

Unclassified

SECURITY CLASSIFICATION OF THIS PAGE (When Data Entered)

REPORT DOCUMENTATION PAGE		READ INSTRUCTIONS BEFORE COMPLETING FORM
1. REPORT NUMBER AFWAL-TR-83-3082, Volume I	2. GOVT ACCESSION NO.	3. RECIPIENT'S CATALOG NUMBER
4. TITLE (and Subtitle) EVALUATION OF THE CRACK GROWTH GAGE CONCEPT AS AN INDIVIDUAL AIRCRAFT TRACKING DEVICE VOLUME I	5. TYPE OF REPORT & PERIOD COVERED Final Report 14 Nov. 1980 - 9 May 1983	
	6. PERFORMING ORG. REPORT NUMBER	
7. AUTHOR(s) F. J. Giessler, J. P. Gallagher	8. CONTRACT OR GRANT NUMBER(s) F33615-80-C-3234	
9. PERFORMING ORGANIZATION NAME AND ADDRESS University of Dayton Research Institute 300 College Park Drive Dayton, Ohio 45469	10. PROGRAM ELEMENT, PROJECT, TASK AREA & WORK UNIT NUMBERS PE 62201 F 24010149	
11. CONTROLLING OFFICE NAME AND ADDRESS AFWAL/FIBEC Wright-Patterson AFB, Ohio 45433	12. REPORT DATE September 1983	
	13. NUMBER OF PAGES 151	
14. MONITORING AGENCY NAME & ADDRESS (if different from Controlling Office)	15. SECURITY CLASS. (of this report)	
	15a. DECLASSIFICATION/DOWNGRADING SCHEDULE	
16. DISTRIBUTION STATEMENT (of this Report) Approved for public release; distribution unlimited		
17. DISTRIBUTION STATEMENT (of the abstract entered in Block 20, if different from Report)		
18. SUPPLEMENTARY NOTES		
19. KEY WORDS (Continue on reverse side if necessary and identify by block number) Crack Growth Gage Individual Aircraft Tracking Force Management Fatigue Crack Growth		
20. ABSTRACT (Continue on reverse side if necessary and identify by block number) An analytical and experimental program was conducted to evaluate the crack growth gage concept for application as an individual aircraft tracking device. Three gage designs were evaluated. Volume I discusses the evaluation of two versions of a stepped thickness gage and a stepped width gage. Volume II discusses the evaluation of a side-grooved constant thickness gage. An analytical evaluation of the change in transfer function corresponding to gage design parameter changes was performed to determine the configura-		

tion of the gages to be tested. Initial spectrum tests were conducted on the first stepped gage design to determine the ranking ability of the gage. Then constant amplitude tests were conducted on the second stepped gage design. A modification of the gage was made to improve spectrum test response. The modified gage was subjected to both constant amplitude testing and spectrum testing.

The analytically derived crack growth rates were compared to the test data. In general, the analysis predicted slightly higher growth rates than observed.

The ability of the gages to perform the IAT function was evaluated by comparing predicted lives based on a normalized crack growth curve. A larger variation in life prediction was observed than was considered desirable for an accurate tracking device. An analytical analysis of expected variations in material properties was made and an analysis of variance was performed. This showed that the variations observed could not be explained by the assumed variation in material properties.

It was concluded that these designs of crack growth gages were not suitable for stand-alone tracking devices due to their variability in response to spectrum loading.

AFWAL-TR-83-3082, VOLUME I



EVALUATION OF THE CRACK GROWTH GAGE CONCEPT AS AN INDIVIDUAL AIRCRAFT TRACKING DEVICE

VOLUME I

ae ^{*University*} University of Dayton Research Institute,
300 College Park Avenue
Dayton, Ohio 45469

September 1983

Final Report for Period 14 November 1980 - 9 May 1983

Approved for public release; distribution unlimited

AIR FORCE FLIGHT DYNAMICS LABORATORY
AIR FORCE WRIGHT AERONAUTICAL LABORATORIES
AIR FORCE SYSTEMS COMMAND
WRIGHT-PATTERSON AIR FORCE BASE, OHIO 45433

NOTICE

When Government drawings, specifications, or other data are used for any purpose other than in connection with a definitely related Government procurement operation, the United States Government thereby incurs no responsibility nor any obligation whatsoever; and the fact that the government may have formulated, furnished, or in any way supplied the said drawings, specifications, or other data, is not to be regarded by implication or otherwise as in any manner licensing the holder or any other person or corporation, or conveying any rights or permission to manufacture use, or sell any patented invention that may in any way be related thereto.

This report has been reviewed by the Office of Public Affairs (ASD/PA) and is releasable to the National Technical Information Service (NTIS). At NTIS, it will be available to the general public, including foreign nations.

This technical report has been reviewed and is approved for publication.

Rodney L. Wilkinson

LT RODNEY L. WILKINSON
Project Engineer

Davey L. Smith

DAVEY L. SMITH, Chief
Structural Integrity Branch

FOR THE COMMANDER

Ralph L. Kuster, Jr.

RALPH L. KUSTER, JR., Colonel, USAF
Chief, Structures & Dynamics Division

"If your address has changed, if you wish to be removed from our mailing list, or if the addressee is no longer employed by your organization please notify AFWAL/FIBEC, W-PAFB, OH 45433 to help us maintain a current mailing list".

Copies of this report should not be returned unless return is required by security considerations, contractual obligations, or notice on a specific document.

PREFACE

This report was prepared by the University of Dayton Research Institute, Dayton, Ohio to summarize all work conducted under Contract No. F33615-80-C-3234. The contract was administered by the Flight Dynamics Laboratory, Air Force Wright Aeronautical Laboratories. 1Lt. Rodney L. Wilkinson was the Air Force Program Monitor.

The program was conducted at the University of Dayton with Dr. J. P. Gallagher as Program Manager. The report was prepared by F. J. Giessler, the Principal Investigator.

Acknowledgement is made of the efforts of Mr. Paul E. Johnson who supervised the testing, Mr. Donald R. Askins, who provided assistance in selection of the adhesive material, Mr. James C. McKiernan who bonded the test specimens, and Mr. Dave Dawicke, Miss Ellen Bornhorst, and Mr. Michael Donahue who assisted in the development and application of the various analysis programs.

A portion of the work was done under a subcontract by Purdue University, School of Aeronautics and Astronautics with Dr. A. F. Grandt, Jr. as the Principal Investigator. The description and discussion of the work done by Purdue is presented in Volume II of this report.

TABLE OF CONTENTS

<u>SECTION</u>		<u>PAGE</u>
I	INTRODUCTION	1
II	SCOPE	10
	1. Crack Growth Gage Design	10
	2. Experimental Data Collection	10
	3. Evaluation of the Crack Growth Gage as an IAT Device	11
III	CRACK GROWTH GAGE DESIGN	12
	1. Previous Crack Gage Developments	12
	2. Current Design Procedure	16
	3. Load Transfer Function Development	17
	4. Selection of Gage Design	21
	5. Modification of Gage Design	35
IV	EXPERIMENTAL DATA COLLECTION	36
	1. Selection of Materials	36
	2. Test Specimen Design	36
	3. Material Characterization	39
	4. Gage Fabrication	48
	5. Gage Installation	56
	6. Testing Procedures	56
V	PRESENTATION AND DISCUSSION OF TEST RESULTS	61
	1. Initial Spectrum Tests	61
	2. Constant Amplitude Tests	69
	3. T-38 Spectrum Tests	77
	4. Load Transfer Tests	79
	5. Comparison With Analysis	79
VI	EVALUATION OF CRACK GROWTH GAGE AS AN IAT DEVICE	88
	1. Requirements for an IAT Device	88
	2. Comparison of Test Results	91
VII	CONCLUSIONS	109
VIII	RECOMMENDATIONS	
	APPENDIX A - DESCRIPTION OF GAGE BONDING PROCEDURE	111
	APPENDIX B - TEST DATA PLOTS	117
	REFERENCES	148

LIST OF ILLUSTRATIONS

<u>FIGURE</u>		<u>PAGE</u>
1	Schematic of a Crack Growth Curve that Provides the Basis for Force Management.	2
2	Crack Length Curves that Provide the Basis for Managing the Air Force Structural Preventative Maintenance (Force Management) Program.	4
3	The Various Elements Inherent in IAT Systems.	6
4	Schematic View of Crack Gage Applied to a Flawed Structural Component.	7
5	Crack Growth Gage Type 1.	13
6	Crack Growth Gage Type 2.	14
7	Crack Growth Gage Modified Type 2.	15
8	Elements in a Crack Growth Analysis.	18
9	General Gage Dimensions.	20
10	Comparison of Stress Intensity Factor Analysis for Gage Type 1.	22
11	Stress Transfer Ratios for Candidate Gages.	25
12	Stress Intensity Factor for the Candidate Gages.	26
13	Shear Stress in Adhesive for Candidate Gages.	27
14	Transfer Function for McDonnell Gage.	28
15	Transfer Function for Candidate Gage A.	29
16	Transfer Function for Candidate Gage B.	30
17	Transfer Function for Candidate Gage C.	31
18	Comparison of Stress Ratios for Adhesive Thickness of 0.01 Inch.	32
19	Comparison of Stress-Intensity Factors for Adhesive Thickness of 0.01 Inch.	33

LIST OF ILLUSTRATIONS (Continued)

<u>FIGURE</u>		<u>PAGE</u>
20	Comparison of Shear Stress in the Adhesive for Adhesive Thickness of 0.01 Inch.	34
21	Test Specimen Design.	37
22	Tensile Test Specimen for 7075-T6 and 7075-T651.	40
23	Center Crack Panel for Crack Growth Rate Tests of 7075-T6 Material.	43
24	Crack Growth Rate Data for 7075-T6 Aluminum, R = 0.1 (0.040 Inch Thick).	44
25	Crack Growth Rate Data for 7075-T6 Aluminum, R = 0.5 (0.040 Inch Thick).	45
26	Straight Line Approximation of Crack Growth Rate Data R = 0.9 and R = 0.5 (0.040 Inch Thick).	46
27	Specimen Geometry for Crack Growth Rate Tests on the 7075-T651 Aluminum.	49
28	Crack Growth Rate Data for 7075-T651 Aluminum, R = 0.1.	50
29	Crack Growth Rate Data for 7075-T651 Aluminum, R = 0.5.	53
30	Dimensions of Gage Type 1 Four Gage Panel.	53
31	Enlargement of EDM Notch Geometry.	54
32	Preliminary Modified Type 2 Gage Shape for Precracking.	55
33	Assembled Test Article (Crack Growth Gages Attached to a Carrier) for Development Tests.	58
34	Scheme for Numbering Crack Growth Gages Attached to a Carrier Specimen.	59
35	View of an Installed Test Specimen.	60
36	Transfer Function for Gage Type 1 Initial Tests.	65
37	Transfer Function for Gage Type 2 Initial Tests.	70
38	Crack Growth Rate Versus Maximum Stress Intensity Factor Analysis Versus Test.	72

LIST OF ILLUSTRATIONS (Continued)

<u>FIGURE</u>		<u>PAGE</u>
39	Transfer Function for Gage Type 2 Constant Amplitude Tests.	74
40	Comparison of Spectra Transfer Functions, Type 2 Gages, Tests 010 and 011.	75
41	Comparison of Spectra Transfer Functions, Modified Type 2 Gages, Tests 014 and 015.	76
42	Transfer Functions for Modified Type 2 Gage for Constant Amplitude and Spectrum Tests.	78
43	Results of T-38 Mild Spectrum Test - Modified Type 2 Gage.	80
44	Results of T-38 Baseline Spectrum Test - Modified Type 2 Gage.	81
45	Results of T-38 Severe Spectrum Test - Modified Type 2 Gage.	82
46	Strain Gage Identification for Load Transfer Test 025.	83
47	Load Ratio Results for Test 025.	84
48	Comparison of Test and Analysis - Crack Growth Rates - T-38 Mild Spectrum.	85
49	Comparis-n of Test and Analysis - Crack Growth Rates - T-38 Baseline Spectrum.	86
50	Comparison of Test and Analysis - Crack Growth Rates -T-38 Severe Spectrum.	87
51	Development of Life Ratio from Normalized Crack Growth Curves.	93
52	Normalized Crack Growth Life Plots.	94
53	Life Ratio Plots for the Type 2 Crack Crack Growth Gage.	96
54	Life Ratio Plots for the Modified Type 2 Crack Growth Gage.	97

LIST OF ILLUSTRATIONS (Continued)

<u>FIGURE</u>		<u>PAGE</u>
55	Computed Mean Values for Spectrum Tests Based on a 7% Material Property Coefficient of Variance.	100
56	Effect of Variation on Unbounded Thickness, Modified Type 2 Gage.	102
57	Effect of Variation in Adhesive Thickness, Modified Type 2 Gage.	103
58	Effect of Variation in Length of Narrow Section, Modified Type 2 Gage.	104
59	Effect of Variation in Length of Wide Section, Modified Type 2 Gage.	105
60	Effect of Variation in Width of Narrow Section, Modified Type 2 Gage.	106
61	Effect of Variation in Width of Wide Section, Modified Type 2 Gage.	107
62	Life Ratio Plots for the Type 3 Crack Growth Gage.	108
A-1	Anodized Area.	115
A-2	Bonding Assembly.	116
B-1	Crack Growth Data for Test 001.	118
B-2	Crack Growth Data for Test 002.	119
B-3	Crack Growth Data for Test 003.	120
B-4	Crack Growth Data for Test 004.	121
B-5	Crack Growth Data for Test 005.	122
B-6	Crack Growth Data for Test 006.	123
B-7	Crack Growth Data for Test 007.	124
B-8	Crack Growth Data for Test 008.	125
B-9	Crack Growth Data for Test 009.	126
B-10	Crack Growth Data for Test 010.	127

LIST OF ILLUSTRATIONS (Continued)

<u>FIGURE</u>		<u>PAGE</u>
B-11	Crack Growth Data for Test 011.	128
B-12	Crack Growth Data for Test 012.	129
B-13	Crack Growth Data for Test 013.	130
B-14	Crack Growth Data for Test 014.	131
B-15	Crack Growth Data for Test 015.	132
B-16	Crack Growth Data for Test 019.	133
B-17	Crack Growth Data for Test 020.	134
B-18	Crack Growth Data for Test 021.	135
B-19	Crack Growth Data for Test 022.	136
B-20	Crack Growth Data for Test 023.	137
B-21	Crack Growth Data for Test 024.	138
B-22	Crack Growth Data for Test 041.	139
B-23	Crack Growth Data for Test 042.	140
B-24	Crack Growth Data for Test 043.	141
B-25	Crack Growth Data for Test 044.	142
B-26	Crack Growth Data for Test 045.	143
B-27	Crack Growth Data for Test 046.	144
B-28	Crack Growth Data for Test 054.	145
B-29	Crack Growth Data for Test 057.	146
B-30	Crack Growth Data for Test 060.	147

LIST OF TABLES

<u>TABLE</u>		<u>PAGE</u>
1	Dimensions for the Candidate Crack Growth Gages	23
2	Mechanical Properties for 7075-T6 Aluminum	41
3	Mechanical Properties for 7075-T651 Aluminum	42
4	Constants for Line Segments Fit to Crack Growth Rate Plots 7075-T6 Aluminum	47
5	Summary of Crack Growth Gage Testing at UDRI	62
6	Spectrum Ranking Capability of the Type 1 Gage	66
7	Initial Test Data Comparison (Type 1 Gage)	68
8	Summary of Spectrum Ranking for Gage Type 2 Tests	71
9	Initial Test Data Comparison (Type 2 Gage)	71
10	Design Goals for a Crack Growth Gage Applied to the Individual Aircraft Tracking Process	89
11	Items to be Considered in the Implementation of an IAT System	92
12	Analysis of Variance Table for Modified Type 2 Gage for T-38 Spectrum Tests	99

SECTION I INTRODUCTION

The work described in this report was done to establish the feasibility of using an instrument known as the crack growth gage as an individual aircraft tracking (IAT) device. The program included both analysis and test of several different gage designs. Testing was carried out under both constant amplitude and spectrum loading conditions. The feasibility of the gages were then evaluated based on a set of IAT requirements.

Current Air Force long-term inspection, maintenance, and repair of aircraft structural components are governed by the Aircraft Structural Integrity Program (ASIP) as defined in Air Force Regulation 80-13, MIL-STD-1530A, and MIL-A-83444 [1-3]. These documents require the continual assessment of structural usage and an evaluation of the damage accumulation in individual airplanes which then determines the schedule for structural inspections, maintenance actions, modifications, airplane rotations, and phaseouts. The structural damage assessment, required to accomplish the overall force management function, is based on a durability and damage tolerance analysis (DADTA) which estimates the available structural life in the presence of crack-like damage. This life is defined as the time to grow a flaw from some initial size to a final critical size. The definitions for both durability life and damage tolerance life are given in References 2 and 3.

The crack growth history used in these analyses for durability and damage tolerance lives is derived from an expected sequence of loads determined from the planned usage of the aircraft. In the design stage, the output from the DADTA is the initial force structural maintenance (FSM) plan. A typical crack growth curve representing the basis for maintenance actions in a given region of the aircraft is shown in Figure 1. For purposes of discussion, this curve will control the retirement of a

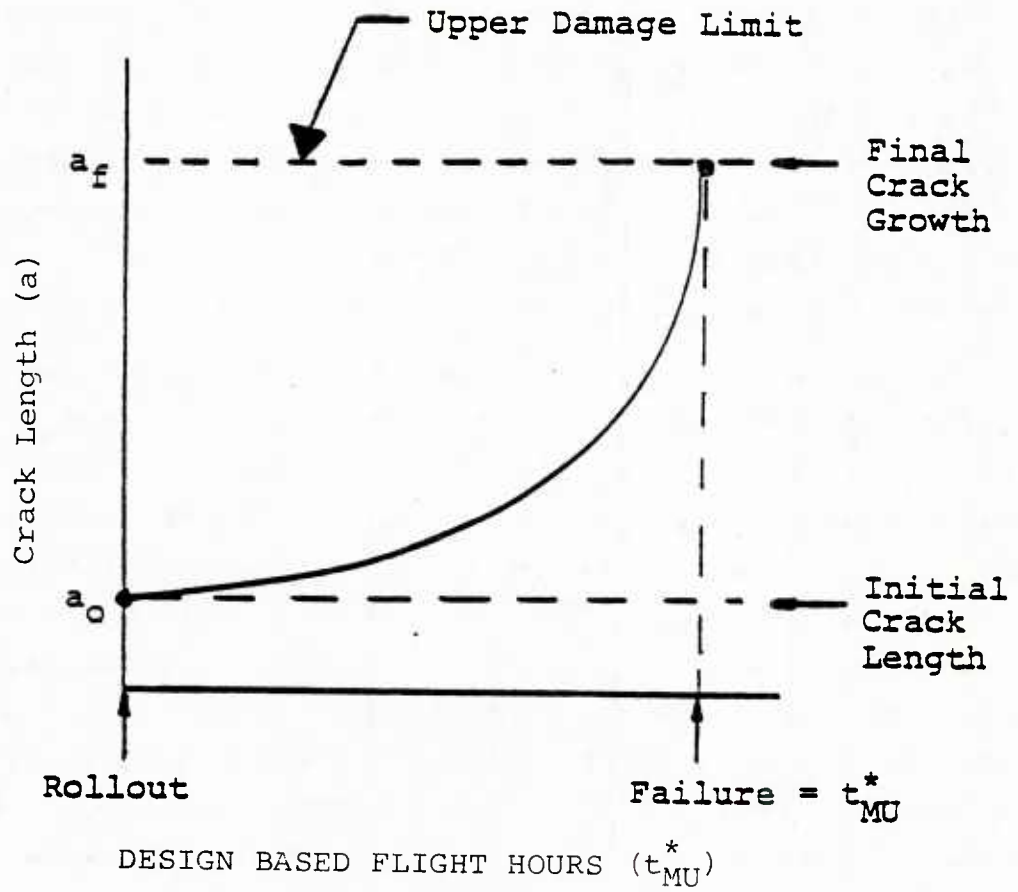


Figure 1. Schematic of a Crack Growth Curve that Provides the Basis for Force Management

structural component that has been designed according to the slow crack growth-noninspectable structure design concepts outlined in Reference 3. The lifetime to failure must be shown by analysis and test to be at least twice the design lifetime. The establishment of the critical structural locations and the corresponding curves, such as shown in Figure 1, provides the basis for the Air Force's structural preventative maintenance (force management) program and the actions dictated by the FSM plan.

After the aircraft force enters service, it is required that the actual usage be monitored to detect changes from the planned usage. This monitoring has two aspects. One aspect is a complete usage evaluation for a representative fraction of the force: the Loads and Environmental Spectral Survey (L/ESS). Between 10 and 20 percent of the aircraft force is commonly used to collect L/ESS data. These data are analyzed and compared to the design usage to arrive at a revised baseline usage. Subsequent data collection is sometimes accomplished using L/ESS equipment to determine if the baseline usage should be changed. The outcome of each change in baseline usage is that new crack growth curves of the type shown in Figure 1 are generated to determine what changes must be made to the FSM plan. These baseline crack growth curves become the basis for the second aspect of the usage monitoring function: the Individual Aircraft Tracking (IAT) program. The IAT program provides data for (1) monitoring the current level of damage accumulation in all structurally critical areas of each aircraft as a function of usage, (2) predicting the time remaining for required maintenance actions, and (3) scheduling aircraft into maintenance depots for actions. The critical areas that are "tracked" for damage accumulation are identified during the DADTA process and provide the basic input to the FSM plan. Figure 2 provides an overview of the interdependence of the FSM plan crack growth curves and the IAT monitored crack growth behavior. More detail on this interdependence is provided in Reference 4.

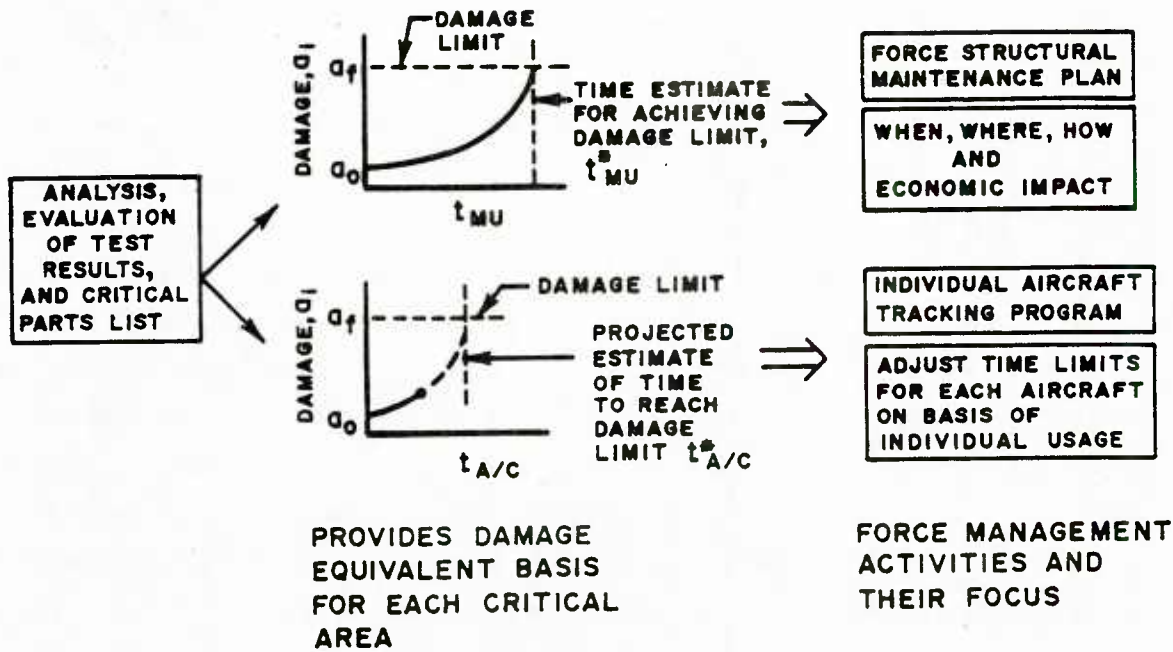


Figure 2. Crack Length Curves that Provide the Basis for Managing the Air Force Structural Preventative Maintenance (Force Management) Program (Reference 4).

We will now focus our attention on the IAT system; i.e., those elements which: (a) define how the individual aircraft's operation history is converted into current levels of crack growth damage, (b) define the remaining structural life, and (c) establish a schedule of maintenance actions for the force of aircraft. Figure 3 identifies the various elements and subelements (or options) built into the IAT systems. The suggested order of operation of the individual elements is defined by the arrows. Individual aircraft data analysis might be accomplished on board the aircraft (as with a microprocessor) prior to the IAT data transfer. However, special and careful attention must be given to the procedures used to periodically change the IAT device when updates occur in the FSM plan as a result of baseline usage changes, new control point additions, etc. Most current IAT systems operate in the manner described by Figure 3.

Currently, the fighter/attack/trainer class of aircraft relies on the recording of motion or load parameters using an acceleration counter or mechanical strain recorder to monitor aircraft response. These types of recorded data require complicated transfer functions to calculate the current level of crack growth damage throughout the aircraft.

Recently, a new concept for monitoring individual aircraft operations was proposed [5] and subsequently elaborated upon [4, 6-16]. This new concept relies on the use of an IAT device called a crack growth gage. The crack growth gage is typically a small structural element which contains a crack and which is attached to a structural component such that it experiences the same loading experienced by the critical area of the component. Figure 4 presents a schematic view of the crack growth gage concept. The type of flaw both in the structure and in the gage will vary with each individual installation.

The crack growth gage device was originally proposed by Howard Smith [17] of the Boeing Company as a fatigue damage monitoring device. The development of a direct transfer function

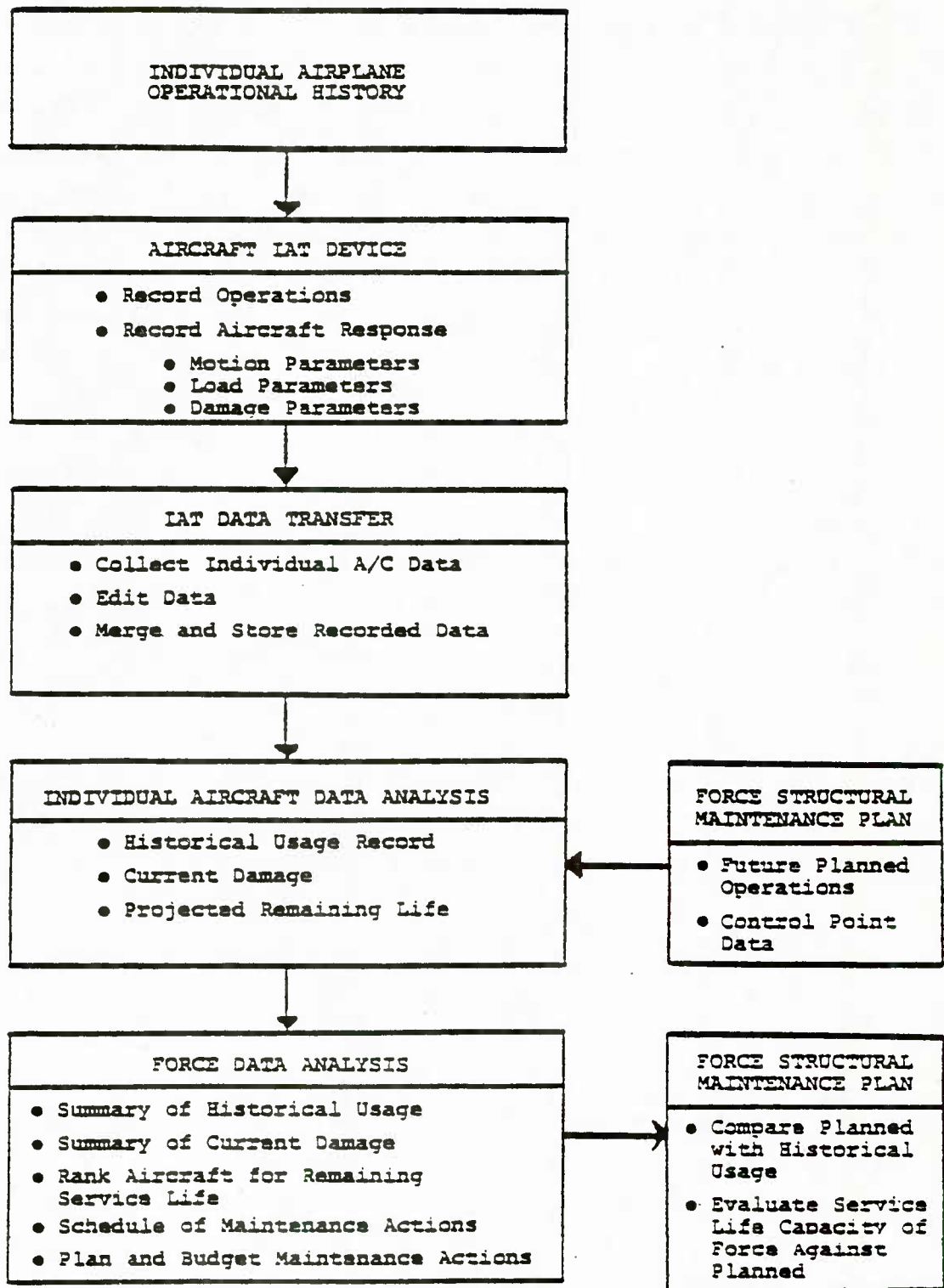


Figure 3. The Various Elements Inherent in IAT Systems

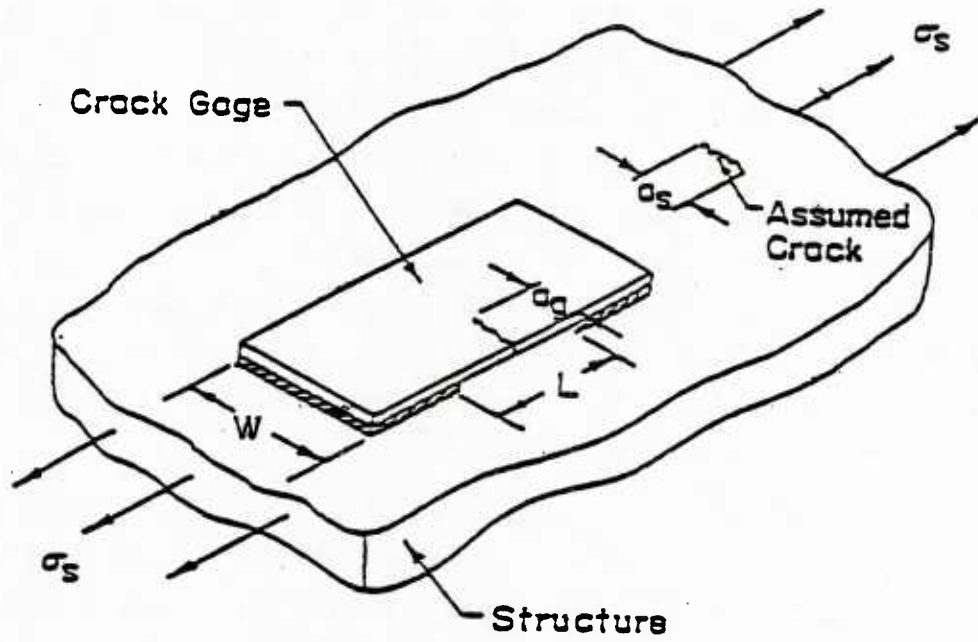


Figure 4. Schematic View of Crack Gage Applied to Flawed Structural Component (Reference 11)

between the crack growth behavior of the gage and of the structural control point provided the technique for applying the crack growth gage to the Air Force requirement for structural damage tracking [5].

While there have been a series of studies that have highlighted the utility of the crack growth gage as an IAT device, fundamental questions remain unanswered. The first and most critical question which was addressed is whether the crack growth gage device will accomplish what Smith's patent suggested, i.e., that it will rank aircraft in a relative manner for maintenance scheduling purposes. "Severely used" aircraft should be scheduled for maintenance prior to an aircraft flying according to a planned (average) operational usage. A "mildly used" aircraft, however, should be scheduled at a later time than those flying according to an average usage. To this date, it has not been clearly demonstrated that the crack growth gage accurately ranks aircraft relative to their usage.

To state this question another way, does the variation of usage significantly affect the crack growth transfer function for a given structural configuration? If the crack growth gage cannot rank aircraft according to usage then the gage is not suitable as an IAT device to schedule maintenance actions.

A second question which has been addressed in the program is whether the crack growth gage has the ability to be a stand-alone IAT system device. The load history integrating effect of the crack growth gage must be assessed as to its ability to provide the ASIP manager with sufficient information to determine aircraft-to-aircraft behavior.

The remainder of this report consists of eight sections and a data appendix. Each section discusses a particular portion of the analytical or experimental part of the program.

The scope of the program is discussed in Section II. Three essential items are identified. First is the design of the crack growth gage, second is the experimental program, and third is the evaluation of the gage as an IAT device.

Section III presents the crack growth gage design method which describes the basis for the gage selection for this program.

The details of the fabrication of the gages and carrier specimens are presented in Section IV.

The results of the experimental program are discussed in Section V. The tests conducted may be divided into three groups. The first group was a series of variable amplitude tests using variations of an available fighter aircraft type loading history. The second group was a set of constant amplitude tests with variations of maximum stress and stress ratio and with and without an overload stress inserted in the history. The third group consisted of three spectrum tests derived from current T-38 usage and identified as mild, baseline, and severe. The reaction of the crack growth gage to the three groups of tests is discussed.

The evaluation of the crack growth gage as an independent IAT device is discussed in Section VI.

Section VII presents a concise formulation of the observations and conclusions of this program and Section VIII presents recommendations.

The Appendix includes a complete set of the data plots obtained during the test program as well as details of the tests.

Volume I of this report presents the work on the stepped gage designs conducted by the University of Dayton and Volume II presents the work on the side-groove gage design conducted by Purdue University under subcontract [36].

SECTION II
SCOPE

The extent of the investigations conducted during the gage design and the experimental testing during gage evaluation portions of the program are discussed in this section.

1. Crack Growth Gage Design

The objective of this activity was to produce two candidate gage designs which along with the side-grooved gage, discussed in Volume II of this report, were to be evaluated as IAT devices.

This effort was composed of the following five elements.

- a. Review of all current literature regarding the application of crack growth gages.
- b. Development of a design procedure.
- c. Evaluation of various gage designs.
- d. Development of an easily applied transfer function for crack growth relations between the structure and the gage.
- e. Selection of two gage designs for the testing phase.

The intent of this effort was to develop an easily applicable method that could be used for future crack growth gage designs as well as for the current program.

2. Experimental Data Collection

The purpose of the experimental activity was to provide the data by which the applicability of the crack growth gage as an IAT device could be evaluated. Essentially three groups of tests were run. The first was a series of initial tests based on a typical fighter aircraft spectrum. The second group was a series of constant amplitude tests designed to determine the response of the gage to changes in stress level and stress range

and to the occurrence of an overload cycle. The third group of tests was spectrum tests representing a baseline, mild, and severe usage of a current USAF fighter/trainer type aircraft.

Six specific elements of the testing program are discussed in this report. These are:

- a. Selection of materials for the gage and the carrier.
- b. Design of the test specimen.
- c. Characterization of the materials.
- d. Fabrication methods for the gages.
- e. Installation of the gages.
- f. Procedures for running the tests.

Details of each of these elements are discussed in the report.

3. Evaluation of the Crack Growth Gage as an IAT Device

The final activity of this program was to use the test results and evaluate the applicability of the crack growth gage as an IAT device. Such an evaluation requires the definition of the requirements of an IAT system. A list of requirements was developed and quantitative measures defined were possible. As the test data became available, it was compared with the requirements. Conclusions were then drawn from these comparisons as to the suitability of the crack growth gage as a stand-alone IAT device.

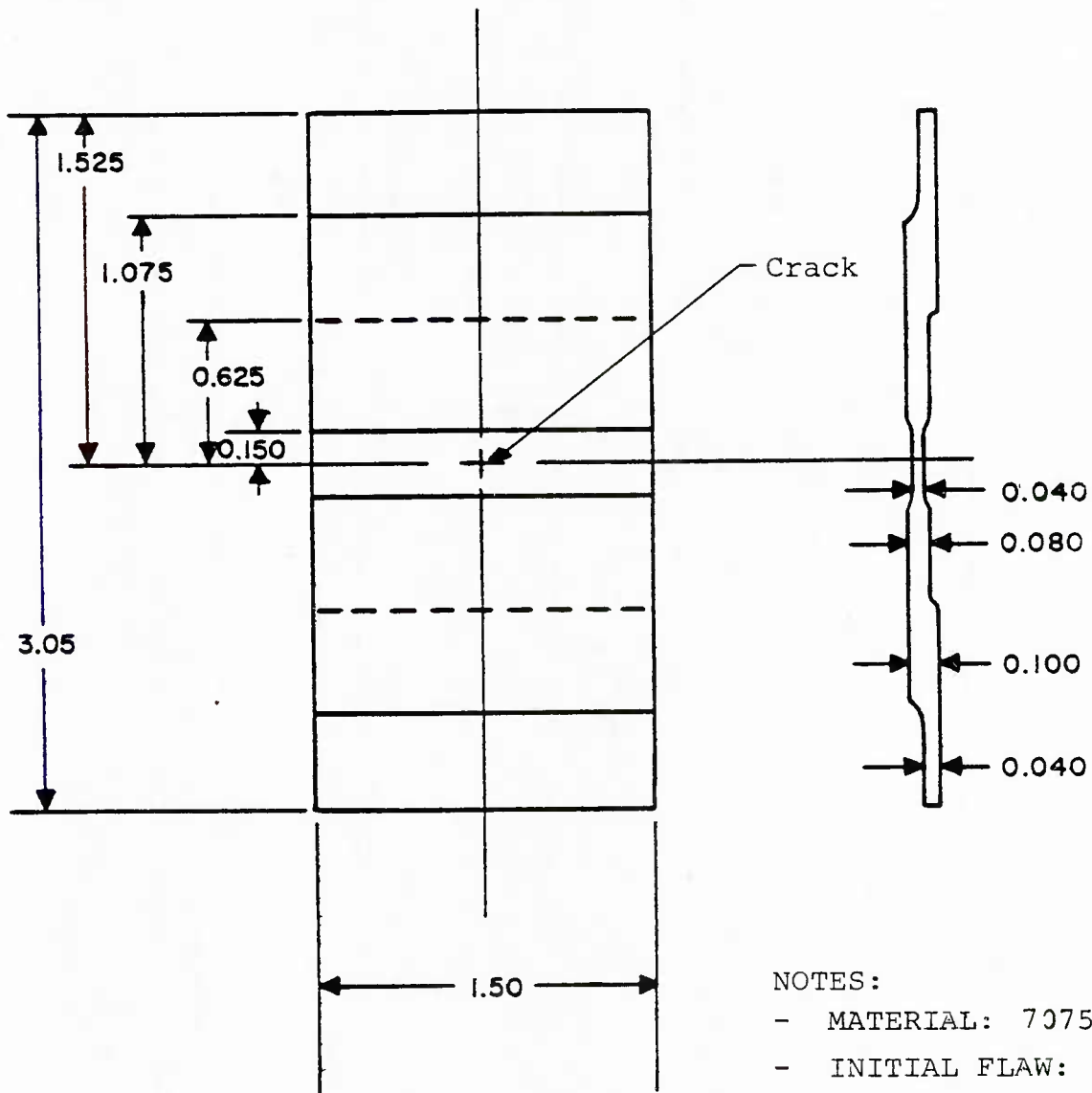
SECTION III
CRACK GROWTH GAGE DESIGN

This section describes the three gage designs which were tested by the University of Dayton. Figures 5, 6, and 7 present these designs. The Type 1 gage, Figure 5, is a duplicate of the gage developed by McDonnell Aircraft Corporation in a previous program [14]. The Type 2, Figure 6, and the modified Type 2, Figure 7, gages were developed to alleviate some of the transfer function spread observed in the Type 1 gage.

1. Previous Crack Growth Gage Developments

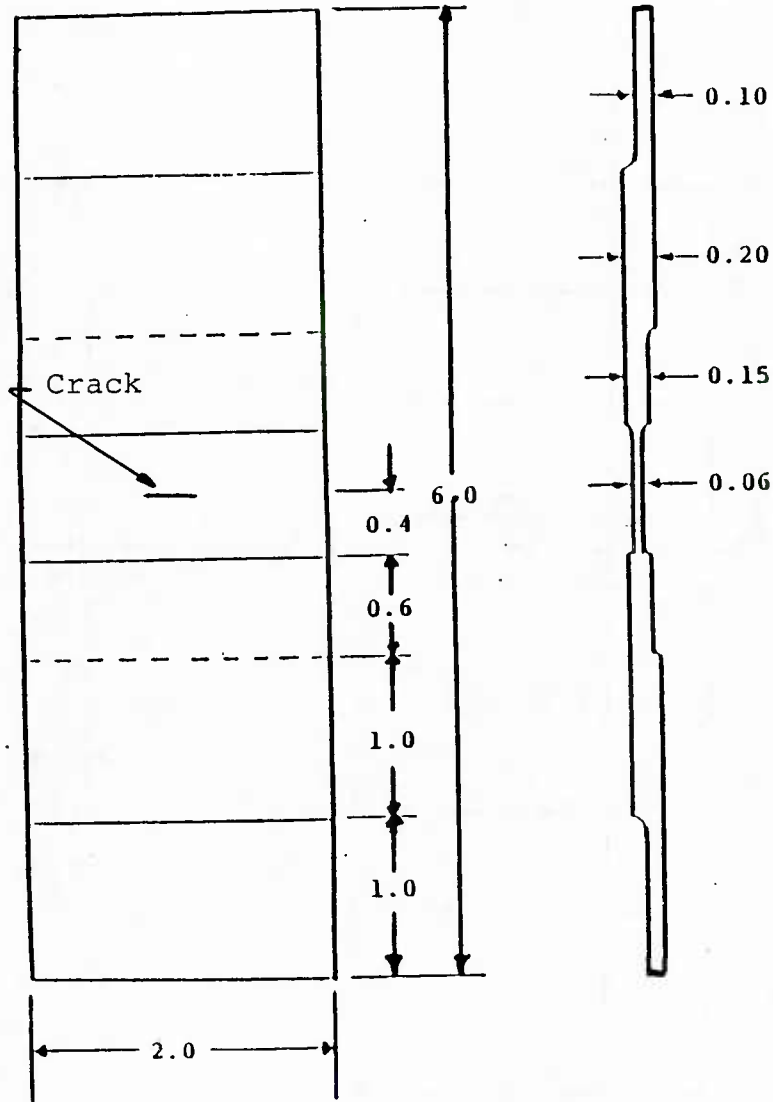
The basic initial design of the crack growth gage is described in three U.S. patents [17, 19, 16]. Since the development of the concept, there has been a series of programs, primarily sponsored by the U.S. Air Force, which have expanded the understanding of the device. A method for analytically developing the transfer function independently from the load history was presented in early reports [4, 5, 6]. It was concluded in Reference 6 that a center cracked gage could provide better correlation over a range of structural flaw lengths than could edge cracked panels. Correlation of test data with analysis showed that the crack growth gage was a principle worthy of additional study [7, 8, 10]. The direct application as an IAT device was also studied [7]. Changing from the original constant thickness gage to a stepped gage design [8, 9, 10, 13, 14, 18] resulted in an increase in sensitivity and a constant stress intensity factor. A trapezoidal design was also investigated in Reference 9 but the analysis showed no significant improvement over the rectangular gage.

Test programs [13, 14] have indicated that the types of load spectra usually associated with fighter/attack/trainer type aircraft operations may induce different behavior in the gage



- NOTES:
- MATERIAL: 7075-T6
 - INITIAL FLAW: 0.200 INCHES
 - ALL DIMENSIONS IN INCHES

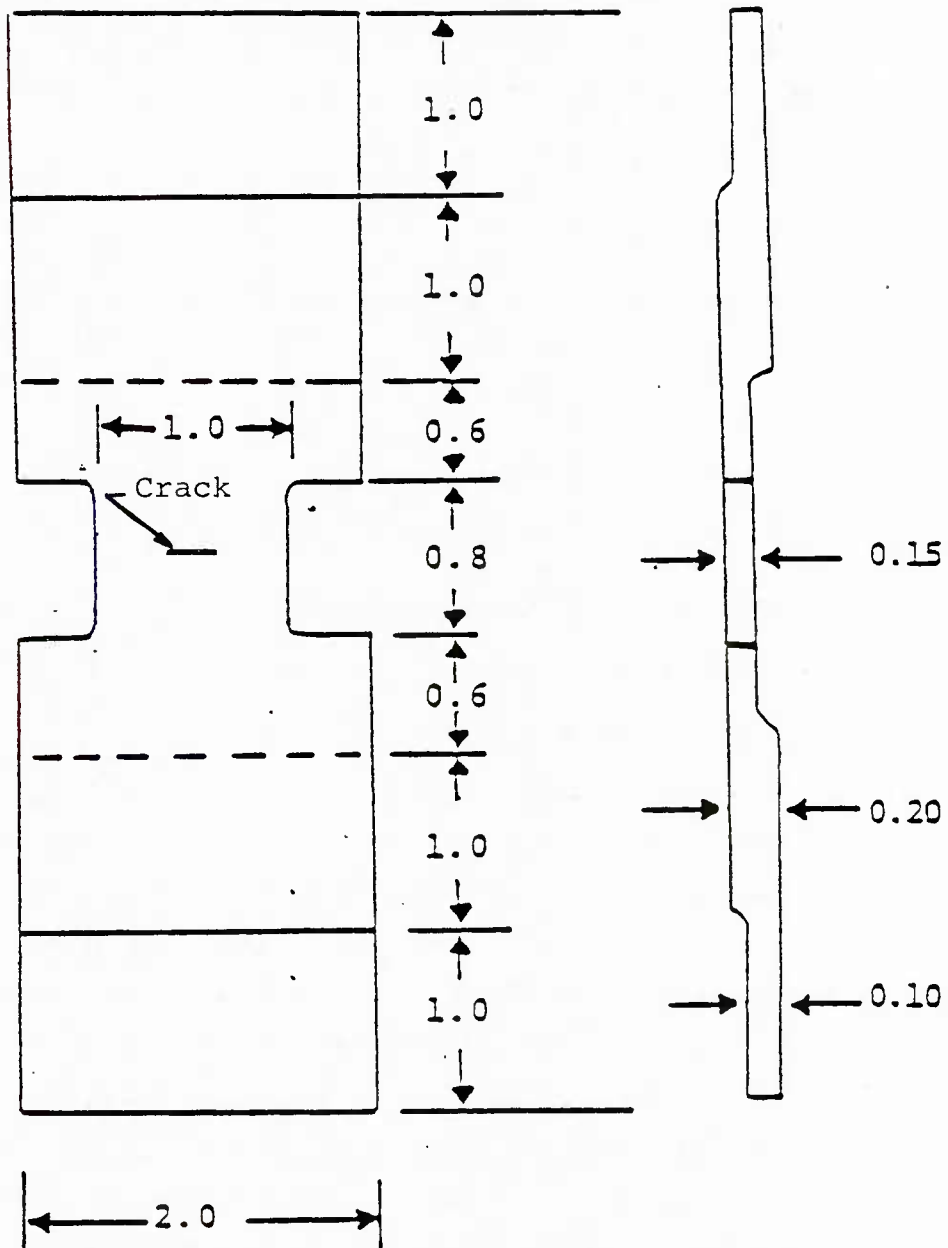
Figure 5. Crack Growth Gage Type 1 (Reference 14)



NOTES:

- MATERIAL: 7075-T651
- INITIAL FLAW: 0.200 INCHES
- ALL DIMENSIONS IN INCHES

Figure 6. Crack Growth Gage Type 2



- NOTES:
- MATERIAL: 7075-T651
 - INITIAL FLAW: 0.200 INCHES
 - ALL DIMENSIONS IN INCHES

Figure 7. Crack Growth Gage Modified Type 2

than in the structure. This is due to the retardation differences between plane stress situations usually found in the gage, and the plane strain situation usually found in the structure.

The thrust of the current investigation was to design a gage which showed reduced sensitivity to spectrum loading variations. However, in order to initiate the investigation, it was decided to conduct a series of spectrum tests with a previously designed gage [14]. This would provide a set of data for comparison purposes.

2. Current Design Procedure

The development of a crack growth gage design requires knowledge of the following elements:

- a. Stress history.
- b. Method to account for stress cycle interactions.
- c. Stress intensity factor for the structure.
- d. Stress intensity factor for the gage.
- e. Crack growth rate data for the structure.
- f. Crack growth rate data for the gage.

The stress history is then applied to the structure and the gage and the resulting crack growth information is used to construct the transfer function. By modifying the stress intensity factor of the gage by varying the geometric and material parameters, a gage design can be developed which will provide the desired relationship between the structure and the gage.

In the current program, the stress histories used were representative of fighter/attack/trainer aircraft usage. Initial tests were conducted using variations of previously used F-4 baseline, mild, and severe spectra [14]. These were used in the analysis to obtain the candidate gage design. Tests were also conducted later using modifications of T-38 operational usage spectra [26]. These spectra were in the form of minimum and maximum cycle end points in a flight-by-flight derived sequence.

The method used to account for cycle interactions in the analysis was a modified Willenborg et al. [32] reducing stress intensity factor model.

The stress intensity factor used for the structure was the Bowie solution for a through-the-thickness radial crack from a hole [22].

The stress intensity factor used for the gage was for a through-the-thickness center crack in a plate. Corrections for finite width and length were obtained using the Isida factor [21]. Corrections for the stepped gage were obtained using the Hilton and Sih factor [22]. In order to relate the gage crack growth to the applied stress of the carrier, a load transfer relation is required. The development of a readily usable relation is discussed in the next subsection.

Crack growth rate data was obtained for both the 7075-T6 material and the 7075-T651 material. Details of these tests are presented in Section IV.

To facilitate the computation of crack growth rates for spectrum loading, the incremental miniblock approach was used [34]. A graphical description of this procedure for crack growth analysis is presented in Figure 8.

3. Load Transfer Function Development

The stress intensity factor relation used for the crack growth gage was:

$$K = \sigma_s \left(\frac{\sigma_g}{\sigma_s} \right) F_1 F_2 \sqrt{\pi a} \quad (3.1)$$

where:

K = Stress intensity factor, ksi $\sqrt{\text{in}}$

σ_s = Stress in structure, ksi

σ_g = Stress in gage, ksi

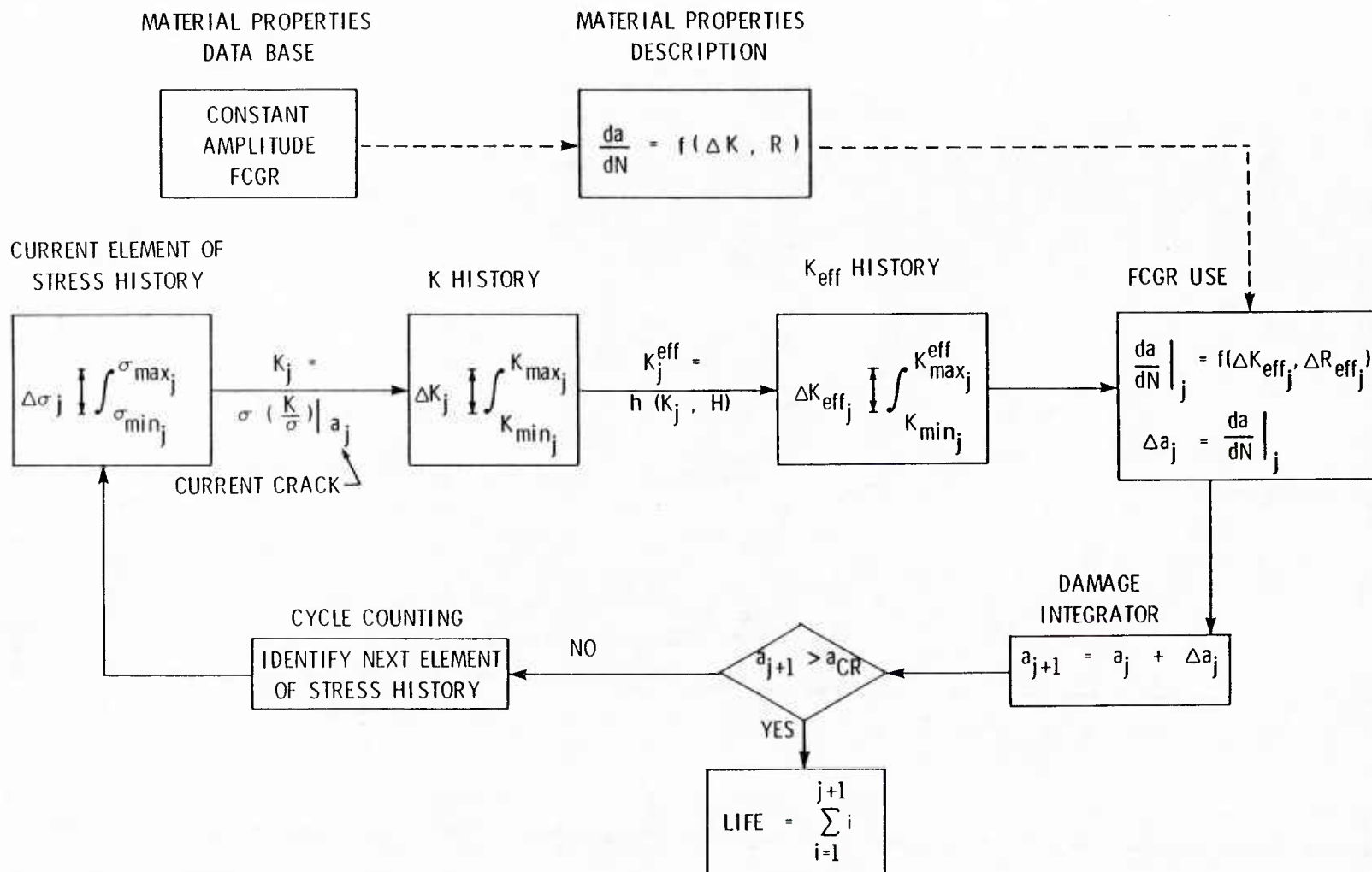


Figure 8. Elements in a Crack Growth Analysis

F_1 = Isida finite length and width correction

F_2 = Hilton-Sih stepped gage correction

a = one-half crack length, inches.

In order to develop a relation for (σ_g/σ_s) , the gage was idealized as shown in Figure 9. Considering the bonded portion of the gage to be rigid, the only deflections are in the unbonded portion and in the adhesive. The analysis is developed by equating the total deflection of these three elements with the deflection of the carrier under the unbonded portion of the gage. This then yields the relation:

$$\frac{\sigma_s (L_1+L_2)}{E_s} = \frac{\sigma_g}{E_g} \left[L_1+L_2 \frac{t_1}{t_2} + \lambda E W t_1 + \frac{t_1+t_3}{L_3} \frac{E_g}{G} \right] \quad (3.2)$$

where:

L_1, L_2, L_3

t_1, t_2, t_3, W } From Figure 9, inches

E_s = structure modulus, ksi

E_g = gage modulus, ksi

G = adhesive shear modulus, ksi

λ = crack compliance, in/kip

The solution for (σ_s/σ_g) gives the relation used.

The crack compliance, λ , was derived from the Irwin-Kies relation:

$$\mathcal{G} = \frac{P^2}{2} \frac{\partial (2\lambda)}{\partial A} \quad (3.3)$$

where:

\mathcal{G} = energy release rate

A = crack surface area

P = load on crack

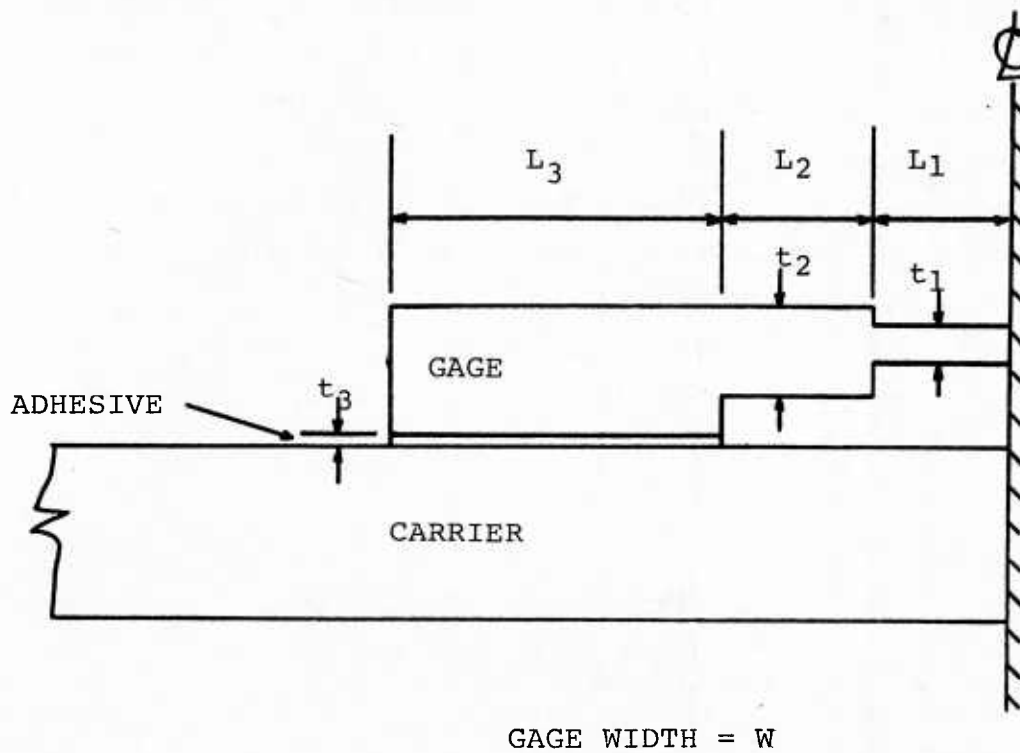


FIGURE 9. General Gage Dimensions

and using:

$$\mathcal{G} = \frac{K^2}{E_g} \quad (3.4)$$

Substituting for the stress intensity factor and writing in terms of a/b , where b is $W/2$, the crack compliance becomes:

$$\lambda = \frac{1}{E_g t_1} \int_0^{a/b} \frac{\pi}{2} \left(\frac{a}{b}\right) (F_1 F_2)^2 d\left(\frac{a}{b}\right) \quad (3.5)$$

This relation is substituted into Equation 3.2 for the final computation form. This relation was compared to the previously developed relation for the Type 1 gage [14] and the comparison is shown in Figure 10. Also shown is a version of Equation 3.2 without the adhesive deflection included. The analysis with the adhesive deflection was used for all subsequent computations.

4. Selection of Gage Design

The selection of a gage design for testing was done by determining the effect on the stress intensity factor relation of several gage geometries. Four candidate geometries are presented in Table 1. The previously developed McDonnell Aircraft Corporation gage [14] was selected as one of the candidate gages since this gage evolved in much the same way as in the present program. Using it for the initial spectrum tests provided data for an evaluation of its characteristics when subjected to spectrum variations. However, it was suspected that its thin crack section might be subject to the previously discussed plane stress/plane strain retardation differences when mounted on a thicker carrier structure.

A second design was sought which might provide some relief from these problems. The three other designs evaluated evolved from an investigation of the effects of dimensional variations on the gage characteristics. The dimensions of these gages (A, B, and C) are given in Table 1.

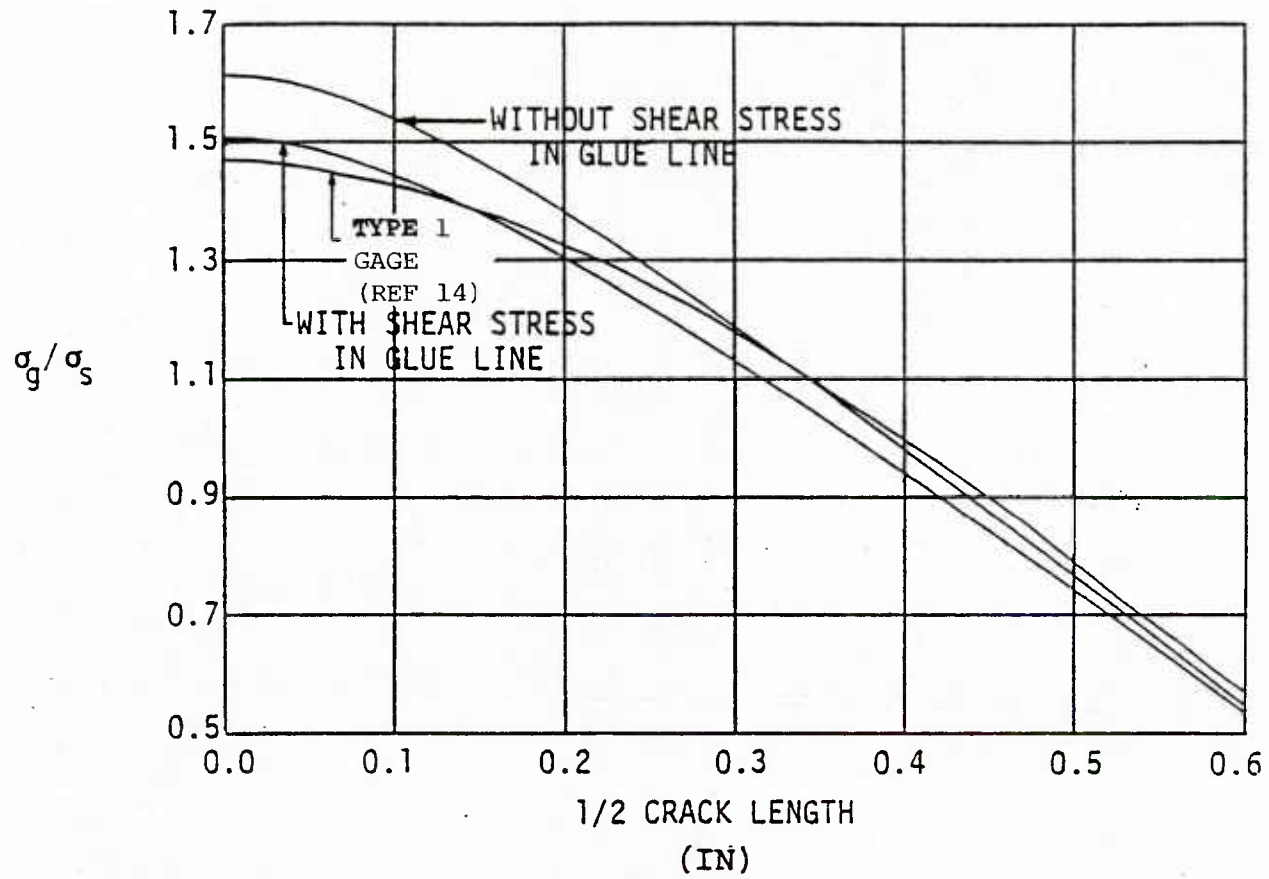


Figure 10. Comparison of Stress Intensity Factor Analyses for Gage Type 1

TABLE 1

DIMENSIONS FOR THE CANDIDATE CRACK GROWTH GAGES

GAGE FEATURE	MCAIR GAGE	GAGE A	GAGE B	GAGE C	
D1	0.15	0.20	0.40	0.20	<p>Initial Crack = 0.200 IN.</p>
D2	0.475	0.70	0.60	0.60	
D3	0.45	1.0	1.0	1.0	
D4	0.45	1.0	1.0	1.0	
T1	0.04	0.05	0.06	0.05	
T2	0.08	0.10	0.15	0.10	
T3	0.10	0.12	0.20	0.12	
T4	0.04	0.05	0.10	0.05	
W	1.5	2.0	2.0	2.0	
MATERIAL.	7075-T6	7075-T6	7075-T651	7075-T6	

Figures 11, 12, and 13 present the stress transfer ratio, stress intensity factor, and adhesive shear stress for each of the candidate gages. The computations were based on an adhesive thickness of 0.004 inches and a maximum carrier stress of 30,000 psi.

Transfer functions for each of the candidate gages were computed based on the F-4 spectra at three load levels. These are presented in Figures 14, 15, 16, and 17. Candidate Gage B shows a very good collapse of the transfer functions for various spectra and load levels.

On the basis of these analyses, candidate Gage B was chosen as the second test gage. The main reasons for this selection were:

- a. High stress intensity factor
- b. Relatively constant stress intensity factor
- c. Low shear stress in the adhesive
- d. Low variation of predicted transfer function, due primarily to use of same material as the carrier structure.

After the initial gages had been manufactured and bonded, it was determined that the average adhesive thickness was closer to 0.01 inches than 0.004 inches. Using this new value, the stress ratio, stress intensity factor, and adhesive shear stress were recomputed for the McDonnell gage and the candidate Gage B. These results are shown in Figures 18, 19, and 20. The changes are small.

For all subsequent discussions, the McDonnell gage is identified as the Type 1 gage and the candidate Gage B is identified as the Type 2 gage.

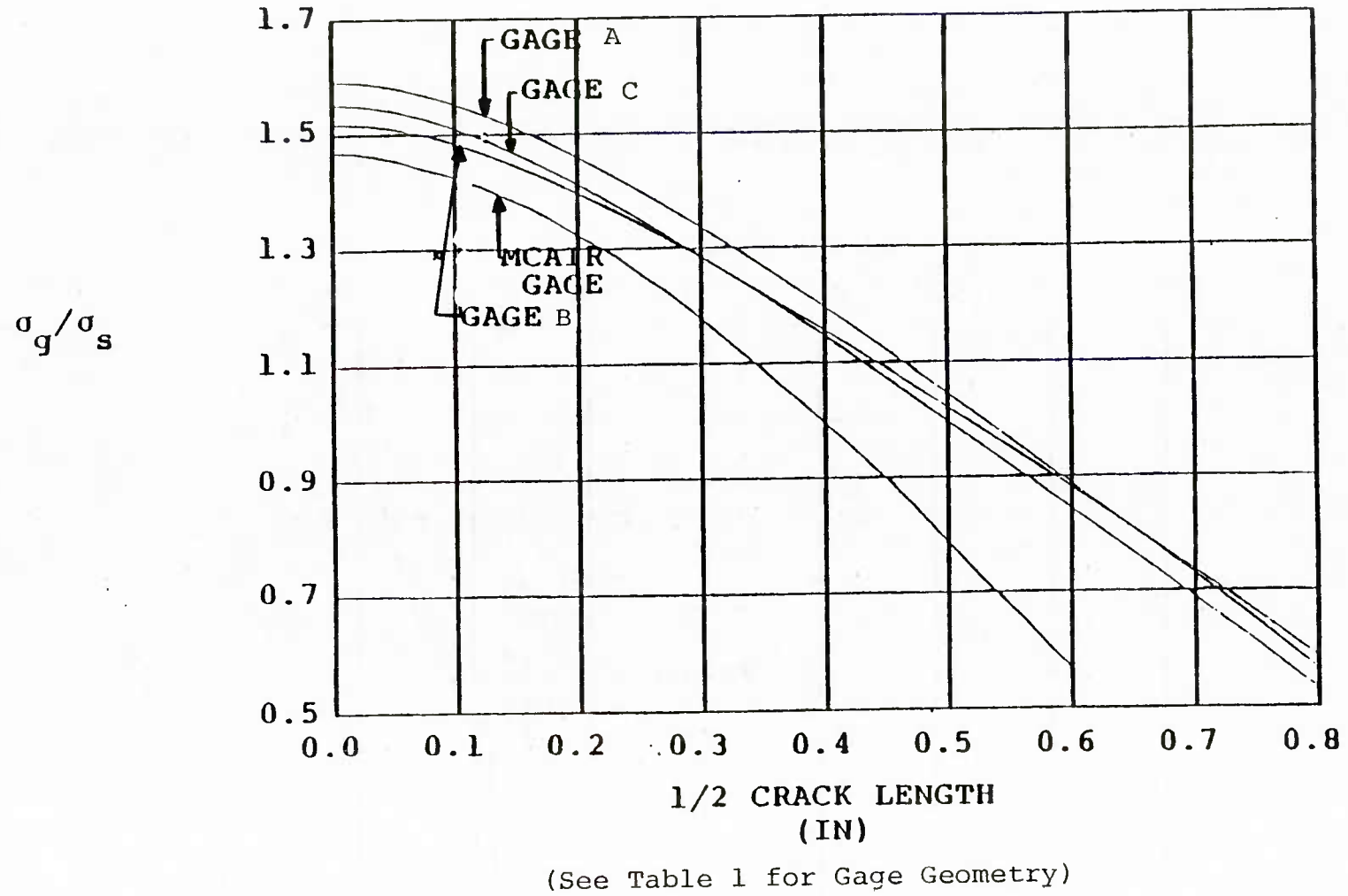
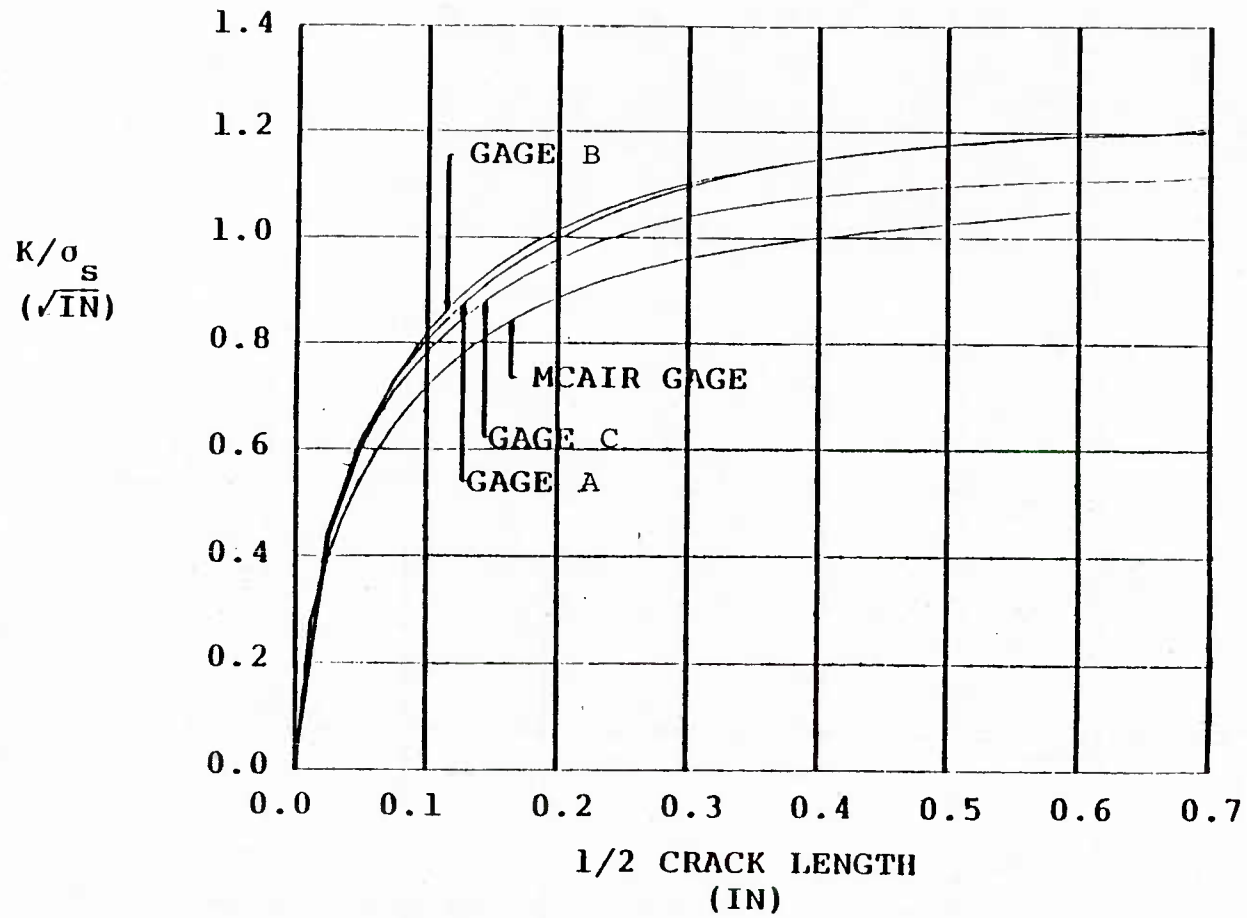
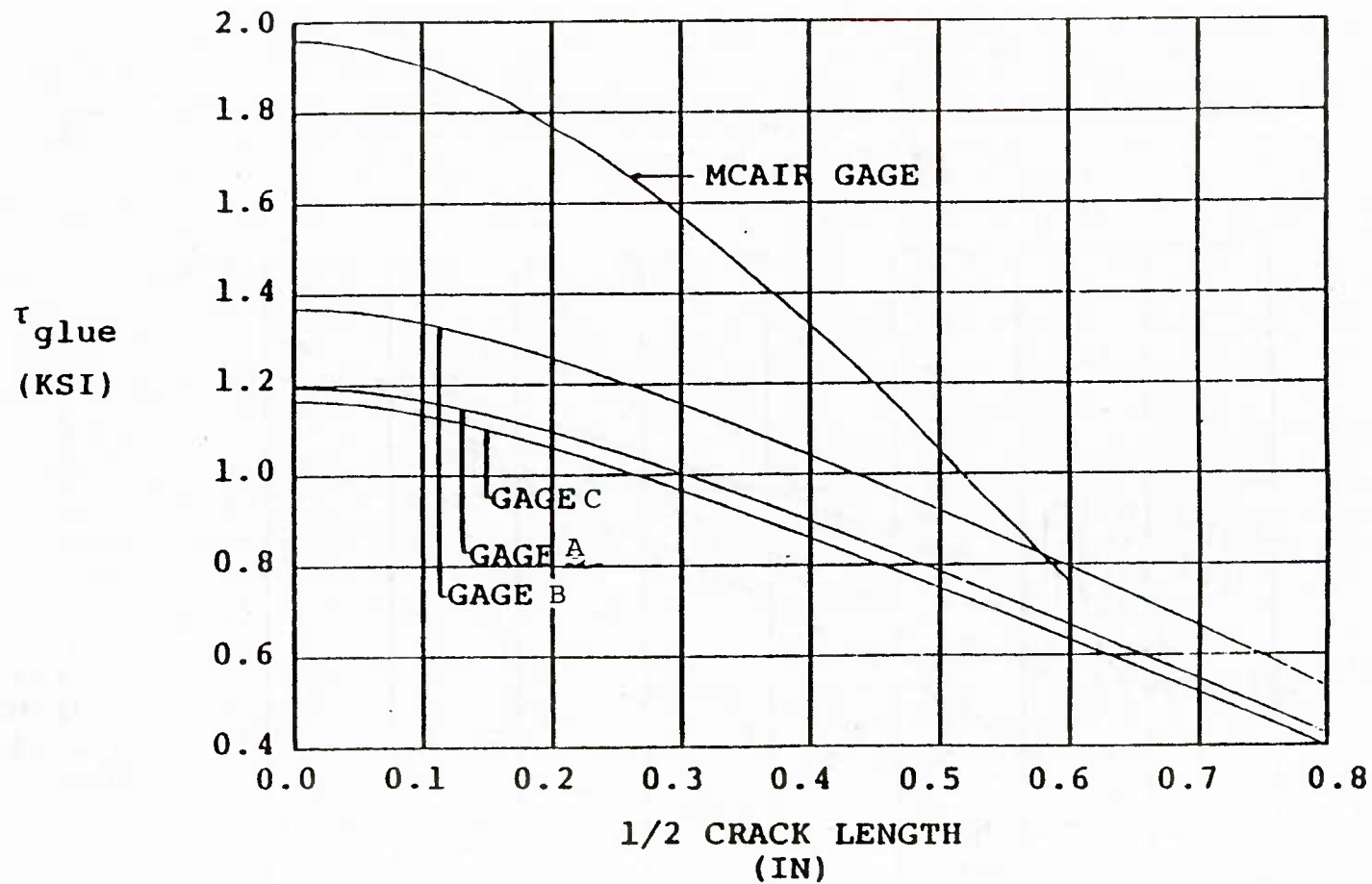


Figure 11. Stress Transfer Ratios for Candidate Gages



(See Table 1 for Gage Geometry)

Figure 12. Stress Intensity Factors for the Candidate Gages



(See Table 1 for Gage Geometry)

Figure 13. Shear Stress in Adhesive for Candidate Gages

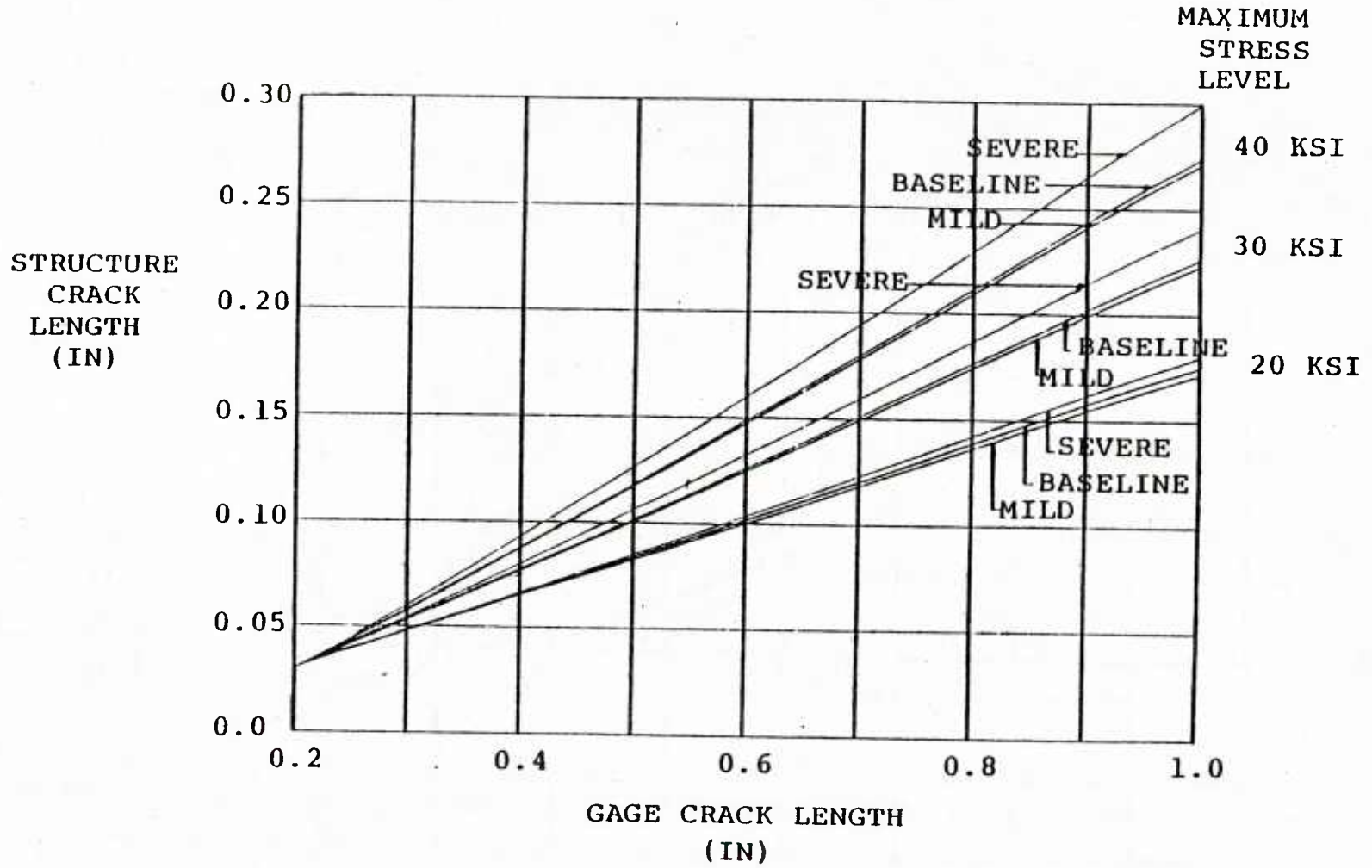
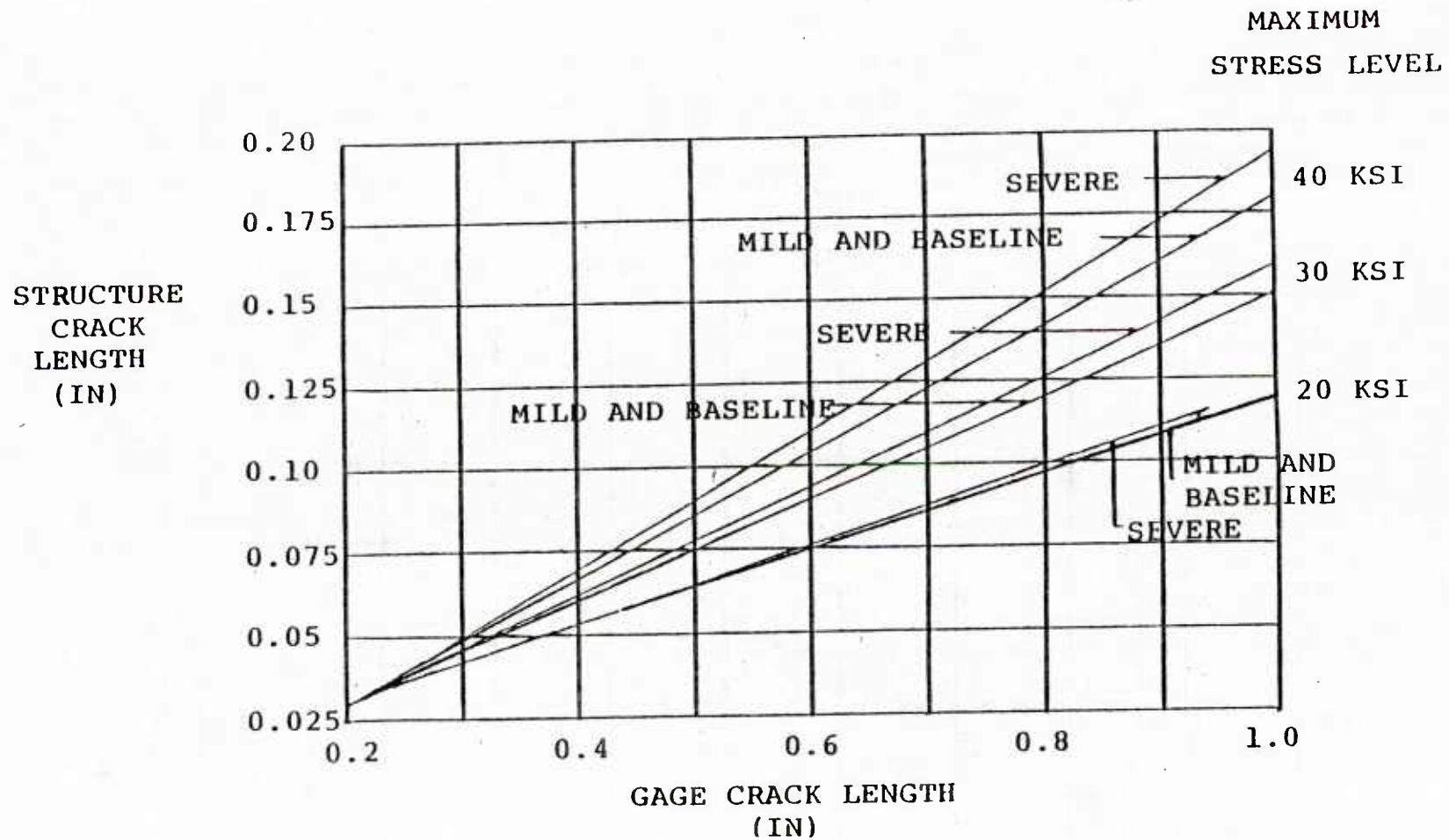
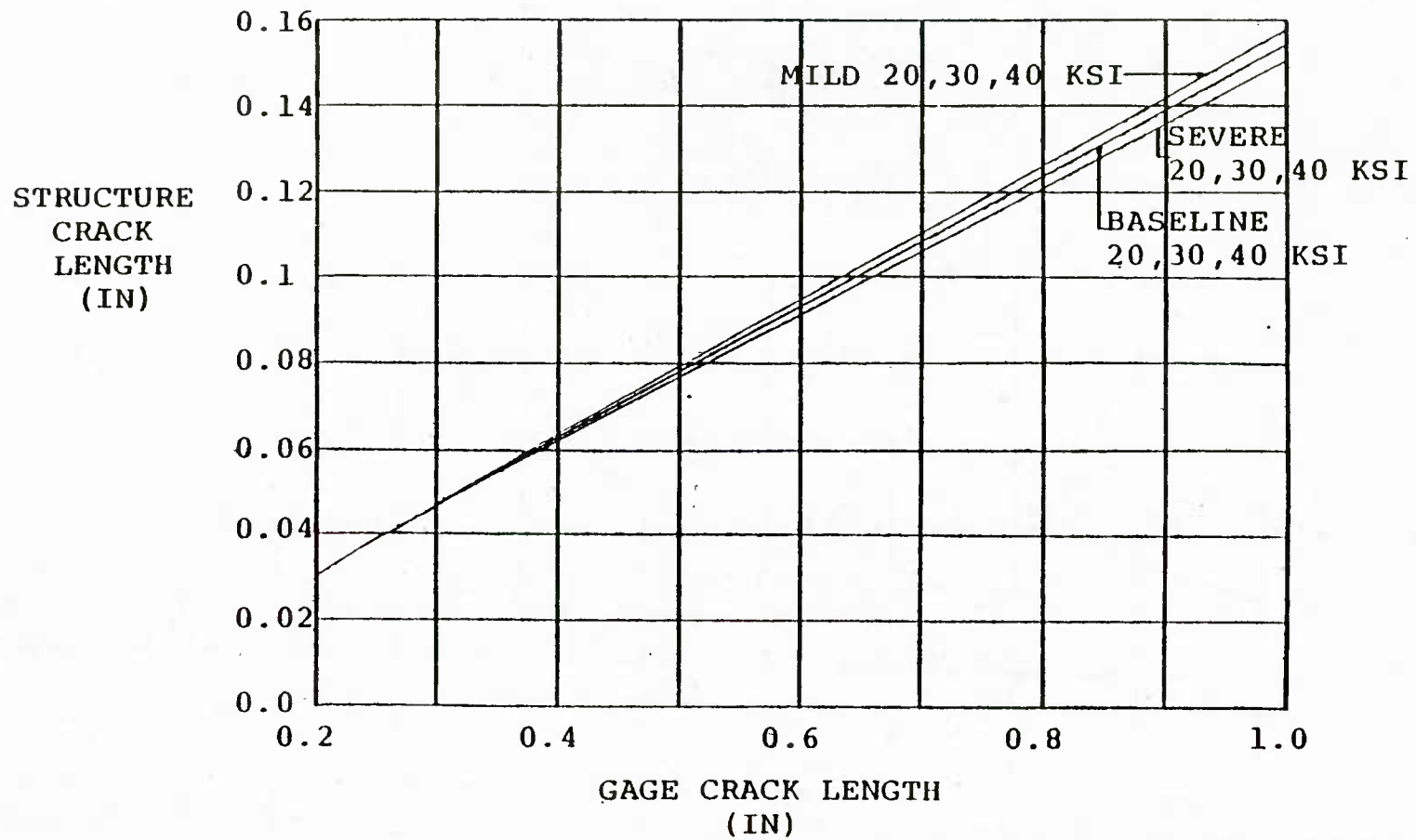


Figure 14. Transfer Function for McDonnell Gage



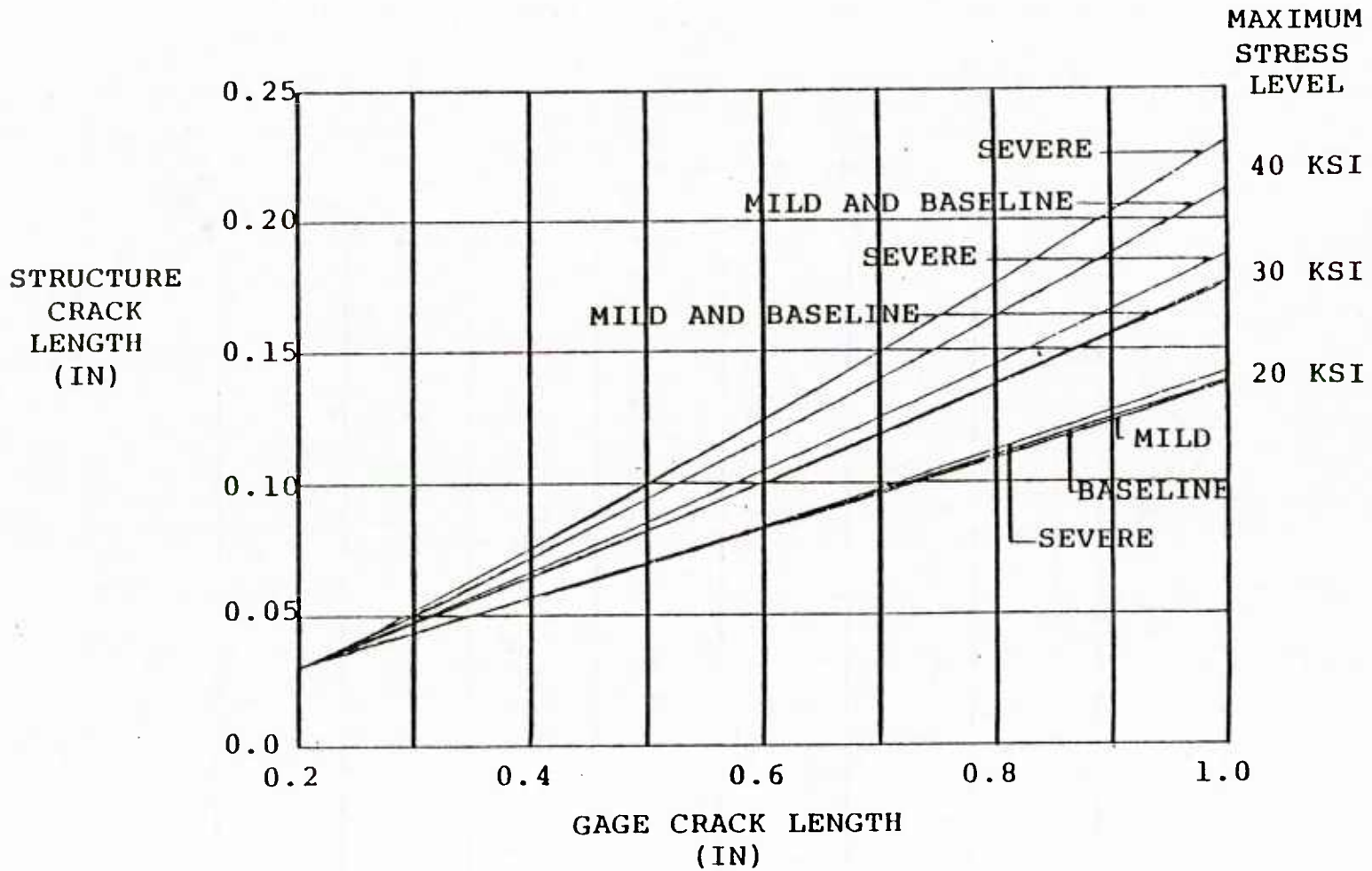
(See Table 1 for Gage Geometry)

Figure 15. Transfer Function for Candidate Gage A



(See Table 1 for Gage Geometry)

Figure 16. Transfer Function for Candidate Gage B



(See Table 1 for Gage Geometry)

Figure 17. Transfer Function for Candidate Gage C

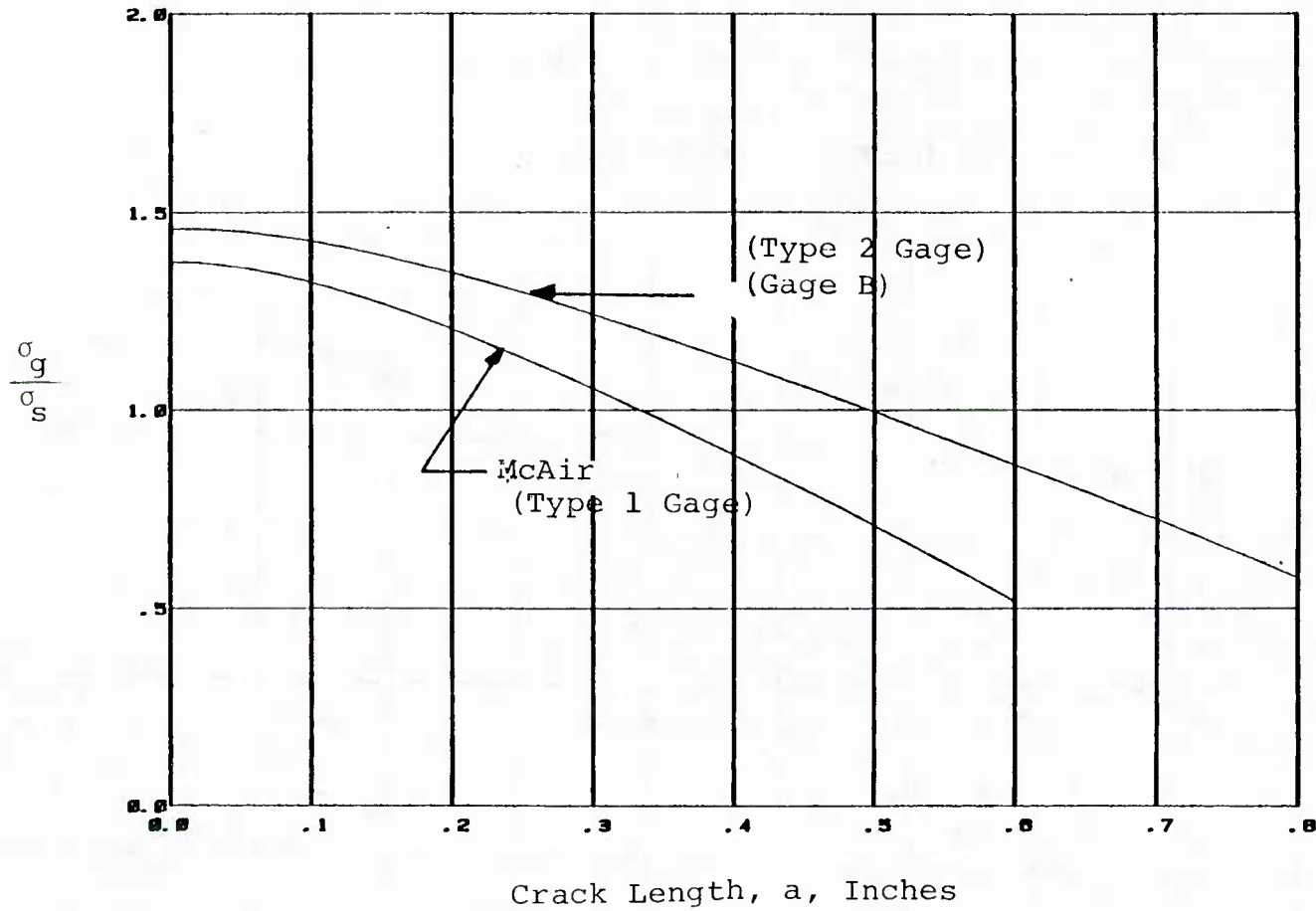


Figure 18. Comparison of Stress Ratios for Adhesive Thickness of 0.01 inch

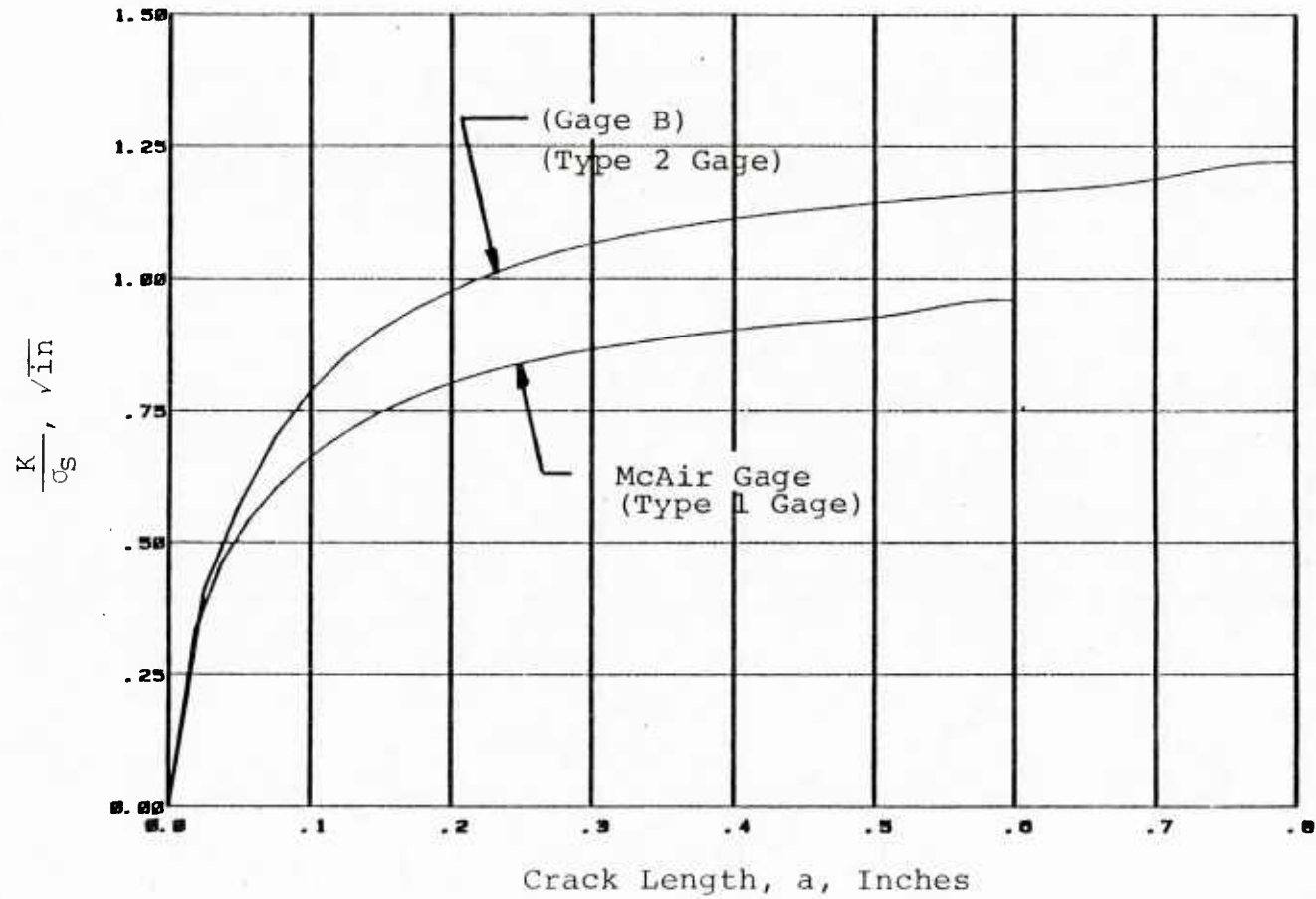


Figure 19. Comparison of Stress - Intensity Factors for Adhesive Thickness of 0.01 Inch

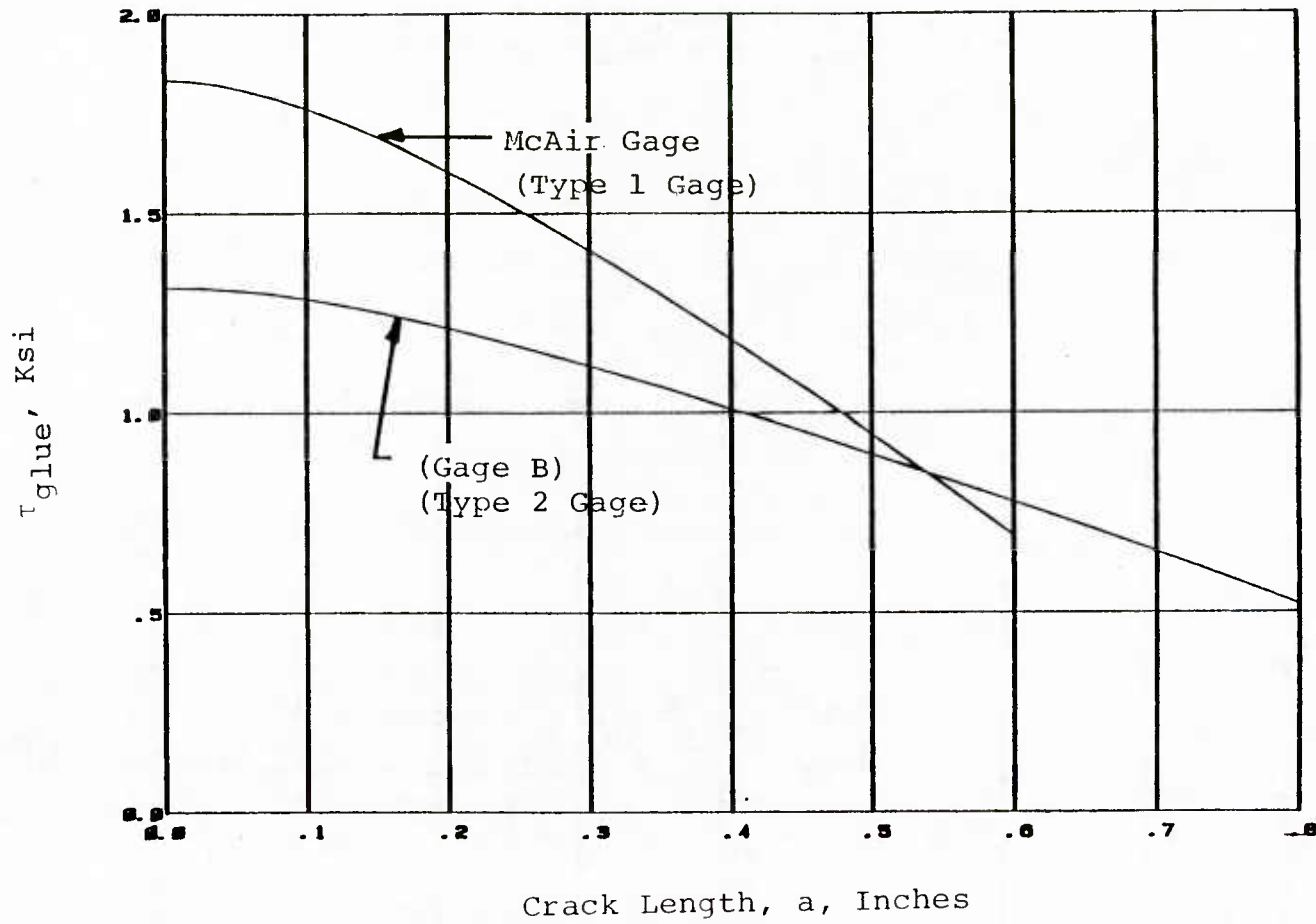


Figure 20. Comparison of Shear Stress in the Adhesive for Adhesive Thickness of 0.01 Inch

5. Modification of Gage Design

After completion of part of the testing on the Type 2 gage, which will be discussed in Section V, it was decided to modify the gage. This modification consisted of increasing the thickness and reducing the width of the cracked section. The final dimensions are shown in Figure 7. This new design was called the Modified Type 2 gage.

This revision necessitated changing the stress intensity factor relations. Defining the cracked section width as W_1 and following the procedure of Section III-3 resulted in a stress transfer relation as follows:

$$\frac{\sigma_g}{\sigma_s} = \frac{L_1 + L_2}{(L_1 + L_2 \frac{t_1}{t_2} \frac{W_1}{W} + \lambda E t_1 W_2 + \frac{t_1 t_3}{L_3} \frac{W_1}{W} \frac{E}{G})} \quad (3.6)$$

The use of this relation in the crack growth rate analysis of the test data showed an offset between the data from the structure and from the gage. As both were of the same material, they should have shown a continuous variation. The difference was considered to be in the stress ratio relation. In the original development the uncracked, unbonded section was modeled with the displacement characteristics of a full width plate. This was determined not to be entirely accurate, as the material in the corners did not contribute fully to the stiffness. The modification was to consider a trapezoidal variation which ignored the triangular corner material, resulting in the relation:

$$\frac{\sigma_g}{\sigma_s} = \frac{(L_1 + L_2)}{(L_1 + \frac{t_1}{t_2} L_2 \frac{W_1}{(W-W_1)} \ln \left(\frac{W}{W_1} \right) + \lambda E t_1 W_1 + \frac{t_1 t_3}{L_3} \frac{E}{G})} \quad (3.7)$$

Application of this relation removed the offset in the crack growth rate plots and was used in all further analyses.

SECTION IV
EXPERIMENTAL DATA COLLECTION

This section presents the details of the various aspects of the testing program. The materials selected, the design of the carrier specimen, the gage fabrication methods, the bonding procedures, and the test methods are discussed. Attention is given to those areas which proved troublesome during the program. Areas which should be approached carefully in any future program are also indicated.

1. Selection of Materials

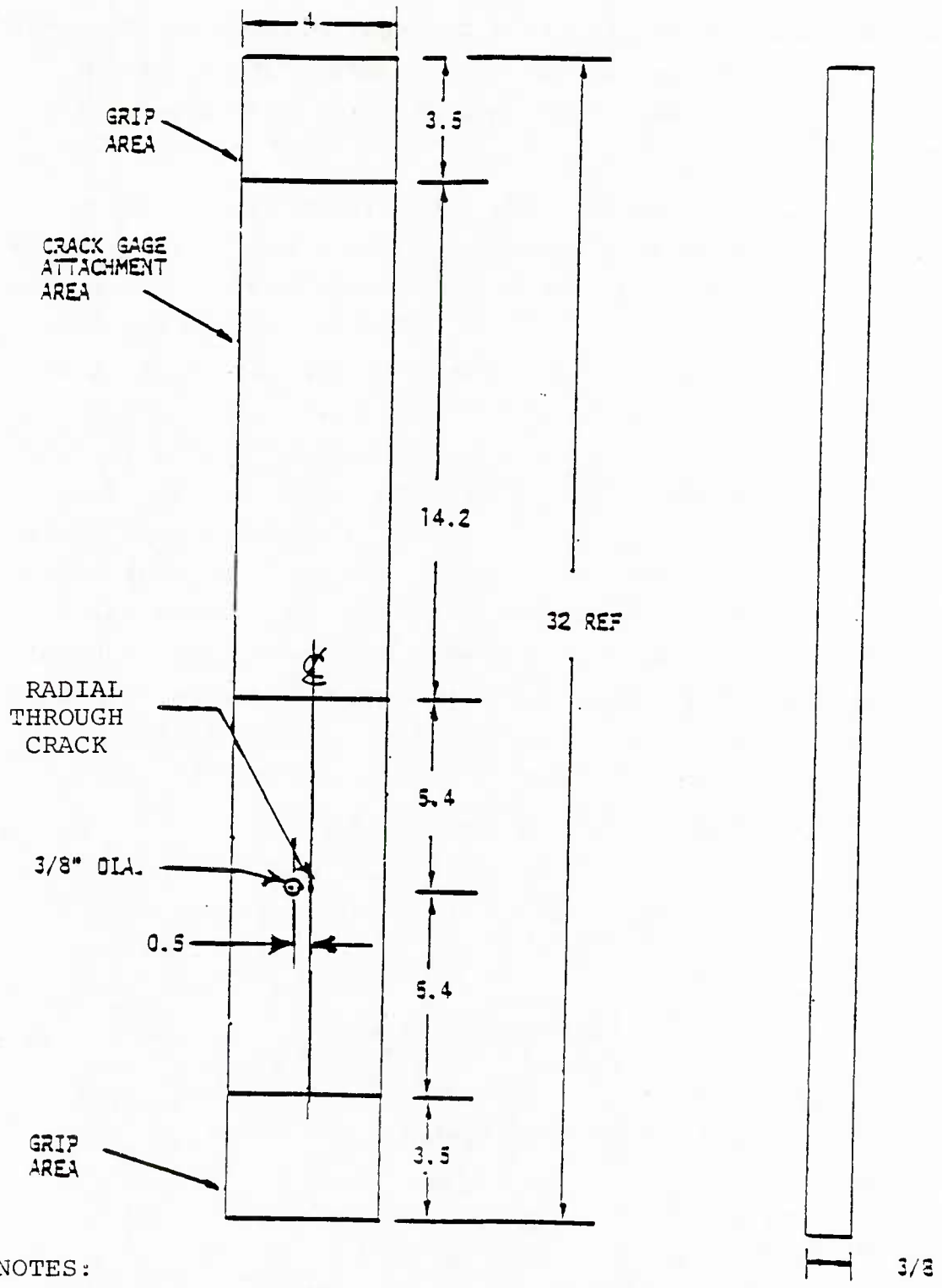
The selection of materials for the carrier specimens and for the crack growth gages was made on the basis of materials used in current fighter/trainer type aircraft as well as those used in previous programs. As a baseline aircraft was to be selected to provide the spectra to be used for variable amplitude loading tests, it was appropriate to select a carrier material which was similar to that used in the baseline aircraft. The selection of the T-38 as the baseline aircraft thus indicated that aluminum alloy 7075-T651 plate material be used for the carrier specimens [54].

The material for the gage was chosen to be 7075-T6 since this would allow some comparisons to be made with previous work [14] if desired.

The carrier material, 7075-T651 was procured in three-eighth inch nominal thickness plates and the gage material, 7075-T6 was procured in one-eighth inch nominal thickness sheets.

2. Test Specimen Design

The design of the test specimen is shown in Figure 21. The simulated structural flaw was a through-the-thickness crack growing radially out of a hole. The center of the hole was located one-half inch off center to allow the crack to grow into



NOTES:

- MATERIAL: 7075-T651
- ALL DIMENSIONS IN INCHES
- INITIAL CRACK = 0.030 INCHES

Figure 21. Test Specimen Design

a region which is relatively free of edge influences. The hole was located so as to be outside the influence of any stress pattern variations caused by either the attached gages or the end grips.

The simulated structural flaw was introduced by first drilling a one-fourth inch diameter hole. A small stress riser was then added and a crack was grown to a length of approximately 0.0925 inches. The loading schedule for precracking began at 22.5 kips and was periodically reduced by ten percent so that the final crack growth was achieved at 6.75 kips. After growing the crack, the hole was drilled and reamed to 0.375 inches in diameter to leave a crack 0.030 inches long as the initial flaw. This procedure was used for all carriers used in this program. Due to machining and crack growing variations, the final crack lengths showed a variation from the 0.030 inch desired value. The mean length was 0.0328 inches with a standard deviation of 0.00228 inches. Thus, the carrier cracks were generally longer than the 0.030 inch design dimension. The University of Dayton fabricated and precracked all of the carriers used by both the University of Dayton and Purdue University.

The stress intensity factor solution used for the simulated structural crack was the following approximation to the Bowie solution

$$\beta = \left[0.6762 + \frac{0.8733}{0.2345 + \frac{a}{R}} \right] \quad (4.1)$$

This is then used in the stress intensity relation:

$$K = \beta \sigma \sqrt{\pi a} \quad (4.2)$$

In these equations

a = crack length from edge of hole, inches

R = radius of hole, inches

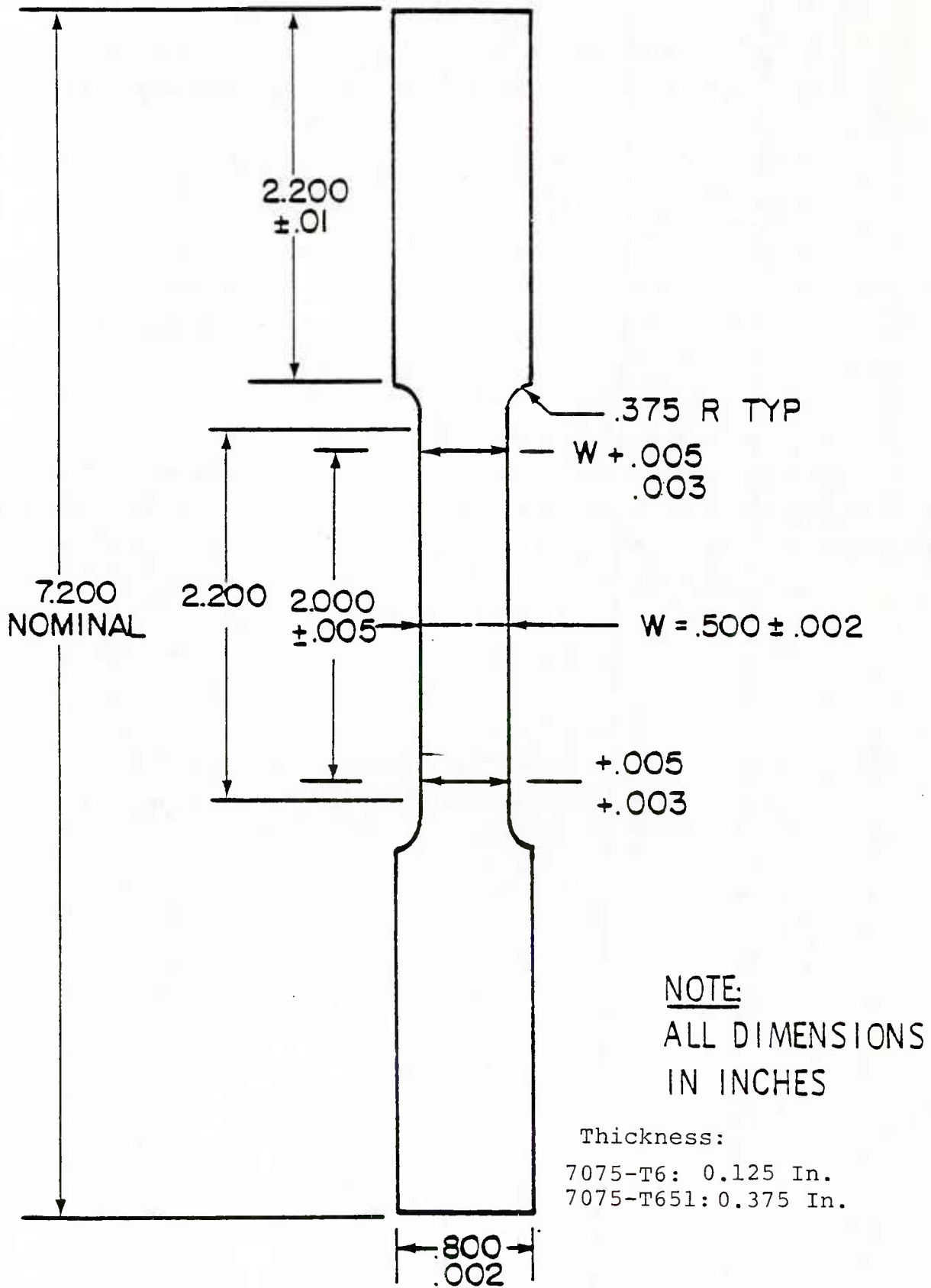
σ = far field applied stress, ksi

The carrier specimens were cut from the 7075-T651 plate material so that the long dimension of the specimen was parallel with the rolling direction.

3. Material Characterization

Two types of material characterization tests were conducted: Tensile tests and crack growth rate tests. These tests were conducted on both the 7075-T6 and the 7075-T651 material. The tensile tests were conducted according to ASTM Test Standard E-8. Figure 22 shows the specimen geometry. The specimens were instrumented on both flat surfaces with T-rosette strain gages. Each gage output was recorded separately. The following mechanical properties were calculated: Young's Modulus, Poisson's ratio, 0.2% offset yield strength, the ultimate tensile strength, and the ductility. In all cases, the variation in the values calculated for both sides of the specimens was less than 2% of the calculated value. The values from the three tests for each material appear in Tables 2 and 3 and are the average of the results from both sides of the specimen. The values for all of the properties except ductility compare well with typical values (B-values) from the Mil-Handbook-5C, also shown in the tables.

The crack growth rate tests for the 7075-T6 material were conducted using the specimen shown in Figure 23. The purchased 0.125 inch thick material was chem-milled to 0.040 inch thick. The tests were conducted at R ratios of 0.1 and 0.5 in a closed-loop electro-hydraulic test machine equipped with hydraulic grips. Loads were selected for various tests to generate crack growth rate data for the range of 10^{-7} to 10^{-3} . The $da/dN-\Delta K$ curves appear in Figure 24 for $R = 0.1$ and in Figure 25 for $R = 0.5$. Visual inspection of the data determined that there were four straight-line segments to the data. Figure 26 presents the least-squares fitted curves for both load ratios. Table 4 presents the constants for the line segment fits using



TENSILE TEST SPECIMEN

Figure 22. Tensile Test Specimen for 7075-T6 and 7075-T651

TABLE 2

MECHANICAL PROPERTIES FOR 7075-T6 ALUMINUM

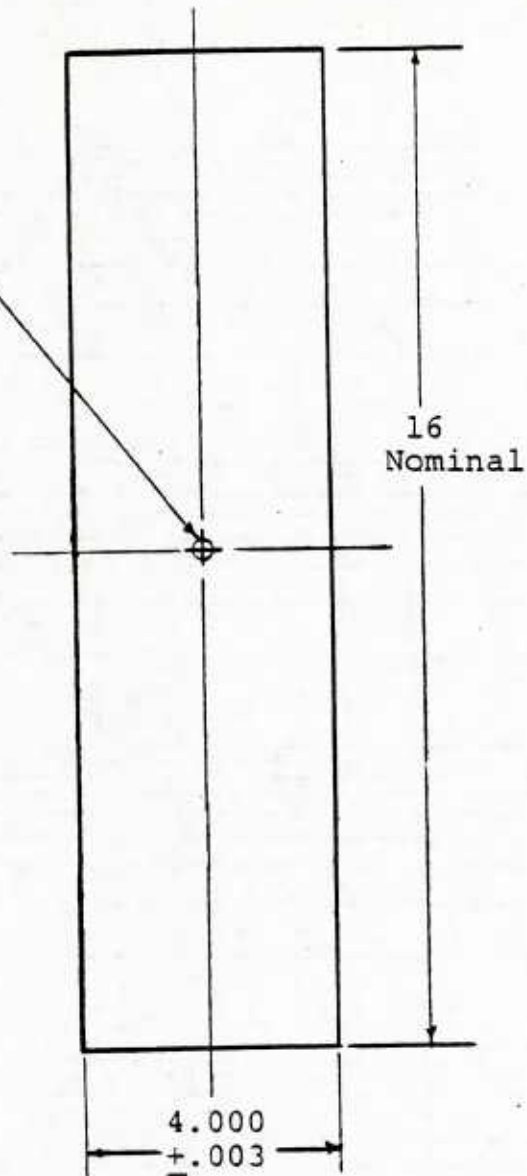
Mechanical Property	Material	7075-T6 Aluminum	HDBK-5C Table 3.7.3.0 (b ₁) B Values 15 Sept 76
	Thickness	0.125 inches	
		Average (3 Tests)	
Young's Modulus, E x 10 ⁶ psi		10.5	10.3
0.2% Offset Yield Stress, σ_y x 10 ³ psi		75.8	72
Ultimate Tensile Stress, σ_{ut} x 10 ³ psi		80.9	80
Poisson's Ratio		0.317	0.33
Elongation in 2 inches, %		10.9	8

TABLE 3
MECHANICAL PROPERTIES FOR 7075-T651 ALUMINUM

Mechanical Property	Material	7075-T651 Aluminum	
	Thickness	0.375 inches	
	Average (3 Tests)		HDBK-5C Table 3.7.3.0 (b ₁) B Values 15 Sept 76
Young's Modulus, E x 10 ⁶ psi	10.0	10.3	
0.2% Offset Yield Stress, σ_Y x 10 ³ psi	79.3	71	
Ultimate Tensile Stress, σ_{ut} x 10 ³ psi	84.7	79	
Poisson's Ratio	0.318	0.33	
Elongation in 2 inches, %	12.5	9	

Starter Hole Radius:

$.062$
 $\pm .002$



NOTES:

- THICKNESS - 0.040 INCHES
- ALL DIMENSIONS IN INCHES

Figure 23. Center Crack Panel for Crack Growth Rate Tests on 7075-T6 Material

DA/DN (IN/CYCLE)

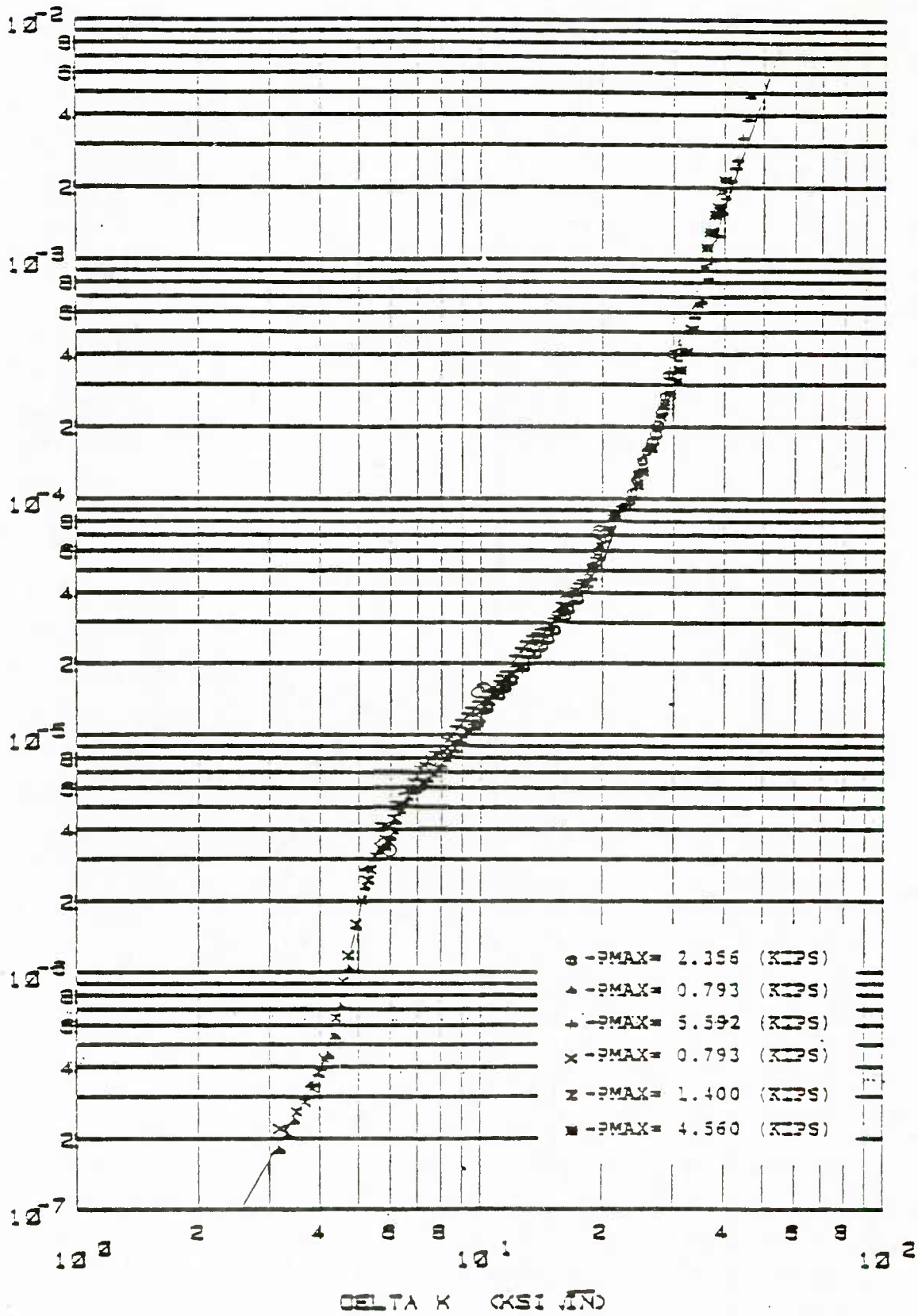


Figure 24. Crack Growth Rate Data for 7075-T6 Aluminum, R = 0.1 (0.040 inch thick)

DA/DN (IN/CYCLE)

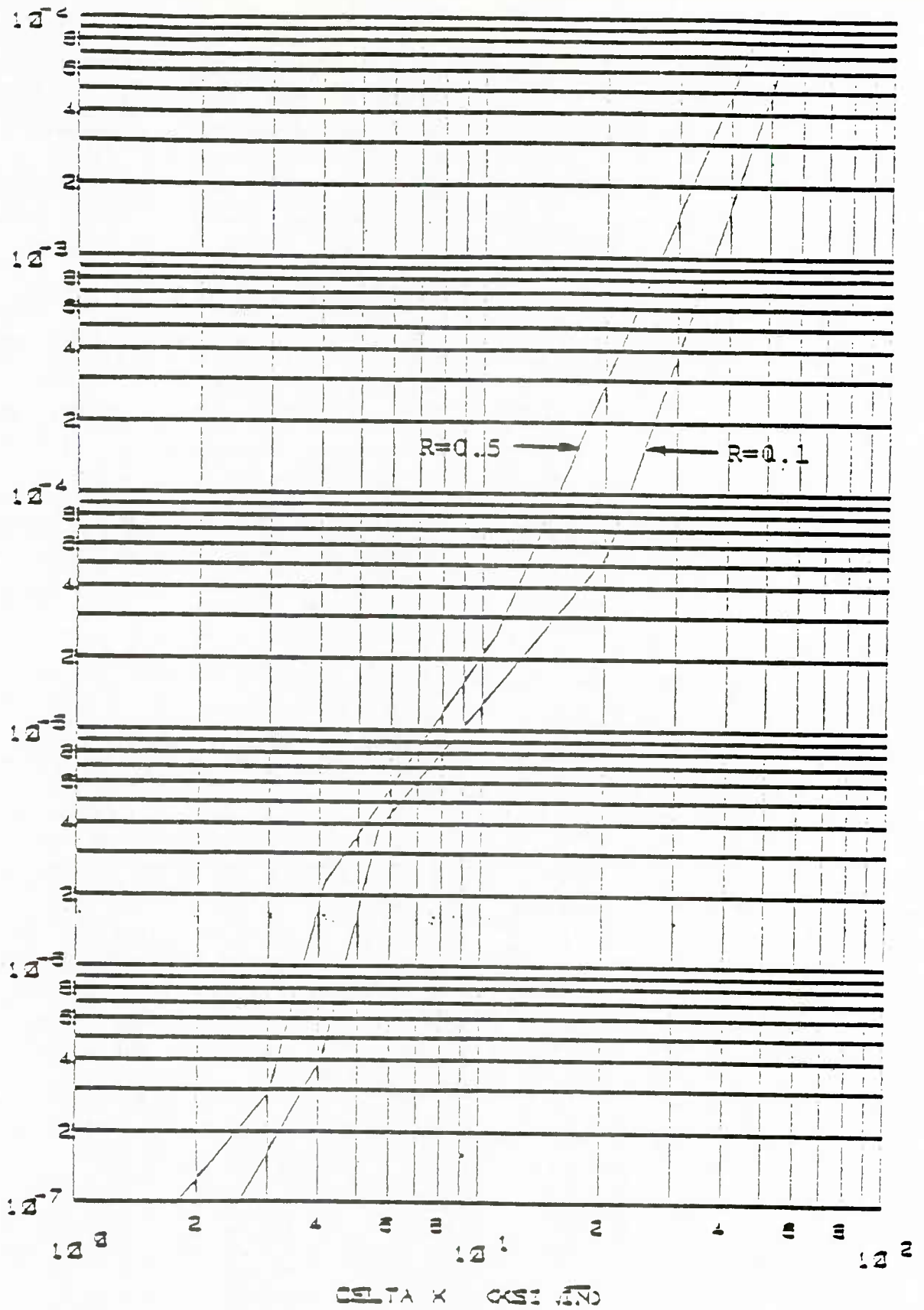


Figure 26. Straight Line Approximation of Crack Growth Rate Data R = 0.1 and R = 0.5 (0.040 inch thick)

DA/DN (IN/CYCLE)

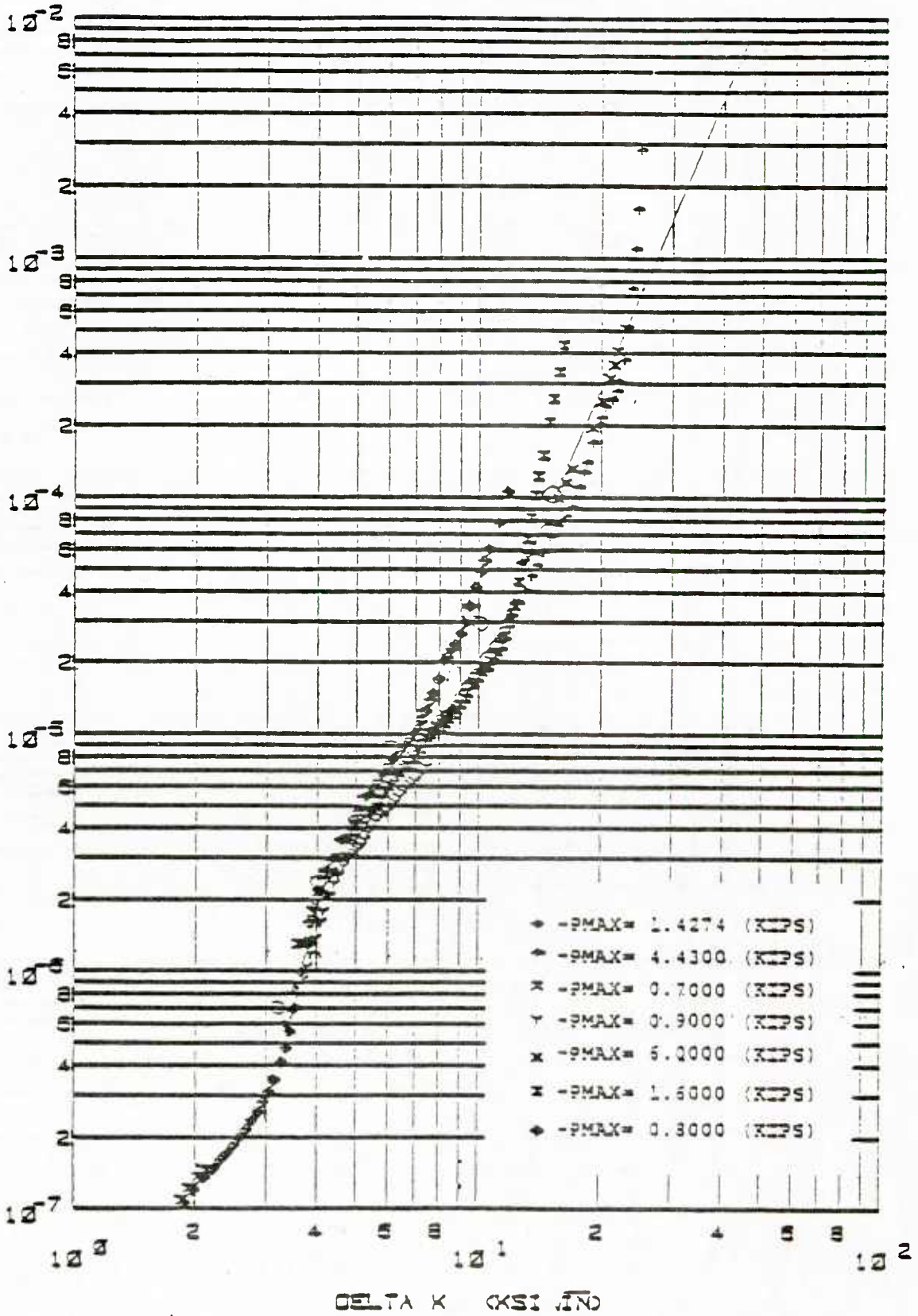


Figure 25. Crack Growth Rate Data for 7075-T6 Aluminum
R = 0.5 (0.040 inch thick)

TABLE 4

CONSTANTS FOR LINE SEGMENTS FIT
TO CRACK GROWTH RATE PLOTS
7075-T6 ALUMINUM

R	ΔK RANGE	C	b
0.1	$\Delta K < 4.077$	6.064×10^{-9}	2.996
	$4.077 < \Delta K < 5.605$	2.032×10^{-11}	7.056
	$5.605 < \Delta K < 20.255$	1.088×10^{-7}	2.070
	$20.255 < \Delta K$	1.907×10^{-11}	4.945
0.5	$\Delta K < 3.017$	2.961×10^{-8}	2.070
	$3.017 < \Delta K < 4.134$	2.219×10^{-10}	6.501
	$4.134 < \Delta K < 10.82$	6.484×10^{-8}	2.501
	$10.82 < \Delta K$	1.779×10^{-8}	4.011

a power law relation. This was used for the initial investigations. The 7075-T6 material was used for the Type 1 gage and for the gages investigated by Purdue University. Volume II discusses the material data model used by Purdue.

The crack growth rate tests for the 7075-T651 material were conducted using the compact tension specimens shown in Figure 27. Tests were run for growth rates between 10^{-7} and 10^{-3} inches/cycle and for R ratios of 0.1 and 0.5. The data for R = 0.1 is shown in Figure 28 and the data for R = 0.5 is shown in Figure 29. A two segment straight-line fit was made to this data using a Walker analysis to fit the equation:

$$\frac{da}{dN} = C [K_{\max} (1-R)^M]^N \quad (4.3)$$

with a break point at

$$K_{\max} (1-R)^{.52} = 7.571$$

The data was fit by the following parameters:

Lower section:

$$C = 0.961 \times 10^{-10}$$

$$M = 0.52$$

$$N = 5.553$$

Upper section:

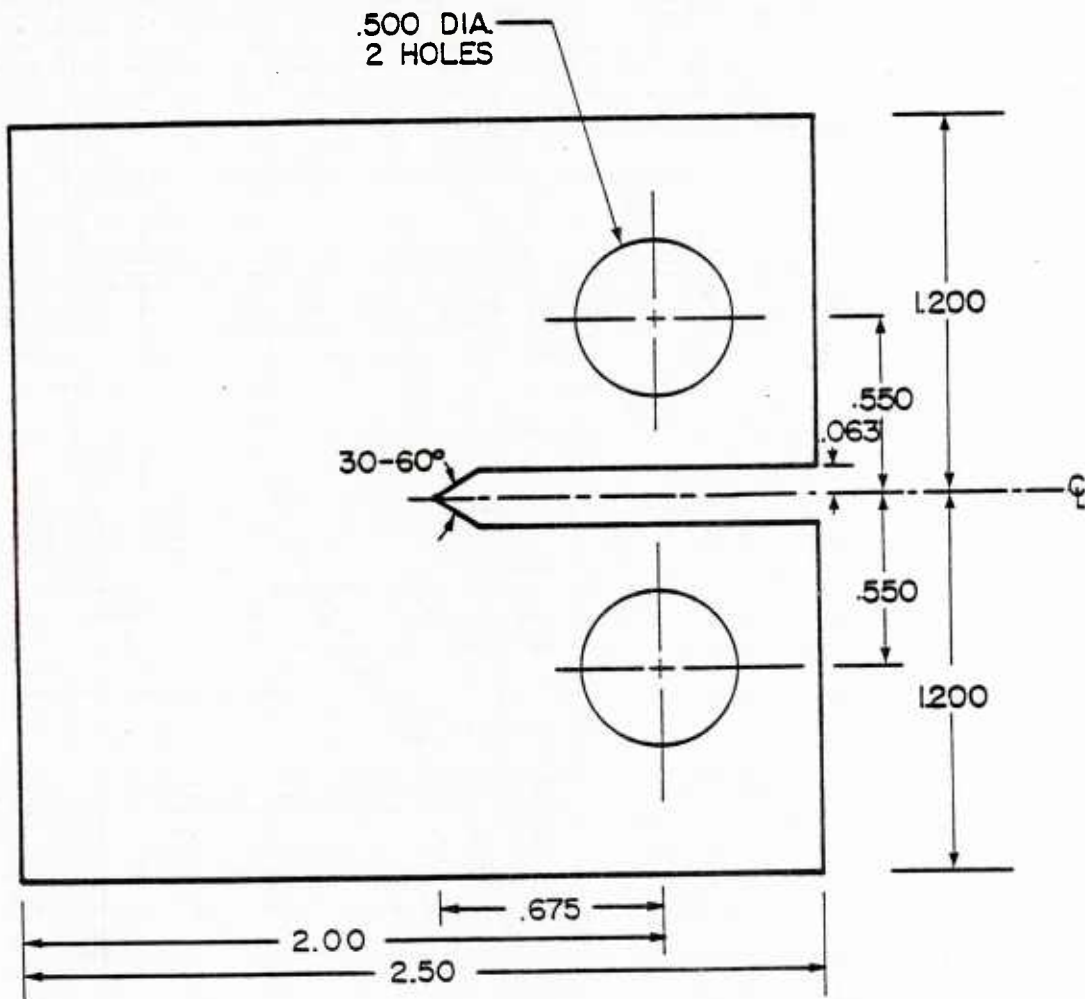
$$C = 0.309 \times 10^{-7}$$

$$M = 0.64$$

$$N = 2.678$$

4. Gage Fabrication

This section describes the fabrication procedures used for the stepped gage design tested by the University of Dayton.



COMPACT TENSION SPECIMEN

NOTES:

1. ALL DIMENSIONS IN INCHES
2. DRAWING IS TWICE ACTUAL SIZE

Figure 27. Specimen Geometry for Crack Growth Rate Tests on the 7075-T651 Material

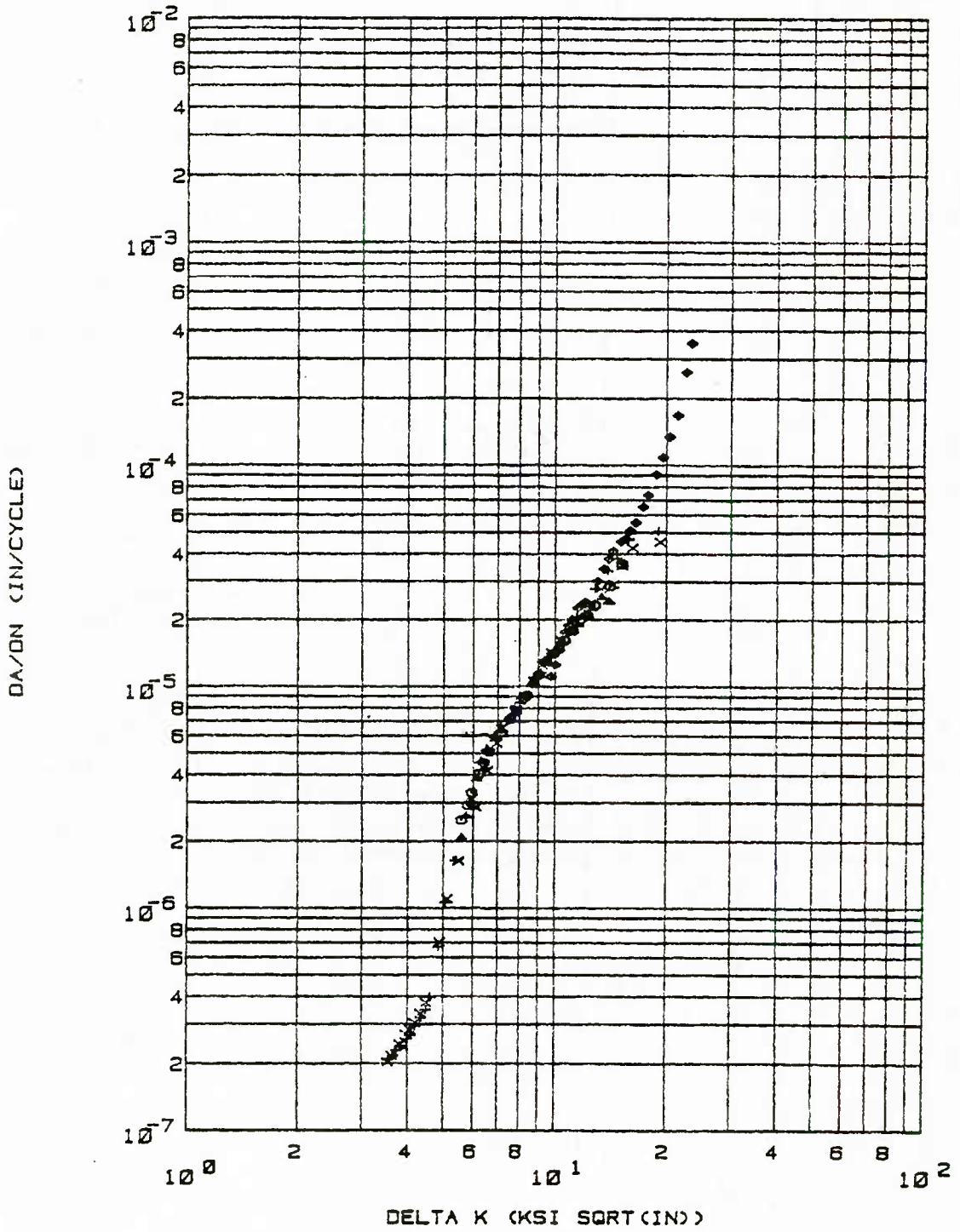


Figure 28. Crack Growth Rate Data for 7075-T651 Aluminum, R = 0.1.

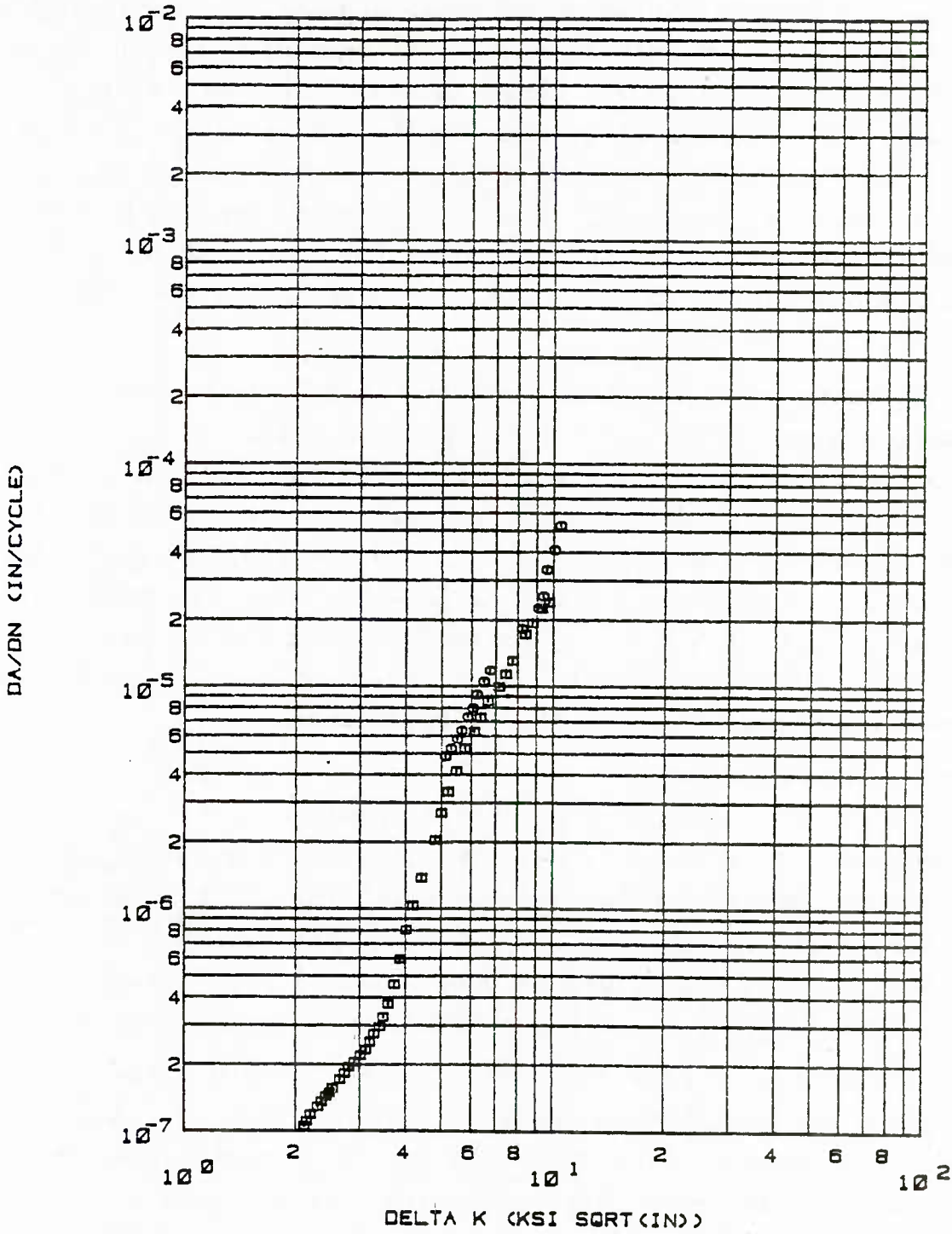


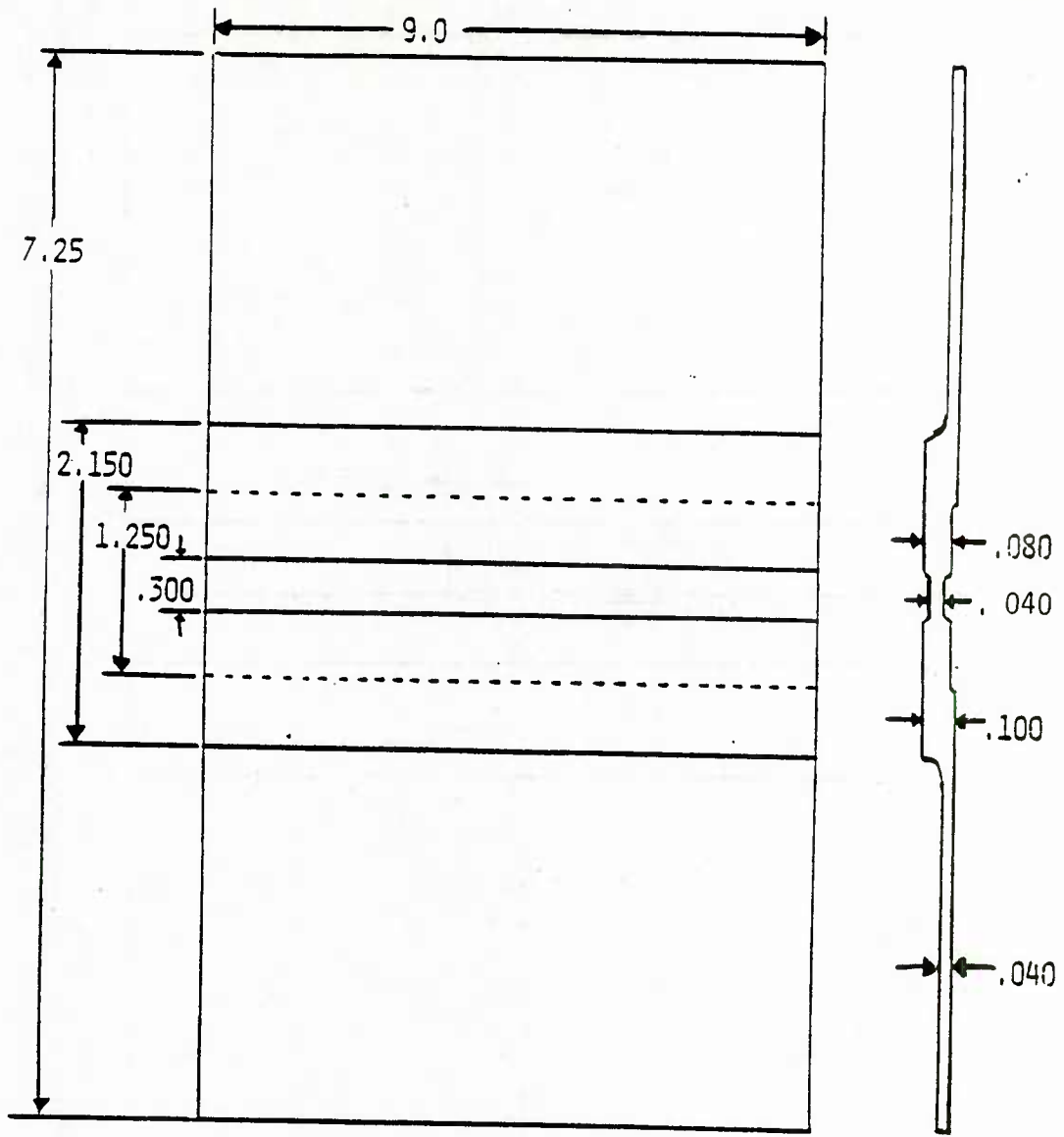
Figure 29. Crack Growth Rate Data for 7075-T651 Aluminum, R = 0.5

The first gage design fabricated was gage Type 1 which was shown in Figure 5. Due to the rather thin center section of this gage, it was decided to do chemical etching to obtain the final gage shape. The initial mechanical machining set the general profile within 0.020 inches and then the gages were chemically etched to the final dimensions. In order to facilitate both the machining and the chemical processing, a four gage panel, shown in Figure 30, was used. This was then cut apart after the final shape was achieved. The length of the panel included end tabs for precracking gripping. After precracking, these were cut off.

The center crack initial flaw was 0.200 inches long. Originally, it was planned to drill a 9 mil central hole, make a 8 to 10 mil wide sawcut 10 to 12 mils long on each side, and then grow to the desired 0.200 inches using a load shedding loading schedule. When this procedure did not yield symmetrical cracks easily, it was decided to utilize an electrical-discharge-machining (EDM) technique. The design of the EDM notch is shown in Figure 31. The total length was later changed to 0.162 inches to allow easier growth of the final crack length.

The asymmetric character of these gages presented a problem during precracking. The cracks initiate on the back side (adjacent to carrier) first. To obtain a straight through-the-thickness crack front, a four-point bending fixture was used. This worked well with the small Type 1 gage but became less satisfactory with the heavier and more asymmetric Type 2 and Modified Type 2 gages.

The fabrication procedure for the Type 2 and Modified Type 2 gages was modified to permit easier precracking. A symmetric preliminary shape which had the final central section dimensions but not the end dimensions was made as shown in Figure 32 for the Modified Type 2 gage design. This blank was then EDM notched and precracked in simple tension and then the



All Dimensions Inches
Final Thicknesses Shown

Figure 30. Dimensions of Gage Type 1 Four Gage Panel

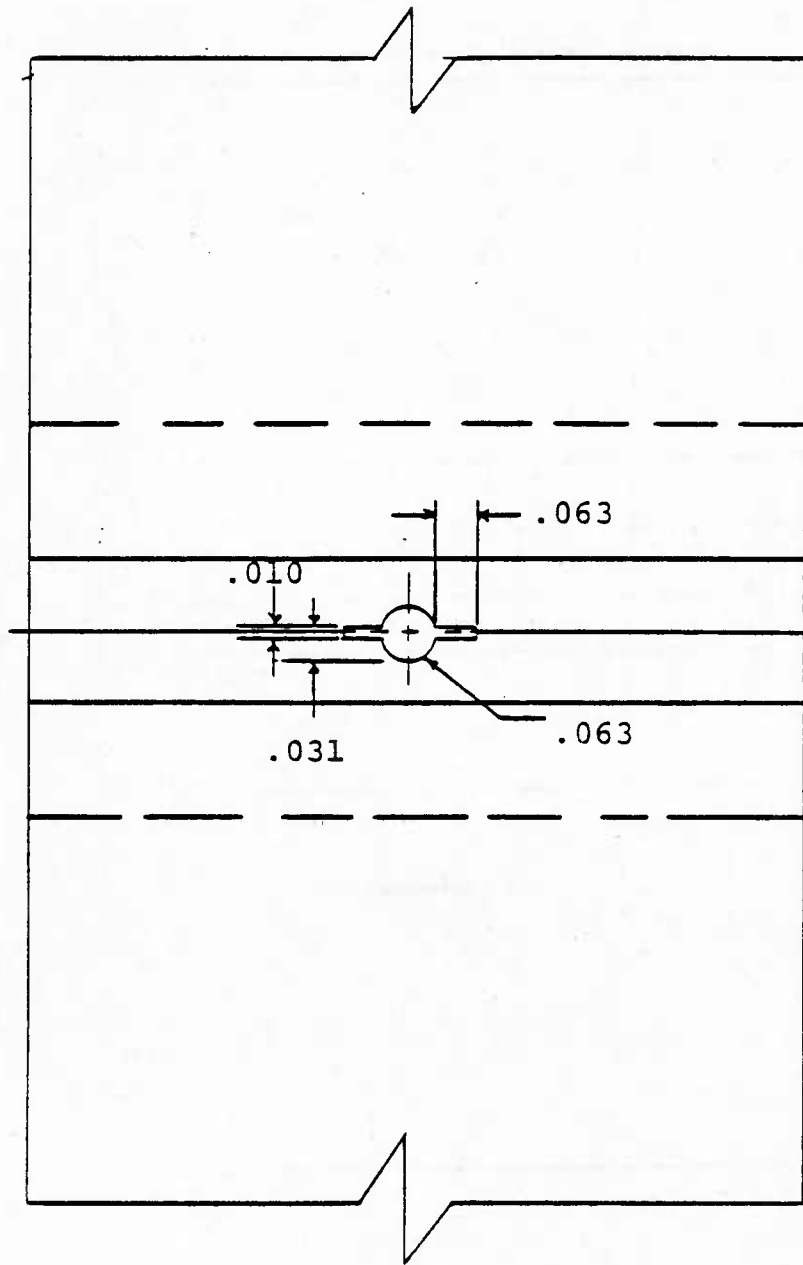


Figure 31. Enlargement of EDM Notch Geometry

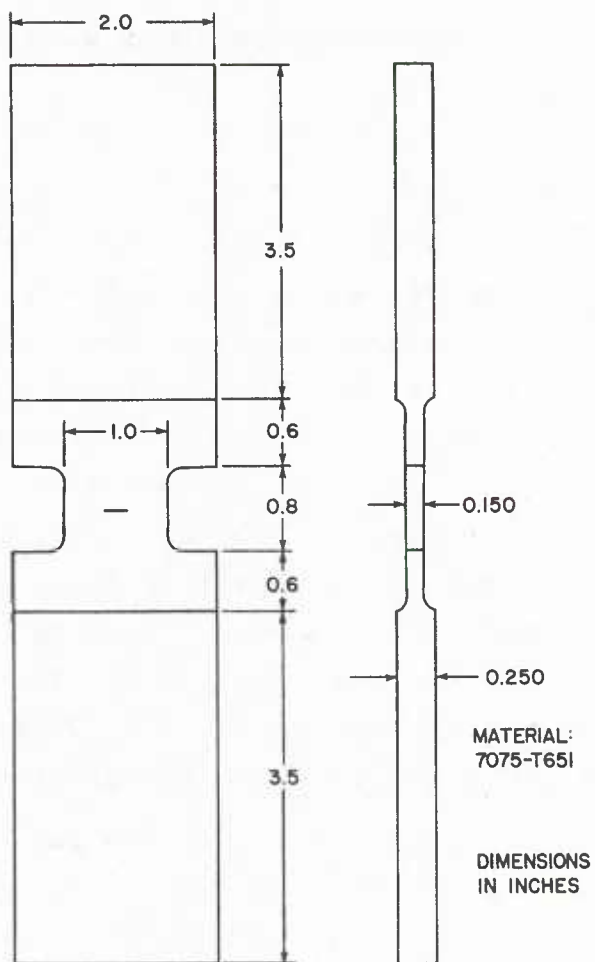


Figure 32. Preliminary Modified Type 2 Gage Shape for Precracking

ends were machined to the final shape. This procedure was used for all of the Modified Type 2 gages and considerably improved the ease of fabrication. Due to the thicker dimensions of the Type 2 and Modified Type 2 gages, they were manufactured entirely by mechanical machining.

5. Gage Installation

The gages were attached to the carriers by adhesive bonding using the structural adhesive FM-73. The bond surfaces were cleaned using the hand phosphor acid anodize (PAA) technique. Each surface was coated with BR-127 primer prior to adhesive application. The FM-73 was cut to size and the gages secured to the carrier, and the assembly was inserted into an oven for the cure cycle. Pressure was applied initially by stacking weights on top of the assembly. This was later changed to the use of a vacuum bag enclosing the assembly. This procedure was then used for the assembly of all test specimens. The University of Dayton also fabricated the specimens tested by Purdue University. Appendix A describes the bonding process in detail.

Figure 33 shows the gage location for the initial tests with the Type 1 gage. Later tests had four gages bonded to each carrier. Figure 34 shows the scheme for identifying the gages. The front was defined as the side with the specimen crack growing to the right.

6. Testing Procedures

The testing was done with the specimens mounted in electro-hydraulic loading machines with hydraulic grips. Anti-buckling fixtures were positioned on each side of the specimens. Micrometer positioned traveling microscopes were used to read the length of each crack. Figure 35 shows the arrangement used for the four gage specimen tests.

The spectrum tests were conducted under computer control. Crack length measurements were made at approximately each 0.025 inch increment of carrier crack growth to show any changes in the growth characteristics of the gages.

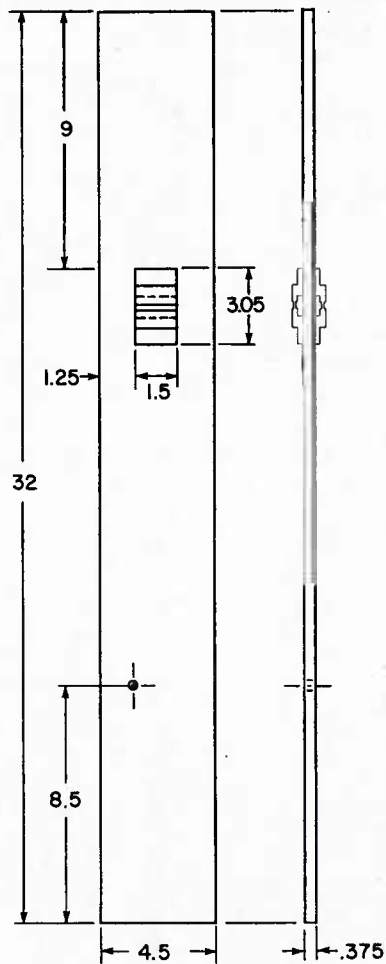


Figure 33. Assembled Test Article (Crack Growth Gages Attached to Carrier) for Development Tests

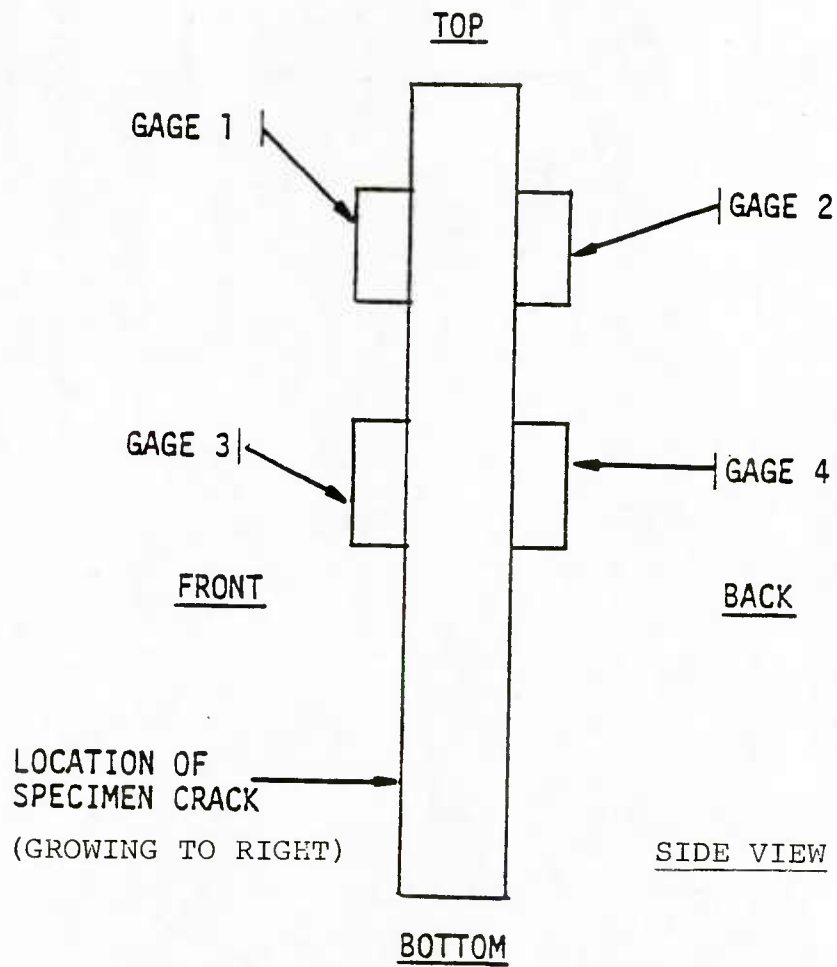


Figure 34. Scheme for Numbering Crack Growth Gages Attached to a Carrier Specimen

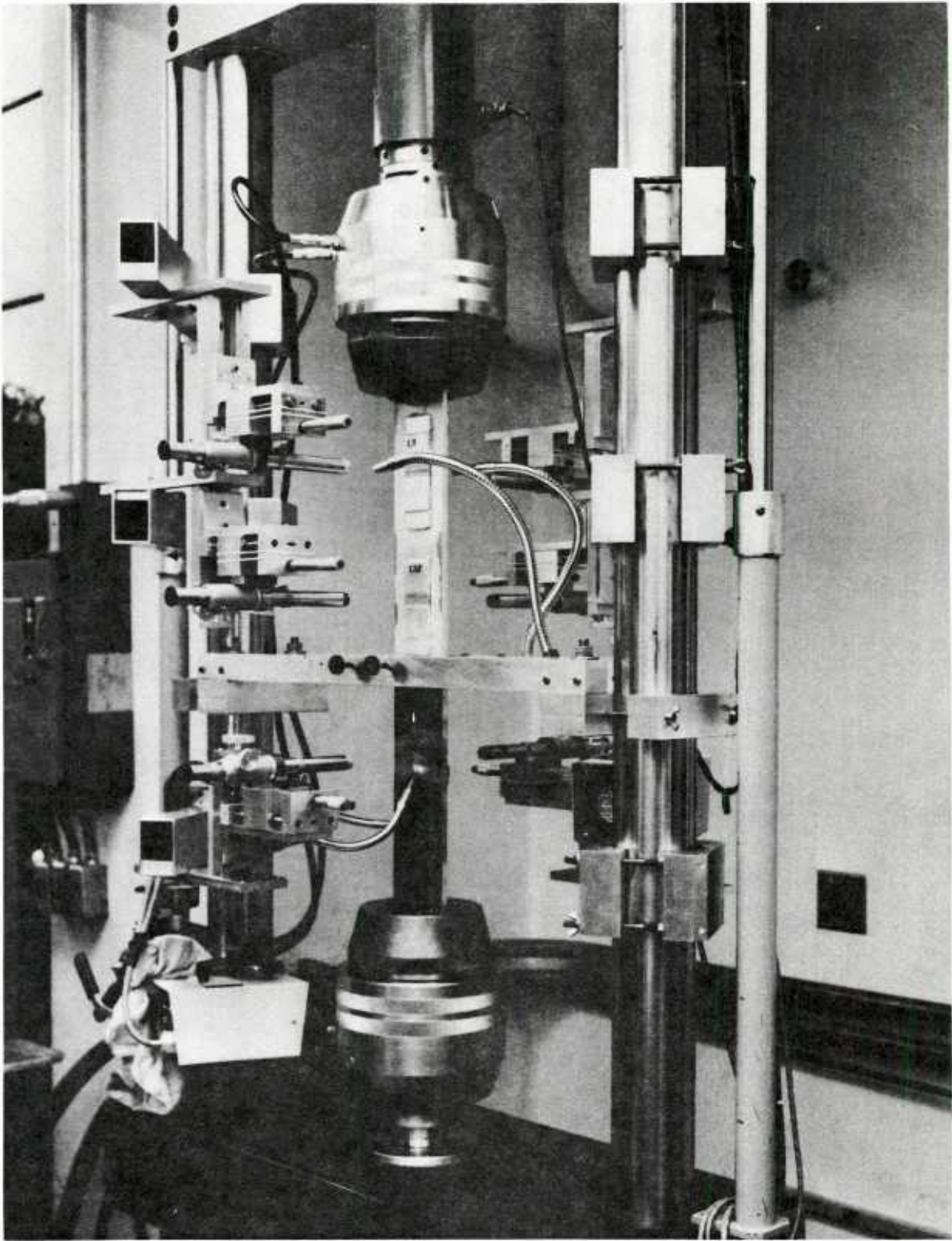


Figure 32. View of an Installed Test Specimen

SECTION V
PRESENTATION AND DISCUSSION OF TEST RESULTS

This section describes the tests conducted and discusses the results. Two types of tests were run: constant amplitude and variable amplitude (or spectrum) tests. Plots of the data from each test are presented in Appendix B.

The first tests were conducted with crack growth Type 1 gages and used variations of spectra developed by McDonnell Aircraft Company [35] for F-4 aircraft fatigue testing. Two gages were mounted back-to-back on the carrier specimen. Later tests were conducted on the Type 2 gage and the Modified Type 2 gage using some of the same spectra for comparison purposes.

A series of constant amplitude tests were conducted using the Type 2 gage and the Modified Type 2 gage. Four gages were mounted on each carrier specimen, two on each side.

Finally, three tests were conducted with the Modified Type 2 gage using variations of spectra by Northrop Corporation for T-38 analysis [26].

The University of Dayton also conducted the three T-38 spectra tests using the side-grooved gage developed by Purdue University. These results are reported in Volume II of this report.

Table 5 lists the tests and their parameters which were conducted at the University of Dayton.

1. Initial Spectrum Tests

Tests 001 through 009 listed in Table 5 were conducted with the F-4 mild, baseline, and severe spectra and five variations of the baseline spectra. The variations were:

- a. High Level - load multiplier increased from 35,000 lb. to 43,000 lb. (test 004).

TABLE 5
SUMMARY OF CRACK GROWTH GAGE TESTING AT UDRI

TEST NO.	TYPE	MAX. STRESS KSI	STRESS RATIO	CARRIER I.D.	GAGE 1		GAGE 2		GAGE 3		GAGE 4		COMMENT
					I.D.	TYPE	I.D.	TYPE	I.D.	TYPE	I.D.	TYPE	
001	SPECT.	23.4	-	002		1		1	-		-		F-4 BASELINE
002	"	"	-	003		1		1	-		-		F-4 SEVERE
003	"	"	-	004	18	1	15	1	-		-		F-4 MILD
004	"	28.7	-	005	5	1	12	1	-		-		F-4 HI-BASELINE
005	"	17.9	-	006	31	1	30	1	-		-		F-4 LO-BASELINE
006	"	23.4	-	007	29	1	28	1	-		-		F-4 BASELINE (DUP)
007	"	"	-	008	13	1	11	1	-		-		F-4 BASELINE (MOD 1)
008	"	23.4	-	009	35	1	34	1	-		-		F-4 BASELINE (MOD 2)
009	"	15.9	-	062	32	1	33	1	-		-		F-4 BASELINE (MOD 3)
010	"	23.4	-	053	L-17	2	L-19	2	-		-		F-4 BASELINE
011	"	28.7	-	051	L-4	2	L-16	2	-		-		F-4 HI-BASELINE
012	"	23.4	-	064	L-24	2	L-25	2	-		-		F-4 SEVERE
013	"	"	-	058	L-20	2	L-22	2	-		-		F-4 BASELINE (MOD 2)
014	"	"	-	010	M-10	2M	M-8	2M	-		-		F-4 BASELINE
015	"	28.7	-	034	M-12	2M	M-11	2M	-		-		F-4 HI-BASELINE
	NOTE:	TEST NOS. 016, 017, 018 NOT USED											
019	C.A.	16.0	-.1	042	M-36	2M	M-42	2M	M38	2M	M46	2M	
020	"	"	+.1	032	L-13	2	L-18	2	L-21	2	L23	2	
021	"	"	+.3	048	M+8	2M	M26	2M	M19	2M	M27	2M	
022	"	25.0	-.1	054	L-1	2	L-5	2	L-26	2	L-27	2	
023	"	"	+.1	067	L-2	2	L-7	2	L-8	2	L-9	2	
024	"	"	+.3	047	M-13	2M	M17	2M	M15	2M	M-16	2M	
	NOTE:	TEST NOS. 025, 026 CONDUCTED BY PURDUE UNIV.											
025	C.A.	VAR	-	029	M41	2M	M50	2M	M55	2M	M56	2M	LOAD TRANSFER
026	C.A.	VAR	-	030	M31	2M	M37	2M	M43	2M	M44	2M	LOAD TRANSFER

TABLE 5 (Continued)
SUMMARY OF CRACK GROWTH GAGE TESTING AT UDRI

TEST NO.	TYPE	MAX. STRESS KSI	STRESS RATIO	CARRIER I.D.	GAGE 1		GAGE 2		GAGE 3		GAGE 4		COMMENTS
					I.D.	TYPE	I.D.	TYPE	I.D.	TYPE	I.D.	TYPE	
	NOTE:	TEST NOS. 027-034 USED BY PURDUE UNIVERSITY TEST NOS. 035-040 NOT USED											
041	C.A.	16.0	- .1	063	L29	2	L-12	2	M-4	2M	M-3	2M	50% OVERLOAD
042	"	"	+ .1	041	L-6	2	L-15	2	L-3	2	L-10	2	"
043	"	"	+ .3	044	M28	2M	M32	2M	M29	2M	M33	2M	"
044	"	25.0	- .1	049	M52	2M	M45	2M	M53	2M	M51	2M	30% OVERLOAD
045	"	"	+ .1	069	L-11	2	L-14	2	L-28	2	L-30	2	"
046	"	"	+ .3	045	M34	2M	M40	2M	M39	2M	M41	2M	"
	NOTE:	TEST NOS. 047-052 USED BY PURDUE UNIVERSITY TEST NOS. 053, 056, 059 NOT USED											
054	SPECT.	30.0	-	057	M20	2M	M23	2M	M21	2M	M25	2M	T-38 ATC (MILD)
055	"	"	-	035	DSG4-24	3	DSG4-23	3	SSG4-31	3	SSG4-24	3	T-38 ATC (MILD)
057	"	"	-	039	M-14	2M	M-24	2M	M-22	2M	M-35	2M	T-38 COMB (BASELINE)
058	"	"	-	038	DSG4-29	3	DSG4-30	3	SSG4-29	3	SSG4-30	3	T-38 COMB (BASELINE)
060	"	"	-	066	M-47	2M	M58	2M	M-48	2M	M-60	2M	T-38 LIF (SEVERE)
061	"	"	-	055	DSG4-34	3	DSG4-37	3	SSG4-32	3	SSG4-34	3	T-38 LIF (SEVERE)
	NOTE:	TEST NOS. 055, 058, 061 DONE BY UNIVERSITY OF DAYTON FOR PURDUE UNIVERSITY - SEE VOL. II FOR TEST RESULTS											

b. Low Level - load multiplier reduced from 35,000 lb to 26,900 lb. (test 005).

c. Low Level Truncation - deleted all cycles having peaks less than 50% of the maximum (test 007).

d. Overload Addition - added a 125% overload every 2,100 cycles after an initial 250,000 cycles (test 008).

e. High Level Truncation - deleted all cycles having peaks greater than 70% of the maximum (test 009).

A composite plot of the gage to structure transfer functions for these tests is shown in Figure 36. The gage crack length used was an average of the front and back gages. As can be seen from the plots in Appendix B, the two gages showed very little variation between the two sides.

An evaluation of the tracking ability of the gage was made in two ways. The ability to rank the severity of different load spectra is a prime requirement of an IAT device. Table 6 summarizes the ranking capability of the Type 1 gage.

In general, the gage ranks the spectra similar to the structure. However, there is one exception. The baseline with 125% overload, Test 008, is not ranked correctly by the gage. This test was run by applying the baseline spectrum until the structure crack reached approximately 0.250 inches and then inserting the overload every 100 hours repeat thereafter. While both the structure and the gage showed the effect by a change in the crack growth rate, the growth of the gage crack was retarded much more than the structural crack. This is attributed to the difference in thickness between the structure and the gage. Such a characteristic is unacceptable in a tracking device.

To further investigate the response of the gage to spectrum loading, the effect of the different transfer functions was determined. This was done by assuming that a structural time period of interest, such as a critical crack length and an inspection time, were related to the gage crack through the

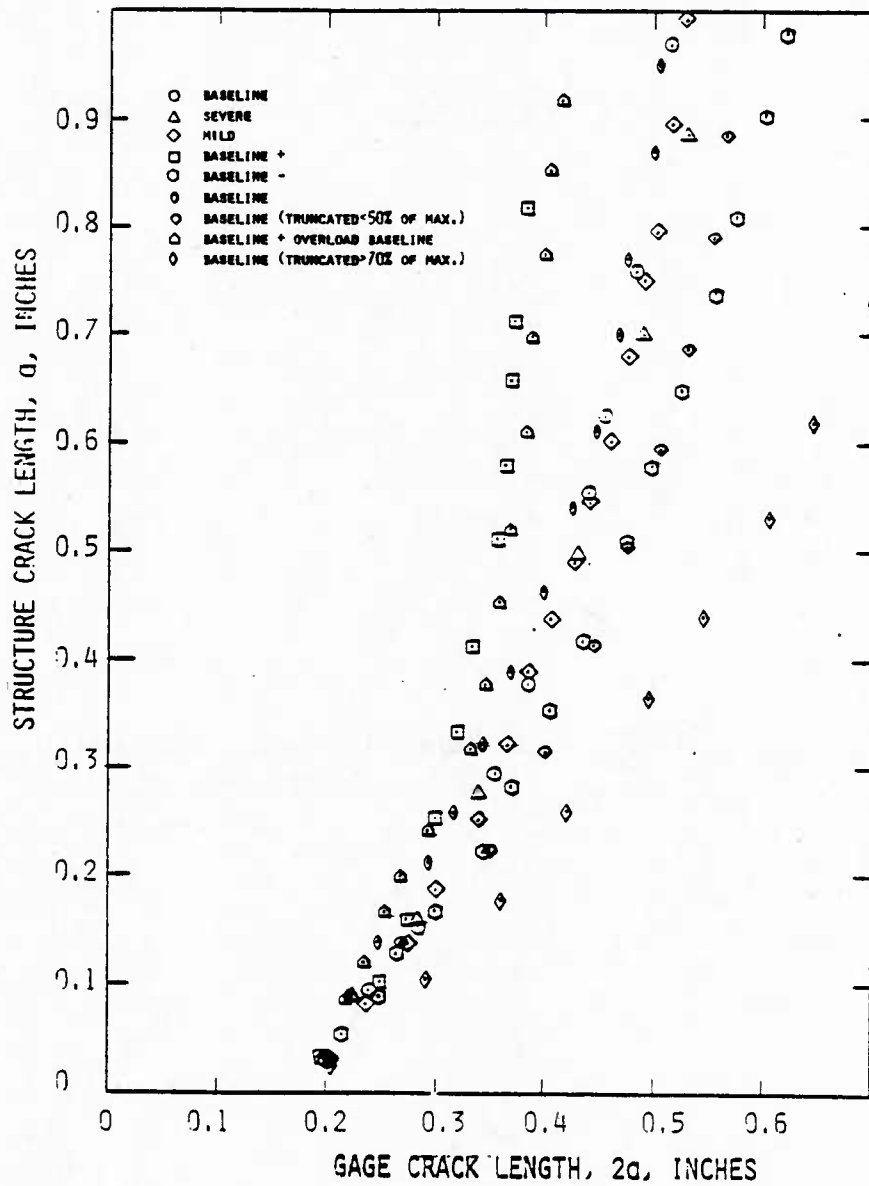


Figure 36. Transfer Function for Gage Type 1 Initial Tests

TABLE 6
SPECTRUM RANKING CAPABILITY
OF THE TYPE 1 GAGE

<u>Rank</u> (1)	<u>Structure</u> (2)	<u>Gage</u> (2)
1	009	009
2	004	002
3	002	004
4	008	007
5	007	006
6	006	001
7	001	008
8	003	005
9	005	003

NOTE: (1) Rank is from fastest to
slowest growing crack.
(2) Entry is test number.

baseline stress spectrum. The structure crack lengths at this gage crack for the other spectra were then determined. Normalizing these with the baseline structure crack readily shows the effect of a different stress spectra. Ratios less than 1.0 are conservative, i.e., the predicted crack is longer than the actual crack. Ratios larger than 1.0 are non-conservative. The predicted crack is shorter than the actual crack. This exercise was done for two gage crack lengths. The results are presented in Table 7. For tests 004 and 008, the results are non-conservative. The results of test 009, while conservative, are considerably more so than the other tests. This raises a question of the efficiency of the gage since if the gage crack is growing much faster than the structure crack, a penalty of cost related to excessive inspection may be incurred.

On the basis of these tests, it was decided that additional spectra tests should be done with the Type 2 gage before proceeding with the constant amplitude tests.

The Type 2 gage is larger than the Type 1. It was designed to have a higher crack growth rate than the Type 1 and because of its thicker cracked section, should show less of the thick-thin retardation effect than the Type 1 gage.

Rather than run all of the tests on the Type 2 gage that were run on the Type 1 gage, it was decided to run only the following spectra:

<u>Test No.</u>	<u>Spectra</u>
010	Baseline
011	High Level Baseline
012	Severe
013	Baseline with Overload

These included the two which were non-conservative and the baseline for the reference and the severe as an additional check on the ranking ability of the gage.

TABLE 7
INITIAL TEST DATA COMPARISON (TYPE 1 GAGE)

<u>Test</u>	<u>Predicted Structural Crack Length</u> <u>Baseline Crack Length</u>	
	For: $2a_G = 0.300$	For $2a_G = 0.400$
001 (B/L)	1.000	1.000
002 (Severe)	0.900	0.983
003 (Mild)	0.975	0.983
004 (B/L ⁺)	1.200*	2.398*
005 (B/L ⁻)	0.875	0.803
007 (TR < 50%)	0.810	0.767
008 (B/L +O/L)	1.250*	1.859*
009 (TR > 70%)	0.625	0.588

a_s = Structure Crack Length, Inches

$2a_G$ = Gage Crack Length, Inches

* = Unconservative

Figure 37 presents the data from these tests. The ranking capability of this gage design is similar to the Type 1 gage and is shown in Table 8.

Comparisons of the gage crack growth plots of Type 1 and Type 2 gages in Appendix B show that the Type 2 did grow faster than the Type 1 gage. Test data comparison of the ability to give conservative tracking results is shown in Table 9. While there is still a non-conservative tendency in the high level baseline spectrum, it is not as pronounced as the Type 1 gage. It can be inferred that the thicker gage has reduced the thick-thin problem.

The crack growth data for the structure, i.e., the radial-through-crack at a hole, was used to evaluate the spectrum analysis program. This program computes the crack growth rate as a function of the maximum stress intensity factor. The test data was converted to this form for comparison. Figure 38 shows a comparison between three sets of data and a power-law fit to an analysis of the low-level baseline stress spectrum. Note that this is not a fit to the data but a fit to crack growth rates obtained from a cycle-by-cycle application of the stress spectrum to the test specimen crack geometry and material properties using the mini-block approach [34].

Based on these results, it was concluded that the analysis procedure is capable of modeling the spectrum crack growth characteristics.

As a result of these tests, it was decided not to do any further testing with the Type 1 gage and to continue the constant amplitude testing with the Type 2 gage.

2. Constant Amplitude Tests

Constant amplitude tests were conducted first using the Type 2 gage mounted four gages on a carrier. Five tests were conducted with this configuration and one test was conducted with two Type 2 gages and two Modified Type 2 gages.

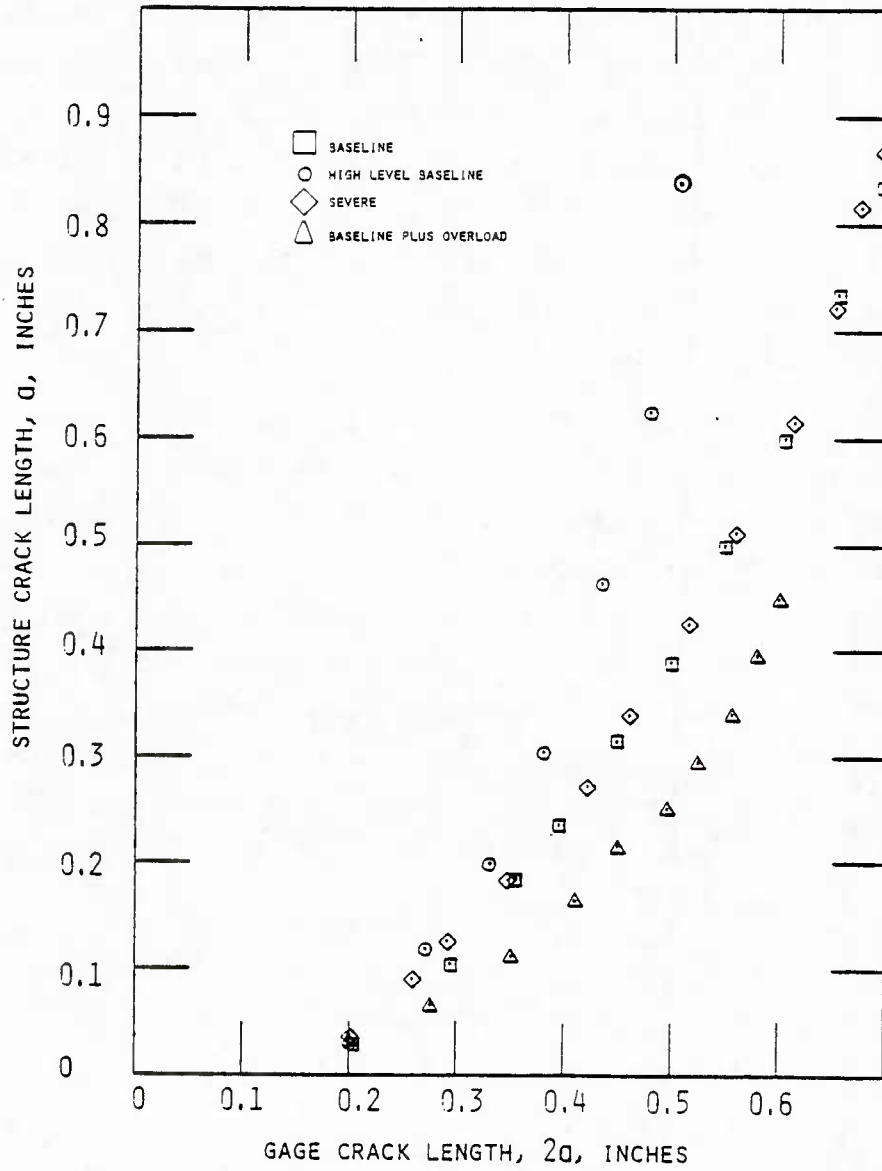


Figure 37. Transfer Function for Gage Type 2 Initial Tests

TABLE 8
SUMMARY OF SPECTRUM RANKING
FOR GAGE TYPE 2 TESTS

<u>Rank</u> ⁽¹⁾	<u>Structure</u> ⁽²⁾	<u>Gage</u> ⁽³⁾
1	011	012
2	012	011
3	010	010
4	013	013

(1) Rank is from fastest to slowest growing crack.

(2) Entry is test number.

TABLE 9
INITIAL TEST DATA COMPARISON
(TYPE 2 GAGE)

<u>Test</u>	<u>Predicted Structural Crack Length</u> <u>Baseline Crack Length</u>	
	For: $2a_g = 0.300$	For: $2a_g = 0.400$
010 (B/L)	1.000	1.000
011 (B/L+)	1.500*	1.620*
012 (Severe)	0.910	1.09

a_s = Structure crack length, inches.

$2a_g$ = Gage crack length, inches.

* = Unconservative

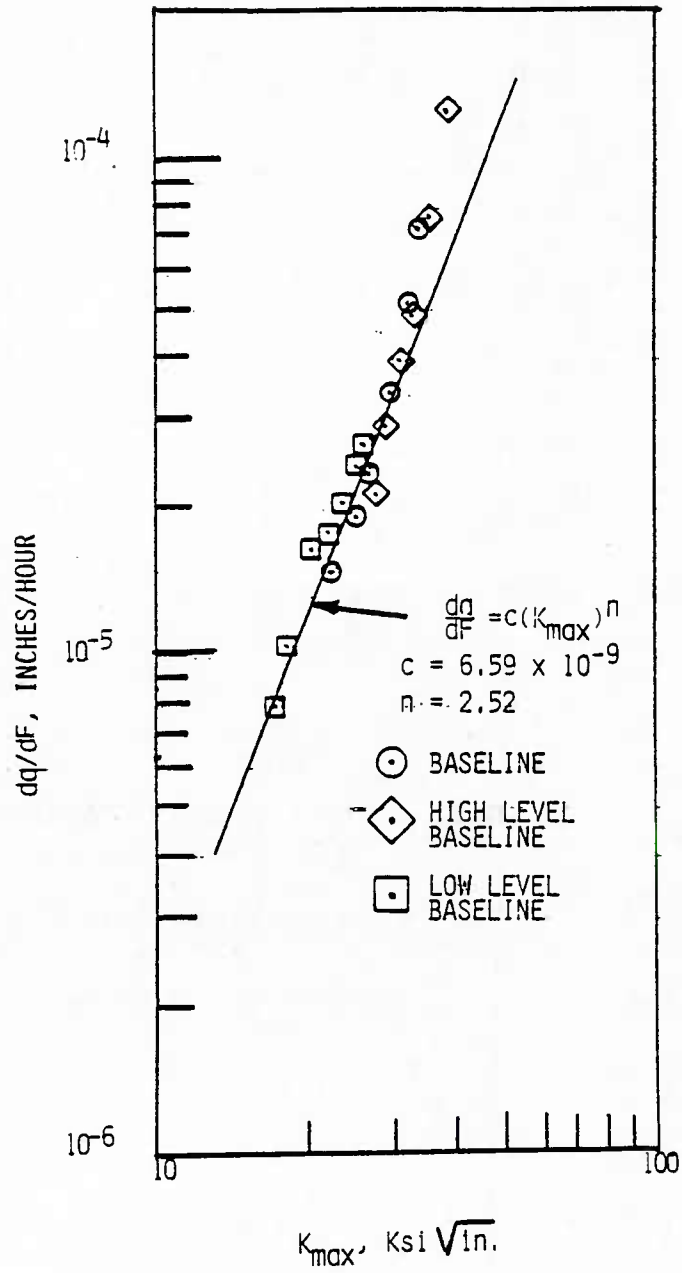


Figure 38. Crack Growth Rate Versus Maximum Stress-Intensity Factor: Analysis and Test.

These tests were:

<u>TEST</u>	<u>GAGE</u>	<u>DESCRIPTION</u>
020	Type 2	16 Ksi MAX, R = 0.1
022	Type 2	25 Ksi MAX, R = -0.1
023	Type 2	25 Ksi MAX, R = 0.1
041	[Type 2]	16 Ksi MAX, R = -0.1
	[modified Type 2]	(with 150% overload cycle)
042	Type 2	16 Ksi MAX, R = 0.1
		(with 150% overload cycle)
045	Type 2	25 Ksi MAX, R = 0.1
		(with 130% overload cycle)

The crack growth data from these tests is presented in Appendix B. Figure 39 presents a summary of the transfer functions for the faster growing gage from these tests. The significant result here is that the results of the overload tests still show evidence of different retardation effects between the gage and the structure. Particularly note the result of test 045. There is also still a considerable spread on the transfer functions for the various loading conditions.

At this point a redesign of the gage was made resulting in the Modified Type 2 gage. The characteristics of this gage were discussed in Section III.

The Modified Type 2 gage was initially subjected to two spectrum tests to see how it would react compared to the Type 2 gage. The F-4 baseline spectrum and the F-4 high level baseline spectrum were run as tests 014 and 015, and compared with tests 010 and 011. Figures 40 and 41 show the transfer functions for these tests. On the basis of the improvement shown in these tests, it was decided to do the remainder of the tests with the Modified Type 2 gage.

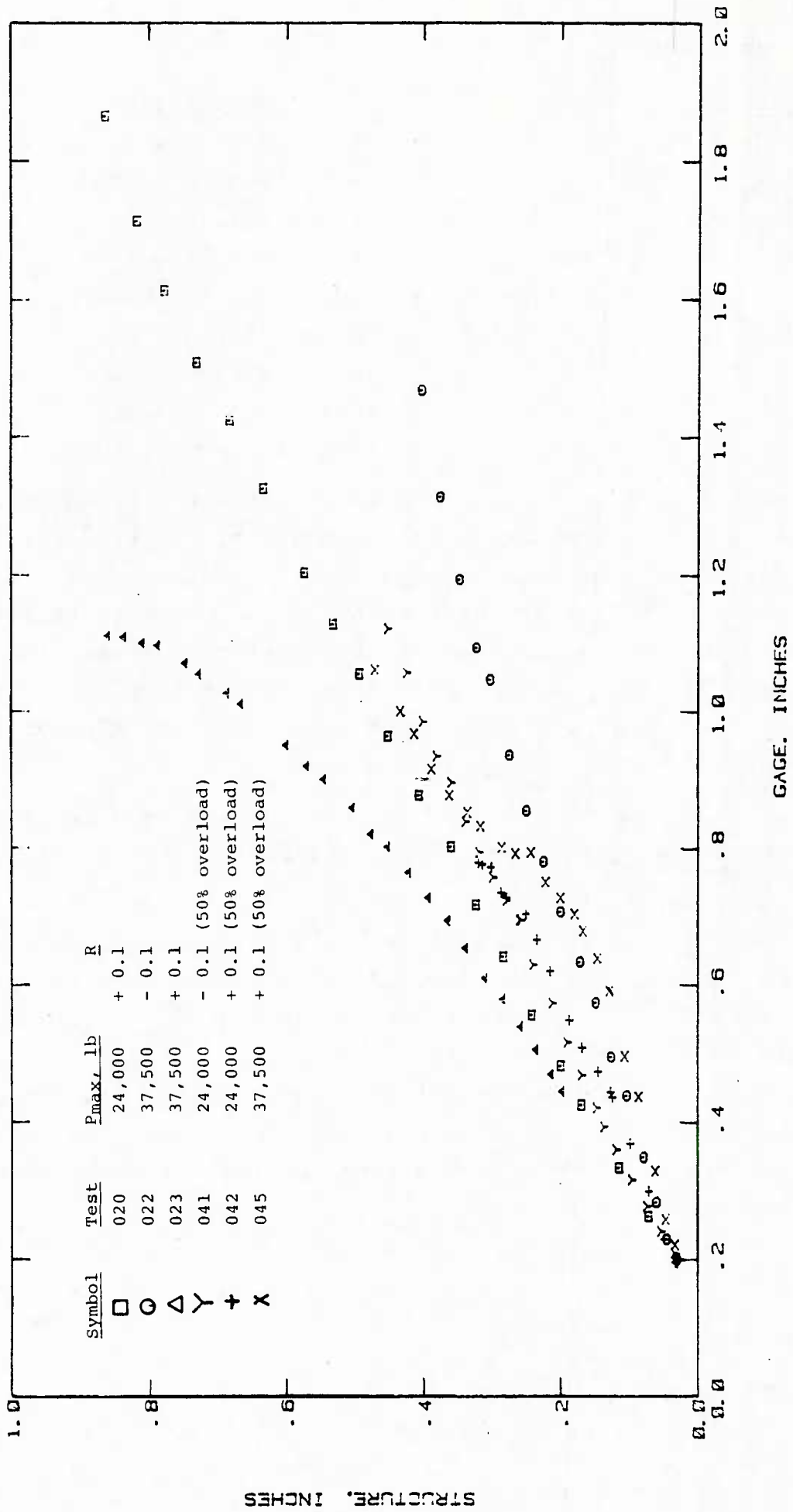


Figure 39. Transfer Function for Gage Type 2 Constant Amplitude Tests

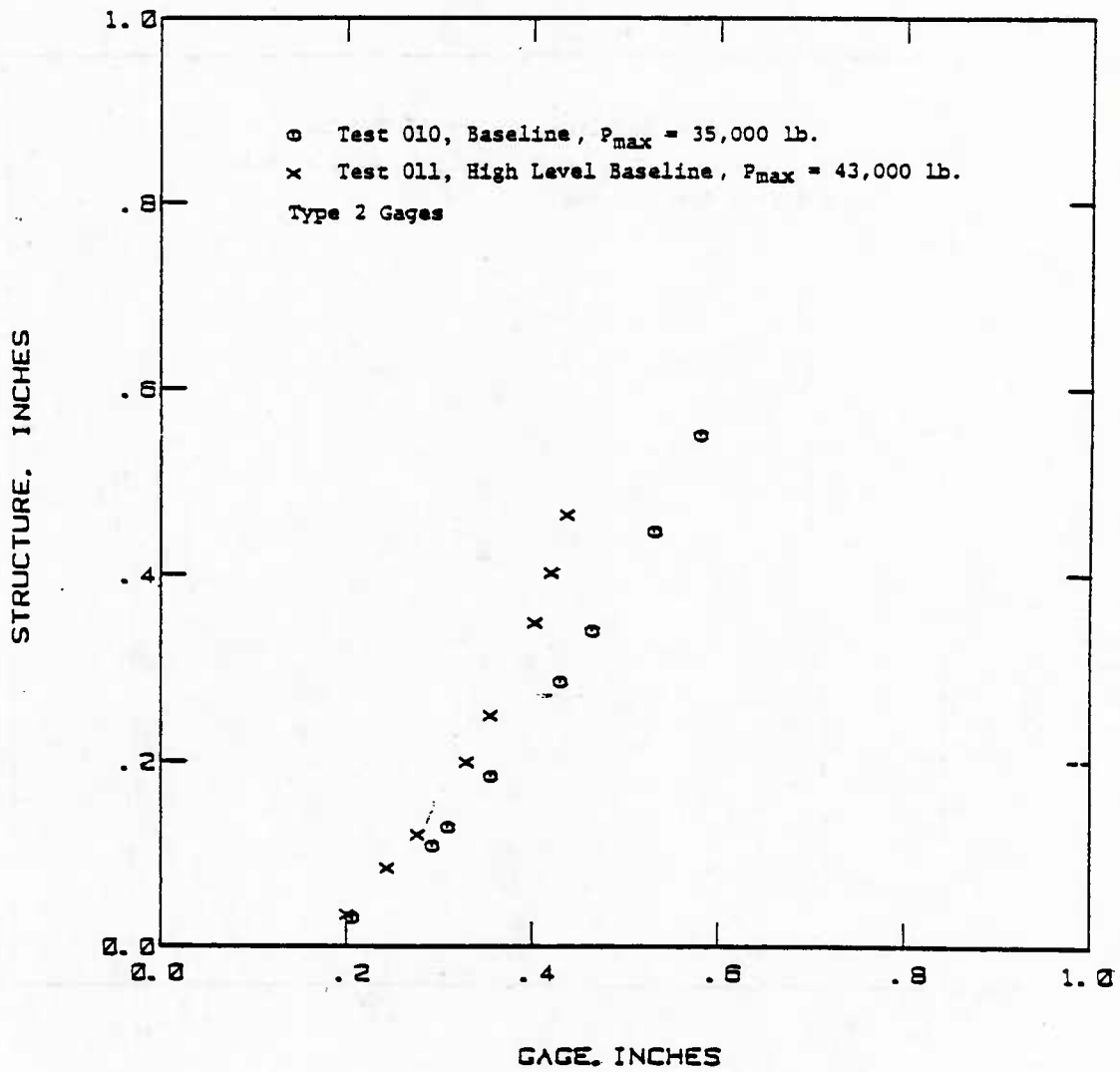


Figure 40. Comparison of Spectra Transfer Functions, Type 2 Gages - Tests 010 and 011.

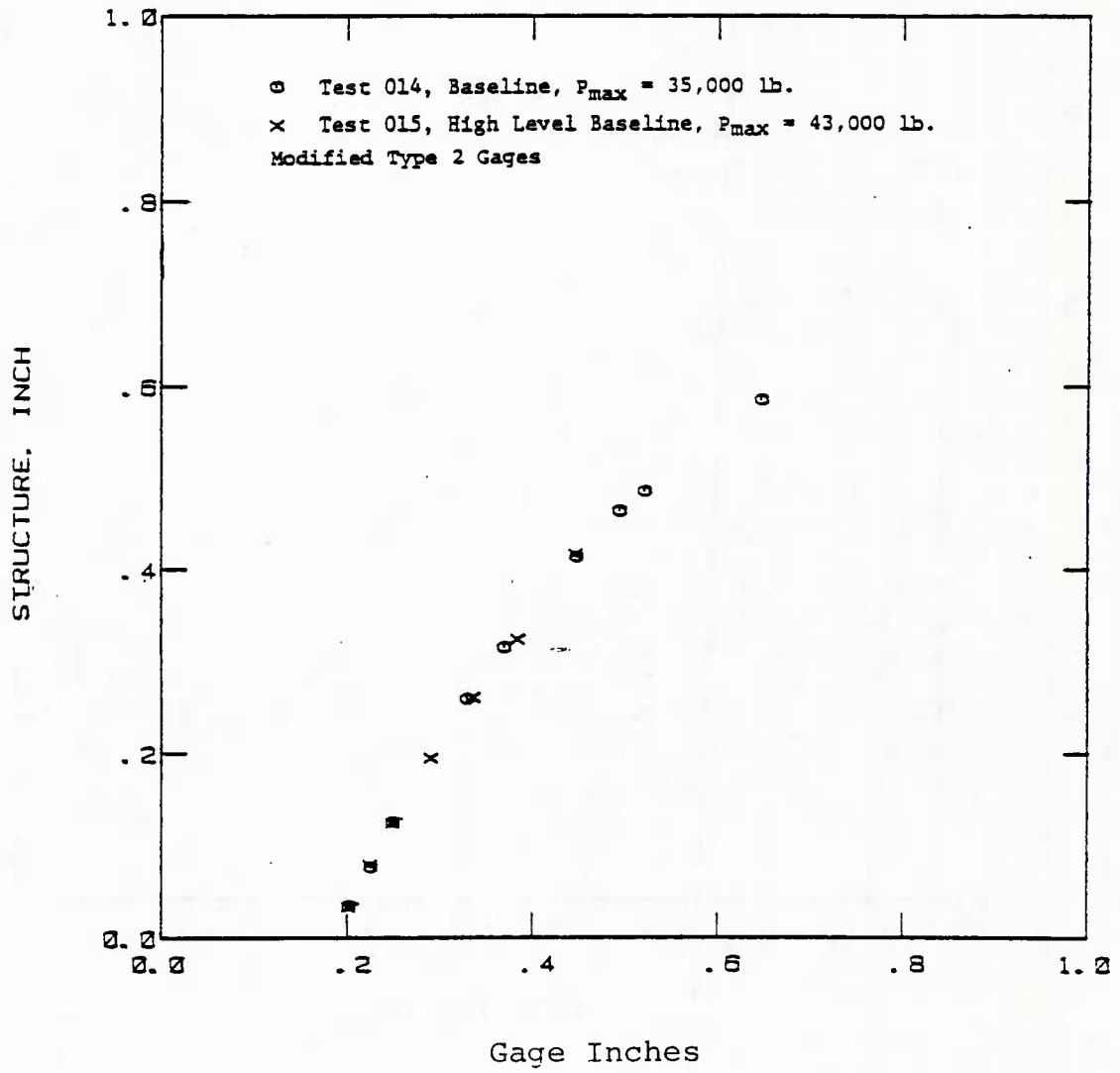


Figure 41. Comparison of Spectra Transfer Functions, Modified Type 2 Gages - Tests 014 and 015

The remainder of the constant amplitude tests were run as follows:

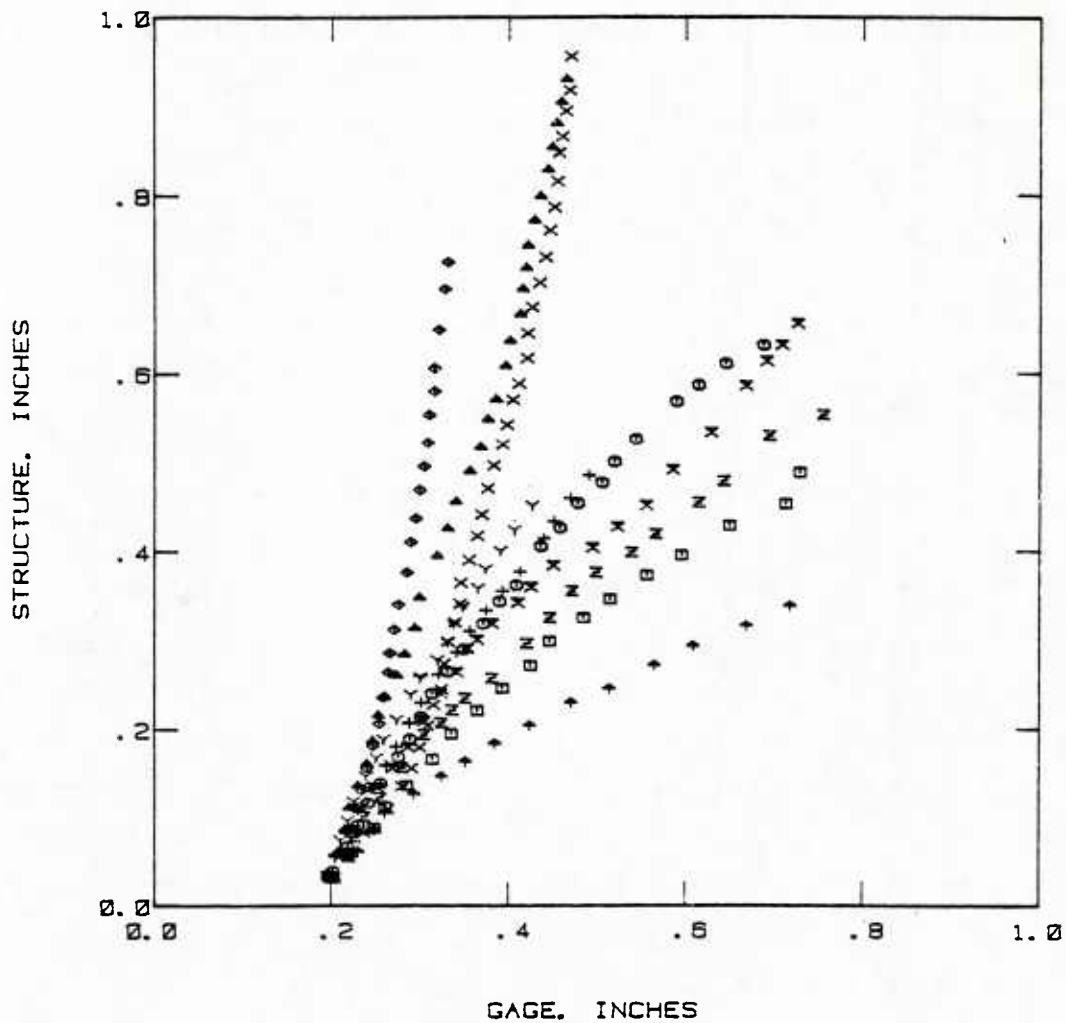
<u>TEST</u>	<u>GAGE</u>	<u>DESCRIPTION</u>
019	modified Type 2	16 Ksi MAX, R = -0.1
021	modified Type 2	16 Ksi MAX, R = +0.3
024	modified Type 2	25 Ksi MAX, R = +0.3
043	modified Type 2	16 Ksi MAX, R = -0.1 (with 150% overload cycle)
044	modified Type 2	25 Ksi MAX, R = -0.1 (with 130% overload cycle)
046	modified Type 2	25 Ksi MAX, R = +0.3 (with 130% overload cycle)

A summary of the transfer function for the fastest growing gage for these tests is shown in Figure 42. This figure also includes the results of the T-38 spectrum tests (054, 057, 060) discussed in the next section. Note that there is still a large variation in transfer functions. Section VI will present discussions of the effect of these variations on the tracking capabilities of the crack growth gage as tested on the program.

3. T-38 Spectrum Tests

To provide a realistic test of the crack growth gage as an IAT device, a series of spectrum tests representing mild, baseline, and severe operational usage of a current aircraft were made. The aircraft chosen was the T-38 and current flight-by-flight stress histories were obtained from the T-38 system office at the San Antonio ALC. Two histories were obtained, one from the Air Training Command (ATC) usage, and one from the Lead-In-Fighter (LIF) usage. The ATC is considered a mild usage and the LIF is considered a severe usage. To construct a baseline usage, flights were selected from both usages and combined. Each history represented 1,000 flight hours.

The histories received were normalized and run at a maximum stress of 30,000 psi. In order to stay within the buckling limit of the test specimen, the histories were modified to limit the normalized compressive stress to -0.1 times the maximum stress. Figures 43, 44, and 45 present the transfer



Symbol	Test	P _{max} , lb	R
□	019	24,000	- 0.1
○	021	24,000	+ 0.3
△	024	37,500	+ 0.3
Y	041	24,000	- 0.1 (50% overload)
+	043	24,000	- 0.3 (50% overload)
X	044	37,500	- 0.1 (30% overload)
◇	046	37,500	+ 0.3 (30% overload)
↑	054	45,000	Var. T-38 Mild
⌘	057	45,000	Var. T-38 Baseline
Z	060	45,000	Var. T-38 Severe

Figure 42. Transfer Functions for Modified Type 2 Gage for Constant Amplitude Spectrum Tests

functions and crack growth rates for these three tests. Analysis of these tests in relation to the IAT capabilities of the gage is presented in Section VI.

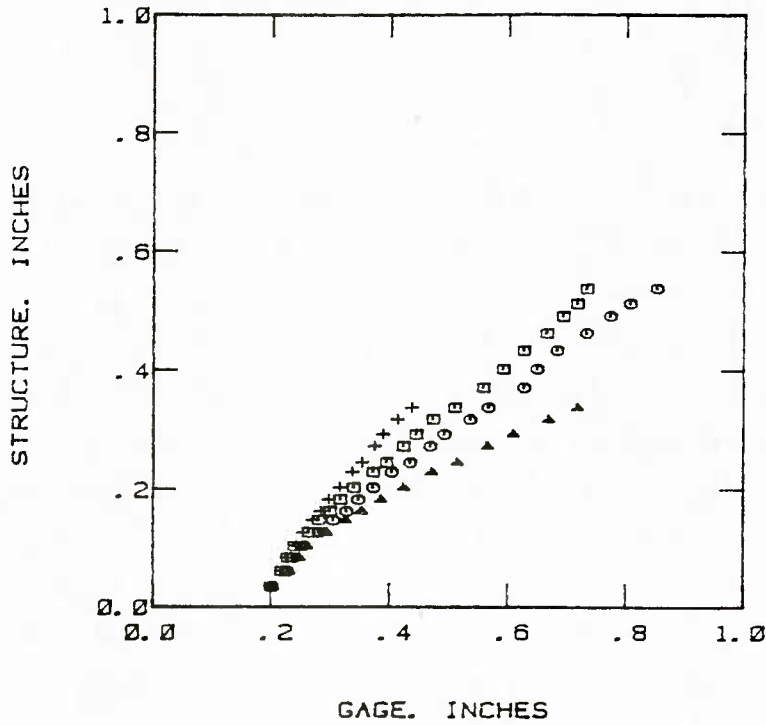
4. Load Transfer Tests

The transfer of load onto the gage from the structure was measured using the modified Type 2 gages. Four uncracked gages were mounted on a carrier specimen and strain gages attached as shown in Figure 46. Static loads were applied in steps from 2.5 Kips to 47.5 Kips. The results are shown in Figure 47. The ratio between the gage strain and the structure strain varied from about 0.82 at the center of the gage to about 1.05 at the edge of the gage. The transfer was constant with load level. The analysis shown in Section III for the modified Type 2 gage (Equation 3.7) presents a stress ratio of 1.16 for an adhesive thickness of 0.008 inches. Measurement of adhesive thickness indicated a mean value of 0.006 inches, and a range of 0.003 to 0.010 inches.

5. Comparison With Analysis

It is essential that the crack growth method used to design the gage provide a good correlation with actual crack growth experience. To determine if the methods used in this program provided this correlation, the T-38 spectra used for test 054, 057, and 060 were processed to obtain a power law fit to the expected crack growth. If the predicted crack growth rates are equivalent to the observed rates then the method can be considered adequate for design use. The results of this analysis are shown in Figures 48, 49, and 50 for the three T-38 spectrum tests. The analysis shows a slightly faster crack growth rate than observed in the tests. This would result in slightly conservative maintenance and inspection scheduling if applied to the development of a force structural maintenance plan.

TEST Ø54 TRANSFER FUNCTION



- X Structure
- O Gage No. 1
- Gage No. 2
- △ Gage No. 3
- + Gage No. 4

TEST Ø54 CRACK GROWTH RATES

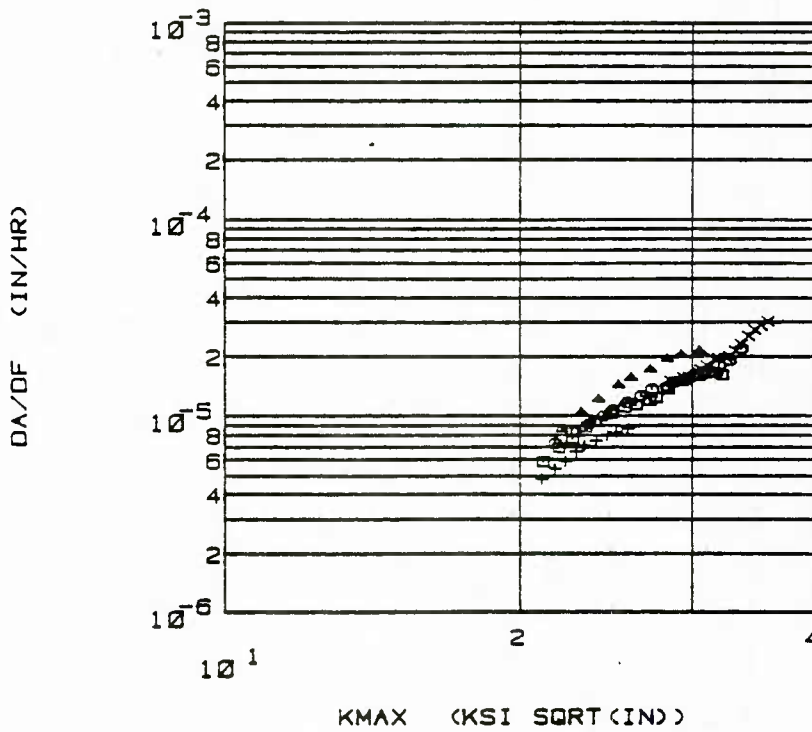
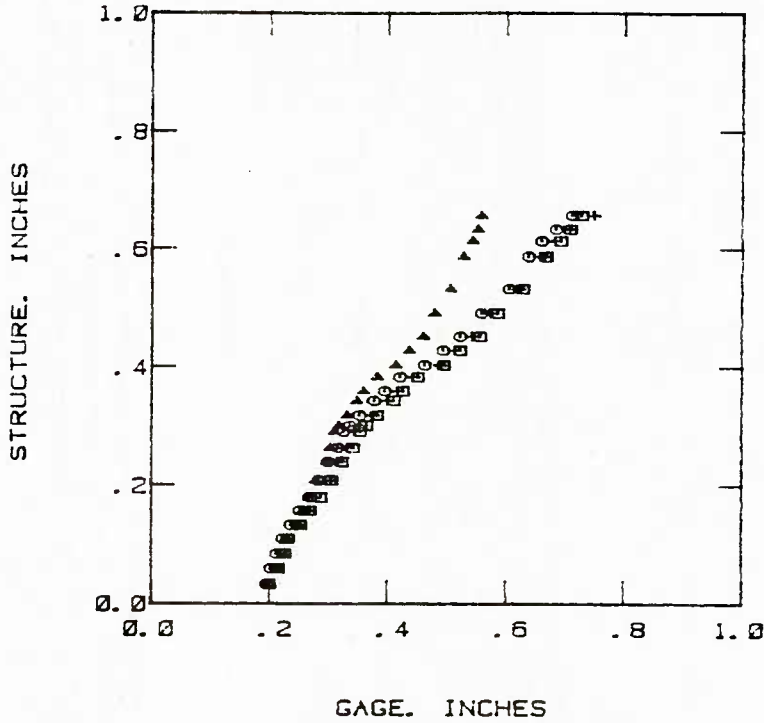


Figure 43. Results of T-38 Mild Spectrum Test - Modified Type 2 Gage

TEST 057 TRANSFER FUNCTION



- X Structure
- Gage No. 1
- Gage No. 2
- △ Gage No. 3
- + Gage No. 4

TEST 057 CRACK GROWTH RATES

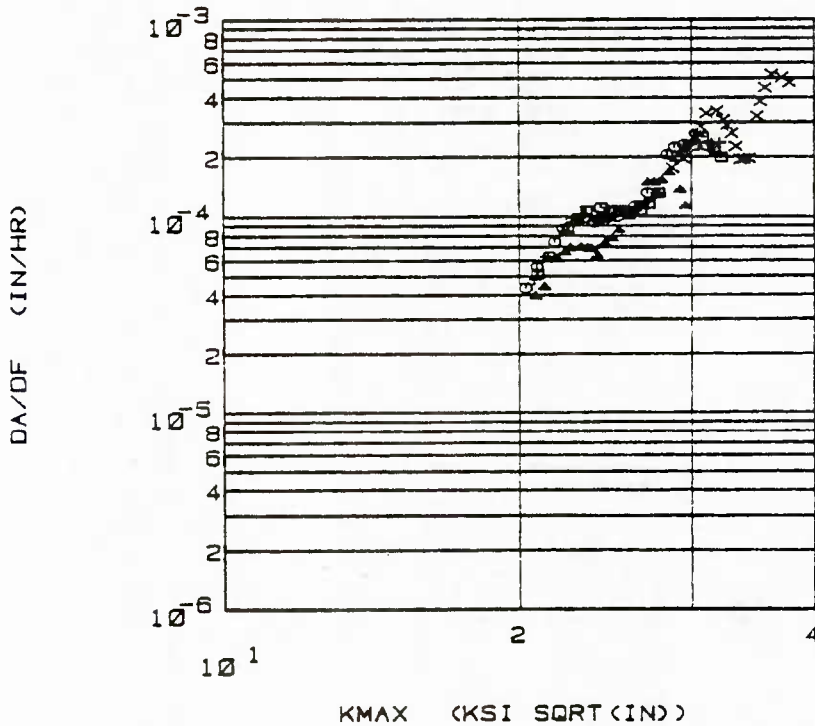
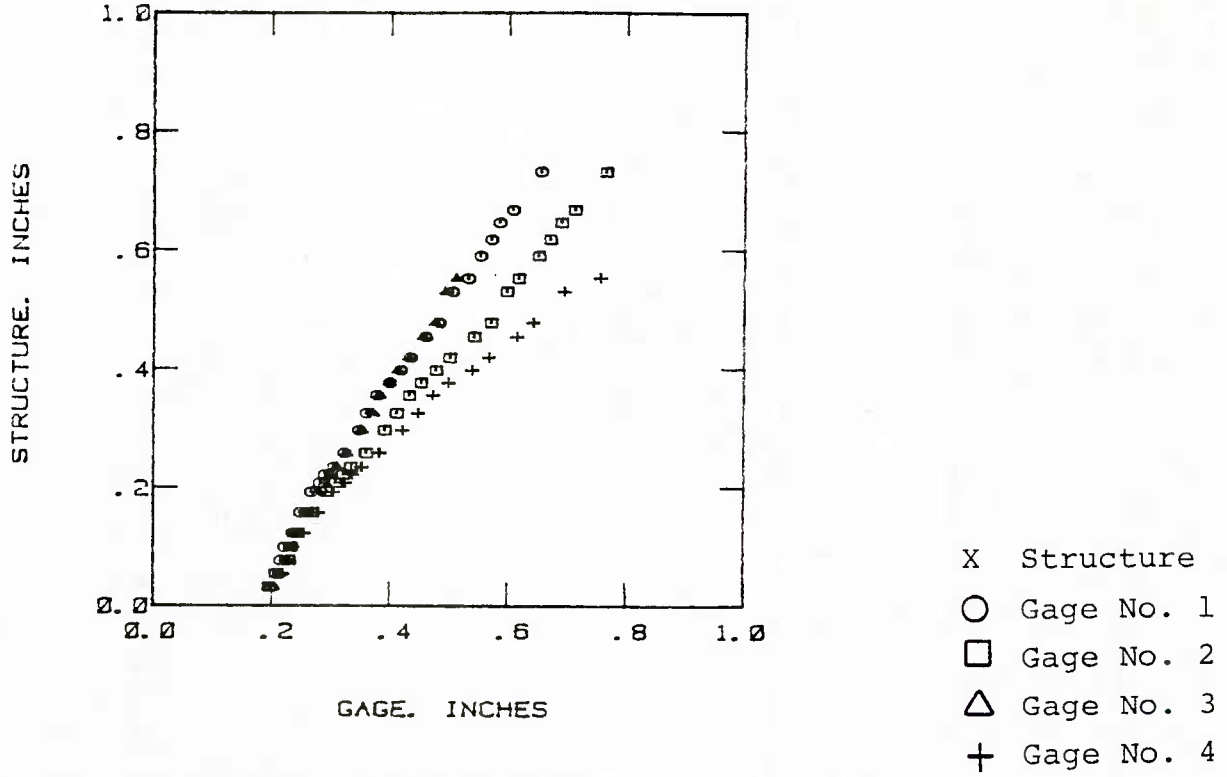


Figure 44. Results of T-38 Baseline Spectrum Test - Modified Type 2 Gage

TEST Ø60 TRANSFER FUNCTION



TEST Ø60 CRACK GROWTH RATES

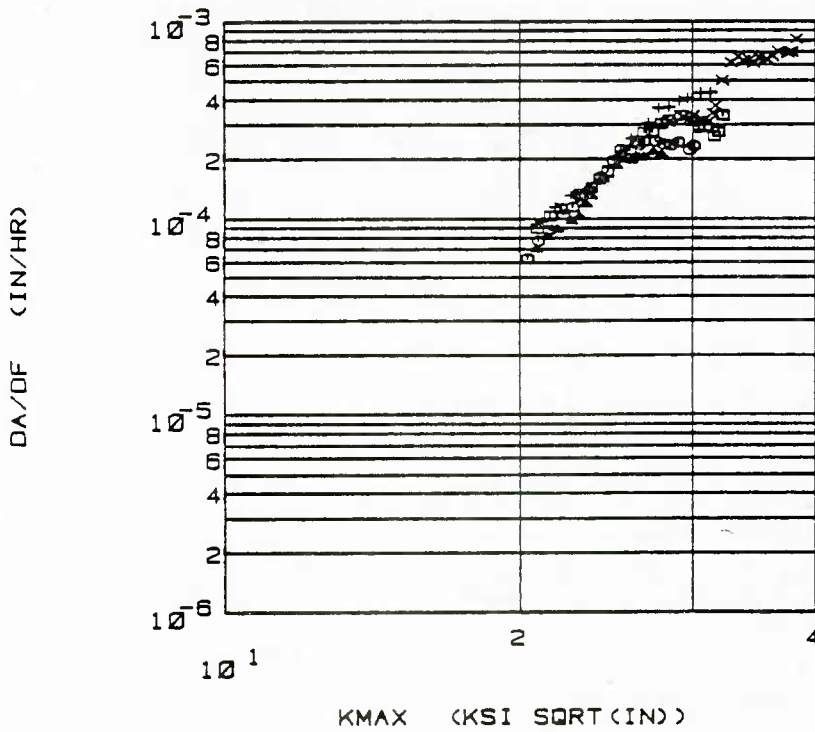
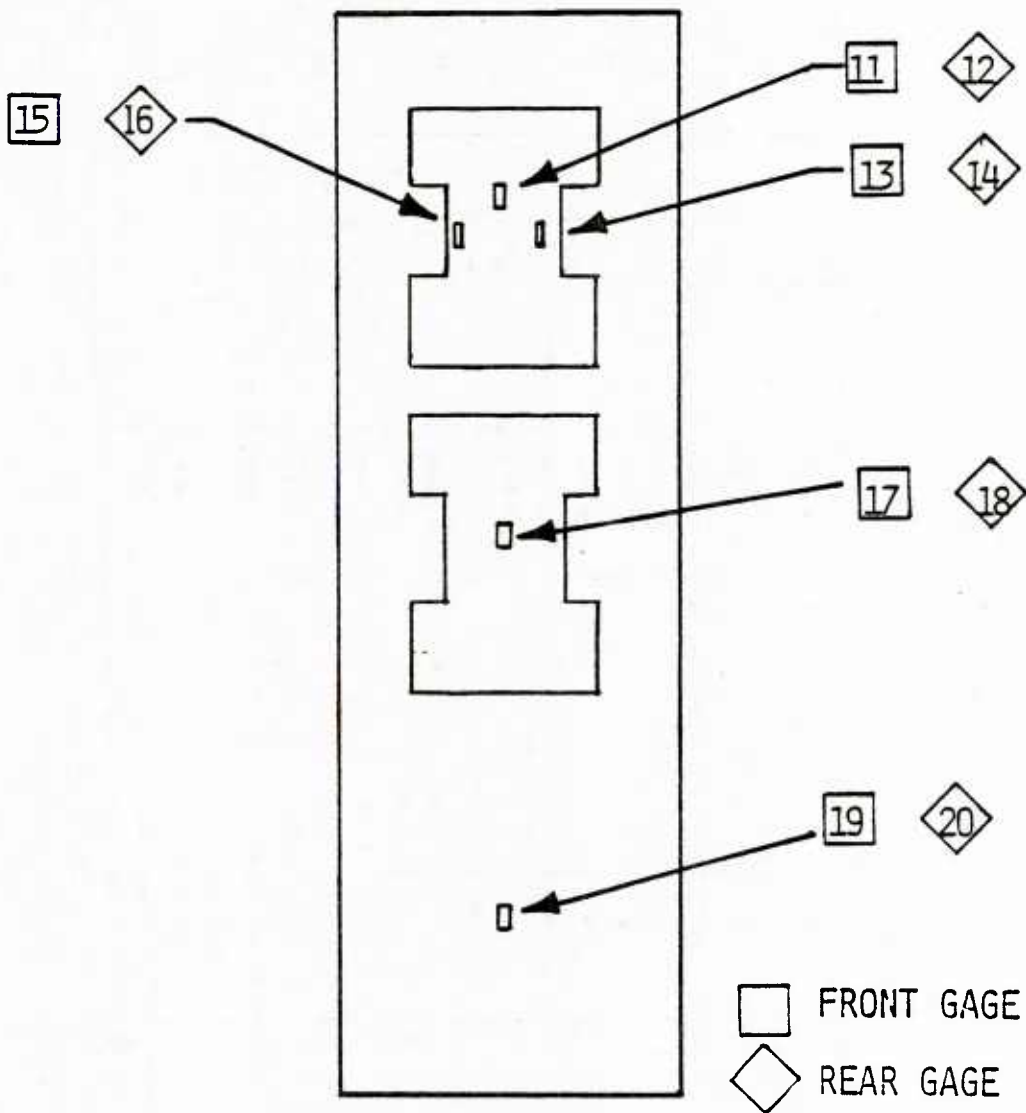


Figure 45. Results of T-38 Severe Spectrum Test Modified Type 2 Gage



STRAIN GAGE IDENTIFICATION - LOAD TRANSFER TEST 025

Figure 46. Strain Gage Identification for Load Transfer Test 025

TEST 025 LOAD TRANSFER

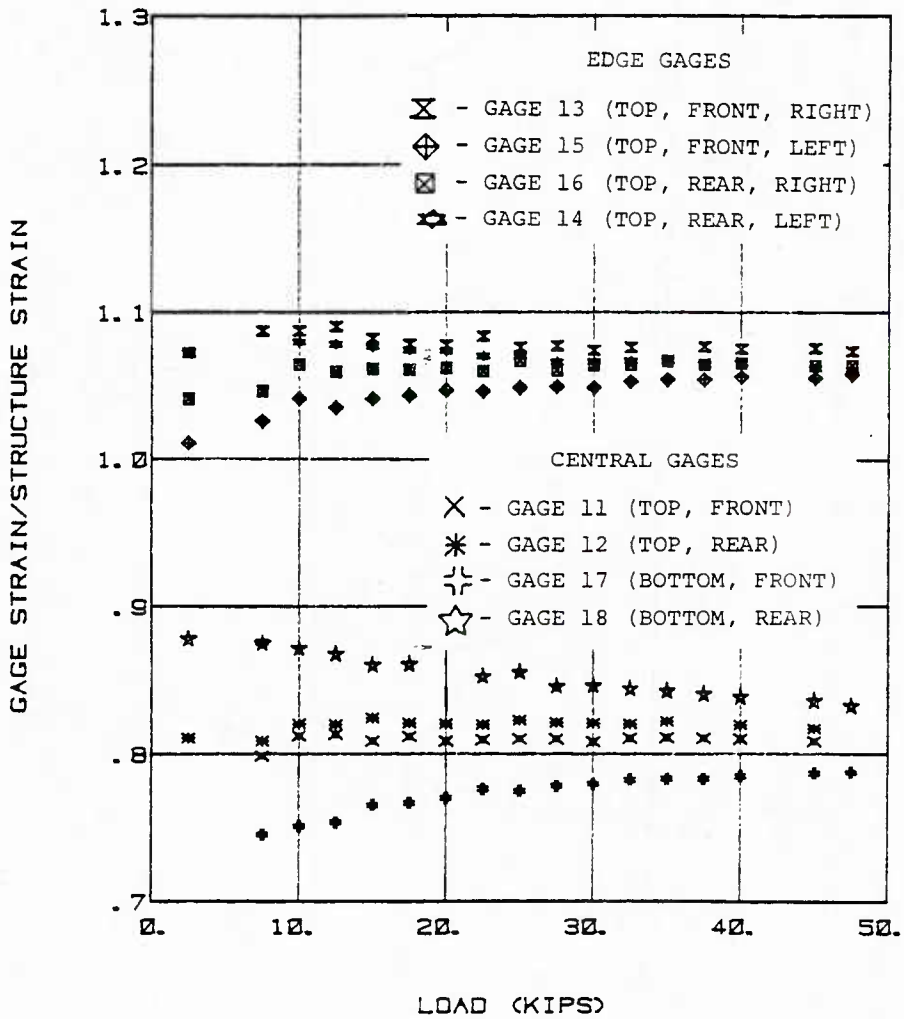


Figure 47. Load Ratio Results for Test 025

TEST Ø54 CRACK GROWTH RATES

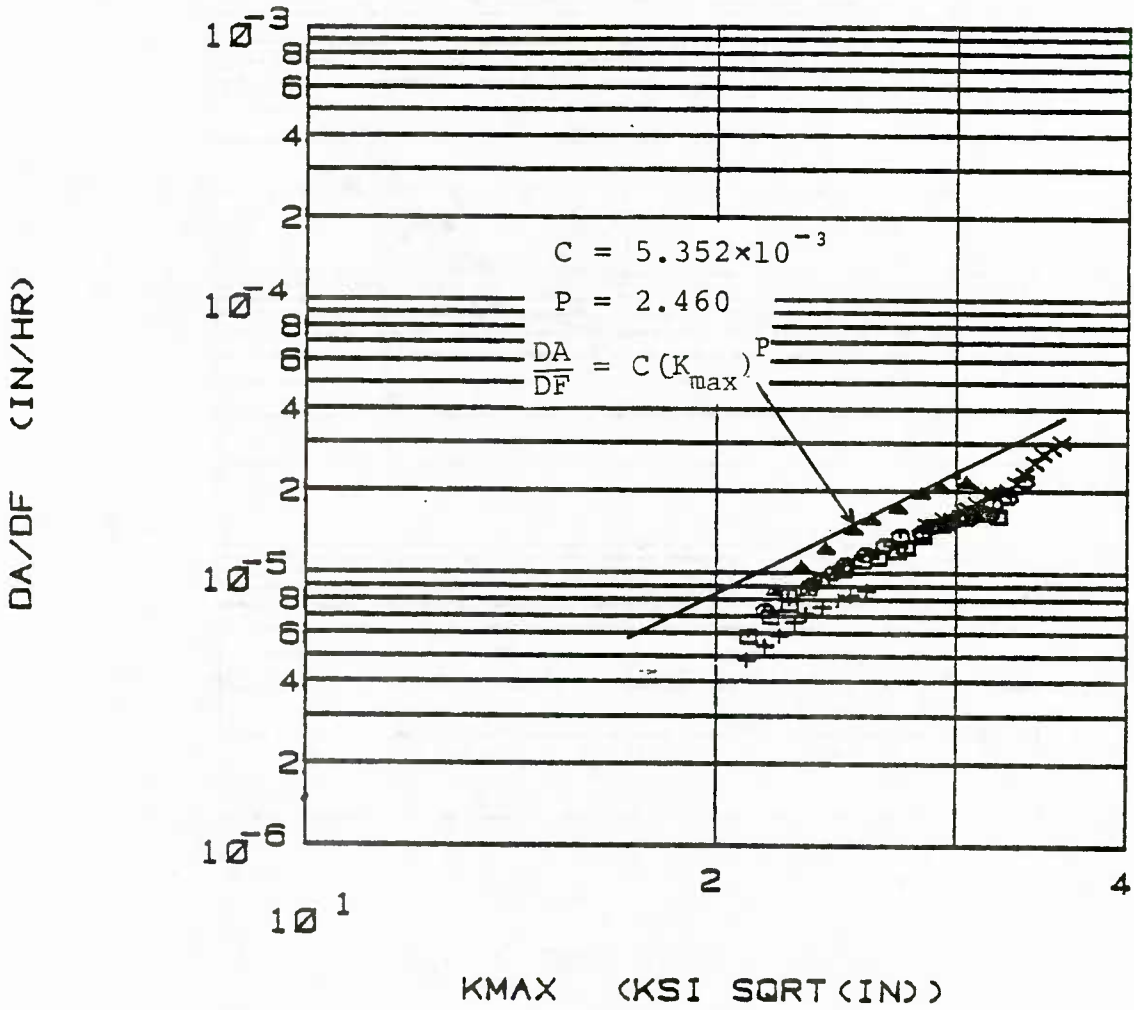


Figure 48. Comparison of Test and Analysis - Crack Growth Rates - T-38 Mild Spectrum

TEST Ø57 CRACK GROWTH RATES

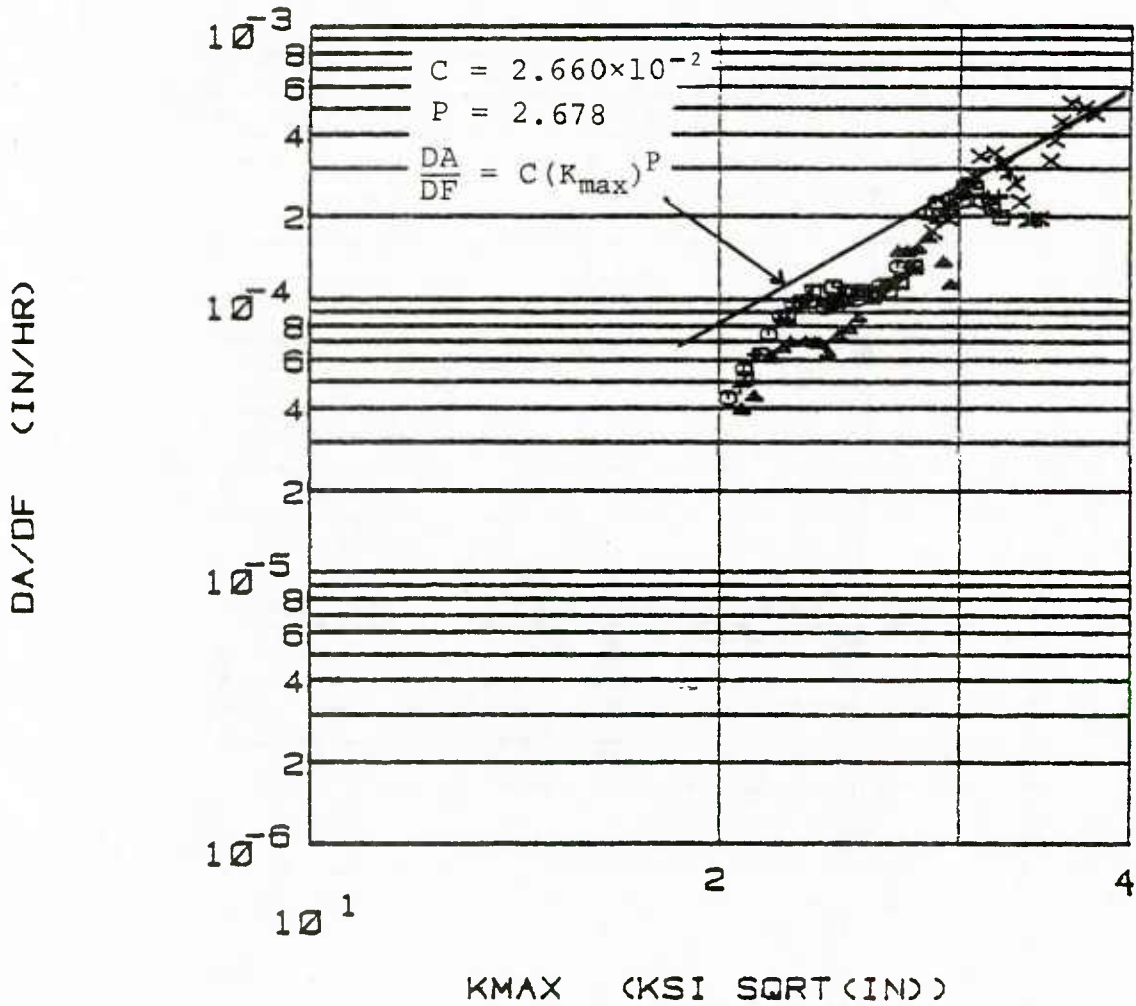


Figure 49. Comparison of Test and Analysis - Crack Growth Rates - T-38 Baseline Spectrum

TEST Ø6Ø CRACK GROWTH RATES

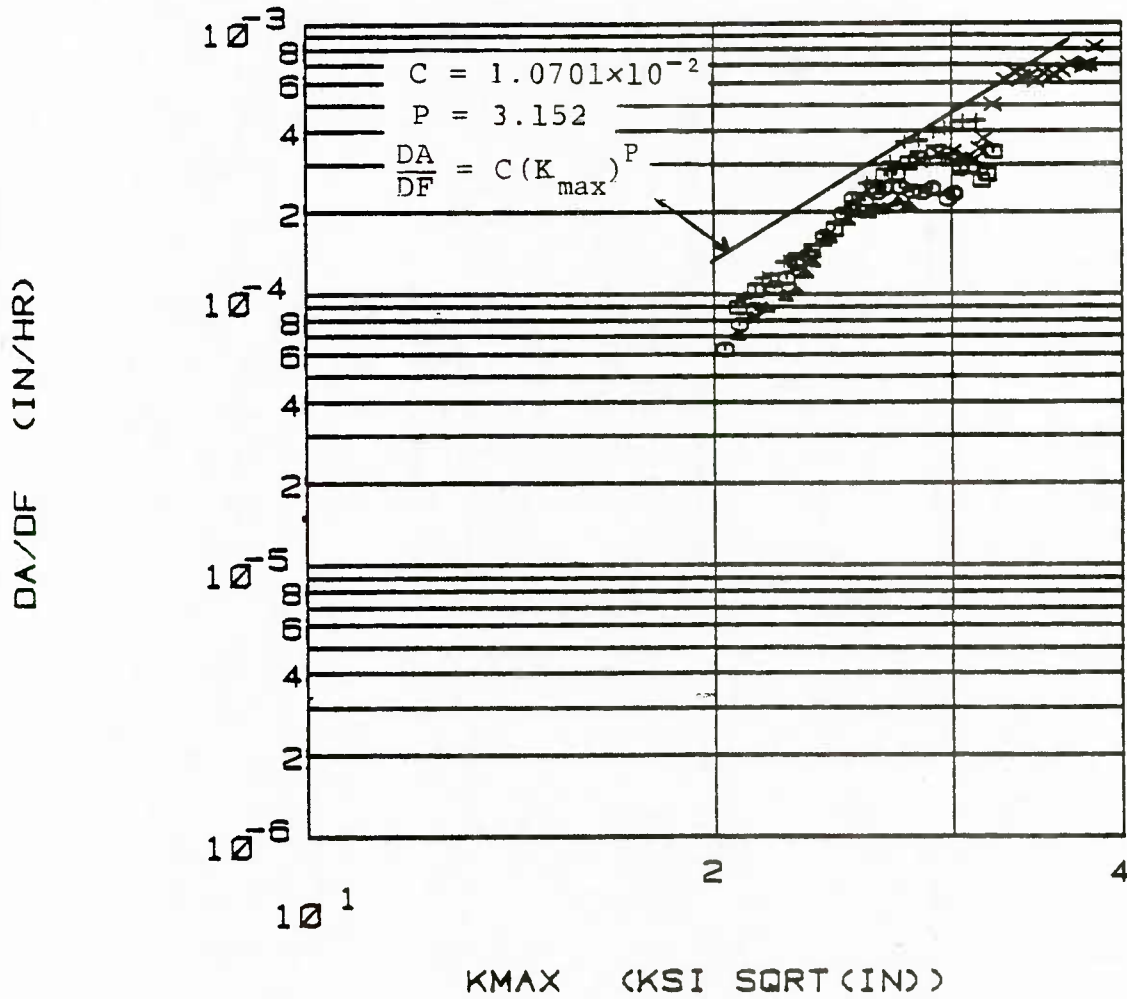


Figure 50. Comparison of Test and Analysis - Crack Growth Rates - T-38 Severe Spectrum

SECTION VI
EVALUATION OF CRACK GROWTH GAGE AS AN IAT DEVICE

The definitive documents that establish and define the Aircraft Structural Integrity Program for all Air Force aircraft are AFR 80-13 and MIL-STD-1530A [1, 2]. One of the basic requirements is the design and implementation of an Individual Aircraft Tracking (IAT) Program. This program is to provide a measure of the usage of each aircraft such that it may be compared to a design or operational mean usage for the purpose of predicting potential flaw growth in critical areas. The establishment and adjustment of inspection and repair intervals for these critical areas is to be based on the individual aircraft usage data. It was for these purposes that the concept of the crack growth gage was developed [15]. This section discusses the requirements of an IAT device and evaluates the crack growth gage for that purpose with respect to the information obtained from the present program.

1. Requirements for an IAT Device

The design goals of an IAT device can be divided into two categories. First are the goals relating to accuracy and reliability. Second are the goals relating to system efficiency. Table 10 is a listing of goals considered to be pertinent to the application of the crack growth gage. While these were all considered in the design of the gages tested, and while many of them received evaluation during the program, the scope of the present program did not include tests for the evaluation of them all. A brief discussion of each goal will indicate how it can be assessed and if it was directly addressed in the current program.

The ranking ability of the gage can be determined by testing to different loading spectra, and comparing the crack growth observed in the gage to that in the structure. This was done as initial testing in the present program.

TABLE 10

DESIGN GOALS FOR A CRACK GROWTH GAGE
APPLIED TO THE INDIVIDUAL AIRCRAFT TRACKING PROCESS

GOALS RELATING TO ACCURACY AND RELIABILITY

1. The gage shall rank aircraft according to usage severity independent of either the structural location monitored or the crack geometry in the structure.
2. Crack growth data from the gage shall be accurately related to the aircraft maintenance schedule.
3. The gage shall be an indicator of relative damage rates.
4. The gage shall not buckle.
5. The gage shall not fail in tension.
6. Crack growth response of gages shall be repeatable from gage to gage.
7. The gage shall not damage the structure.
8. The tracking system based on the gage shall not require information beyond what is collected under current tracking systems.
9. The gage shall not create a safety hazard should it fail.
10. The gage shall reliably predict crack growth for structural cracks having various starting crack lengths.
11. Gages shall be readily replaceable without losing continuity in the tracking system and without damaging or degrading the structure.
12. Gage response shall not be sensitive to normal manufacturing tolerances.

GOALS RELATING TO SYSTEM EFFICIENCY

13. The crack growth increment shall be great enough that it can be easily detected.
14. The gage shall be easily readable.
15. Reading of the gage shall not alter gage operation.
16. The gage shall be convenient to attach.

TABLE 10 (Concluded)

DESIGN GOALS FOR A CRACK GROWTH GAGE
APPLIED TO THE INDIVIDUAL AIRCRAFT TRACKING PROCESS

17. The gage shall remain securely attached.
18. The gage shall be economical to manufacture.
19. Translation of crack growth data for data processing shall be conveniently accomplished.
20. The gage shall be of a convenient size.
21. The cost of a system of aircraft tracking based on the crack growth gage shall be less than current systems.

The relation of crack growth data to Aircraft Maintenance Scheduling is determined by an evaluation of the predicted life expended with the actual life expended. If the gage either over predicts or under predicts the life expended by too large a fraction, the aircraft will either be scheduled for too much maintenance or too little maintenance. A range of plus or minus ten percent has been chosen as a reasonable allowance. Such an evaluation is presented in the next subsection for the current data.

The remainder of the design goals are considered self-explanatory. In the current program, no gages buckled or failed in tension prior to the predicted life.

The implementation of an IAT system requires the consideration of many other items. Table 11 lists these items and presents some of the questions which need to be answered when developing the IAT system.

2. Comparison of Test Results

The results obtained from the Type 2 and modified Type 2 spectrum and constant amplitude tests must be compared and evaluated according to their application to an IAT program. This can best be done by determining the variation in prediction of fraction of life expended for the two gage types.

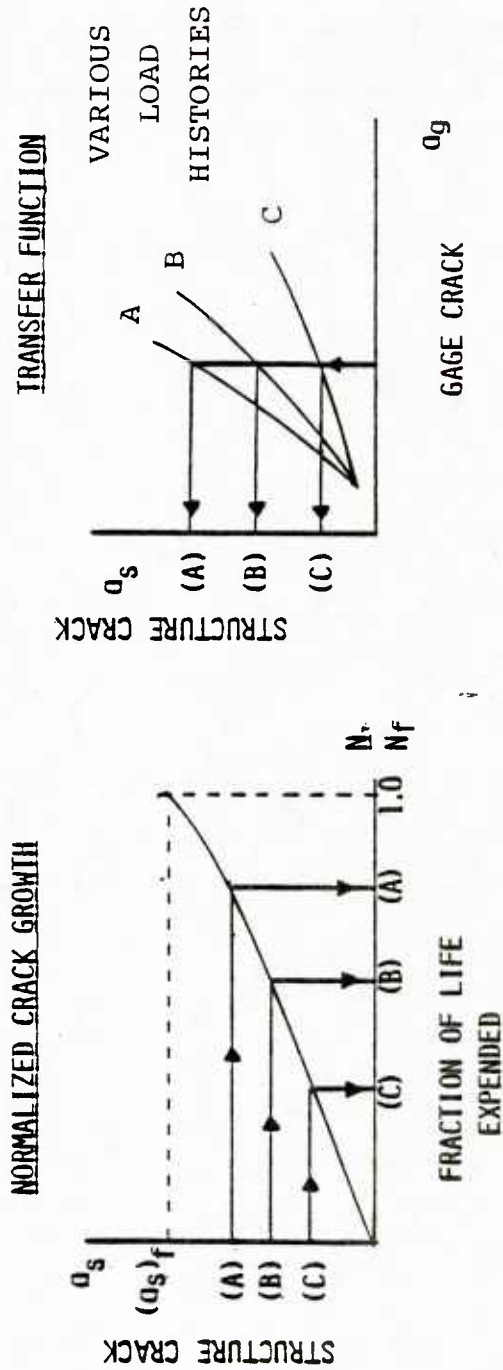
The use of a normalized crack growth curve has been developed as a means of tracking damage on aircraft structures [24]. The type of normalized curve in which the structural crack is plotted against the normalized expended life has been shown to be essentially invariant with stress history. This type of curve is used in this report to evaluate the two gages.

The development of a life ratio from the normalized crack growth curve is illustrated in Figure 51. The life ratio is defined as the ratio of predicted life expended to the actual life expended. A life ratio greater than 1.0 is conservative

TABLE 11
ITEMS TO BE CONSIDERED IN THE
IMPLEMENTATION OF AN IAT SYSTEM

1. Field Support
 - a) Type (What is to be done?)
 - b) Level (What training is required?)
2. Data Transfer (Field to ASIMIS)
 - a) Method of field transcription
 - b) Supplemental information
 - c) Special forms
3. Computer Transcription
 - a) Reading of field form
 - b) Checking of data
 - c) Addition to database
4. Damage Index Computation
 - a) Crack growth related to baseline usage
 - b) How to detect serious usage changes
5. What is reading frequency?
 - a) Crack growth increment per flight?
 - b) How critical is tracking (Monthly, Quarterly)
(i.e., collect Monthly, report Quarterly)
6. Does gage have any location restrictions?
 - a) A baseline spectrum must be known
 - b) Accessibility is important to reading
7. How many gages required to track baseline A/C?
 - a) Number of critical locations
 - b) Transfer of locations possible?
8. How are gages installed?
 - a) Type of adhesive
 - b) Pressure/temperature requirements
 - c) Cure times
 - d) Protection

LIFE RATIO DETERMINATION



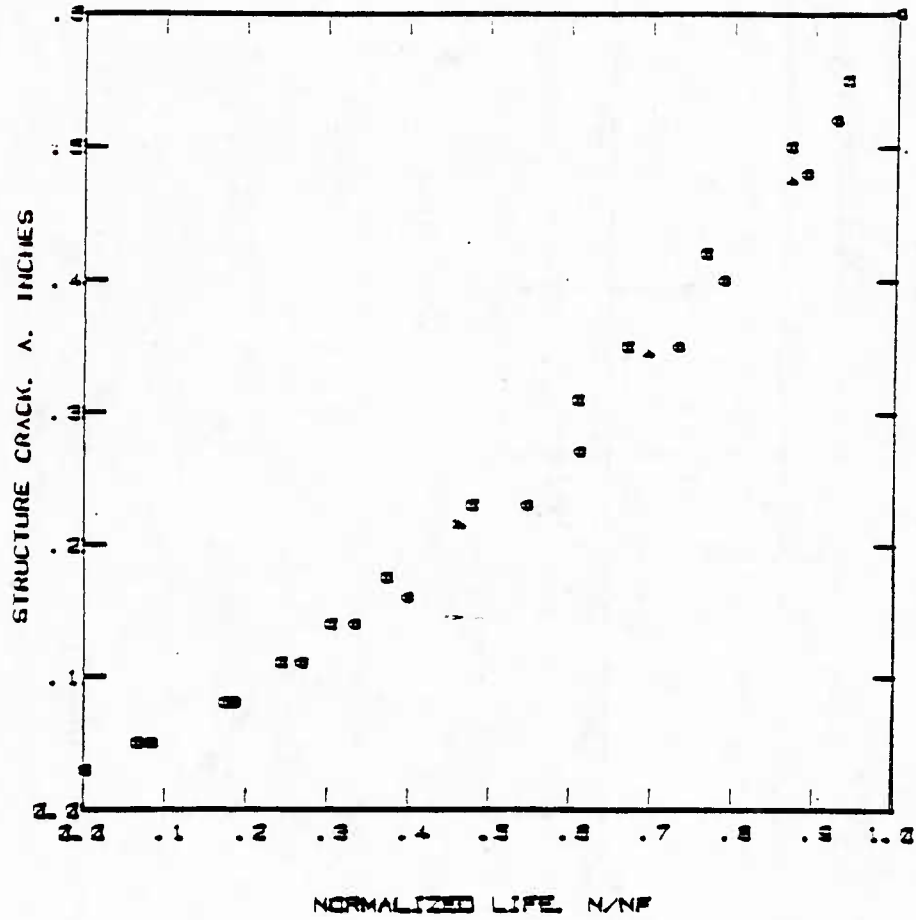
LET LOAD HISTORY B BE THE PREDICATED SEQUENCE
 THEN LIFE RATIO IS N_{PRED}/N_{ACTUAL}
 FOR LOAD HISTORY A:

$$(N_{PRED}/N_{ACTUAL}) = (N/N_f)_B / (N/N_f)_A$$

SIMILARLY FOR LOAD HISTORY C.

Figure 51. Development of Life Ratio From Normalized Crack Growth Curves

NORMALIZED LIFE



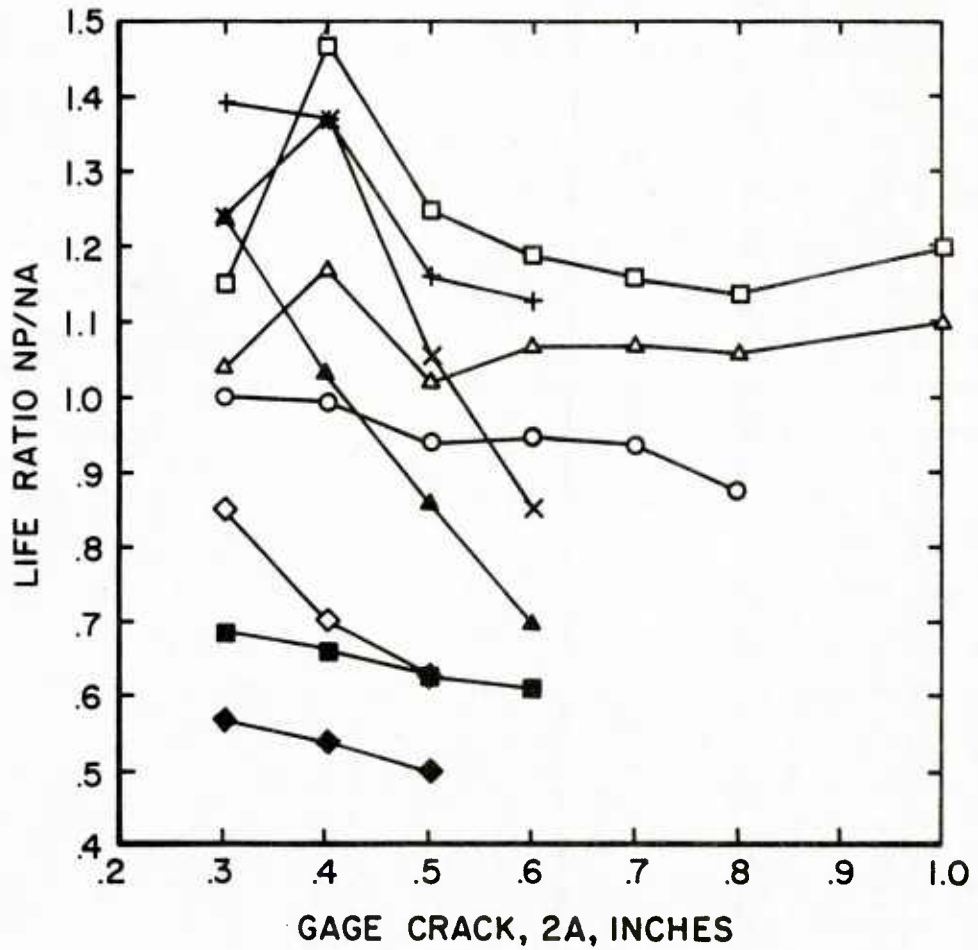
<u>Symbol</u>	<u>Test</u>	<u>Condition</u>
□	019	$S_{max} = 16,000$ psi, $R = -0.1$
○	020	$S_{max} = 16,000$ psi, $R = +0.1$
△	015	$S_{max} = 28,700$ psi, F-4 High Lever Specimen

Figure 52. Normalized Crack Growth Life Plots

and a life ratio less than 1.0 is non-conservative. Life ratios equal to 1.0 indicate an exact prediction of life expended. For this analysis, the range of acceptable variation was taken as ± 10 percent. A review of the error in current tracking methods presented in Reference 37 showed that the probable error in predicting the months to a maintenance action is no less than 10 months in a prediction of 100 months. This error would result in an expected standard deviation of about 15 percent. Thus the present criteria is slightly more stringent than may be currently available. The entire question of acceptable error in tracking methods has only recently begun to be extensively addressed and much more work is needed before firm criteria can be established.

For the analysis of the current data from Type 2 and modified Type 2 gages, a normalized crack growth curve for the structure was constructed. The basis for these plots was test 020 for the Type 2 gage tests and test 019 for the modified Type 2 gage tests. Figure 52 shows the plots of this computation. A value of 0.60 inches was chosen as the final value of structural crack length for life determination. The results of test 015 are also shown on the plot. This indicates that both spectrum and constant amplitude tests can be represented by the same mean normalized curve. Computation of life ratios as indicated in Figure 51 resulted in the data plotted in Figures 53 and 54.

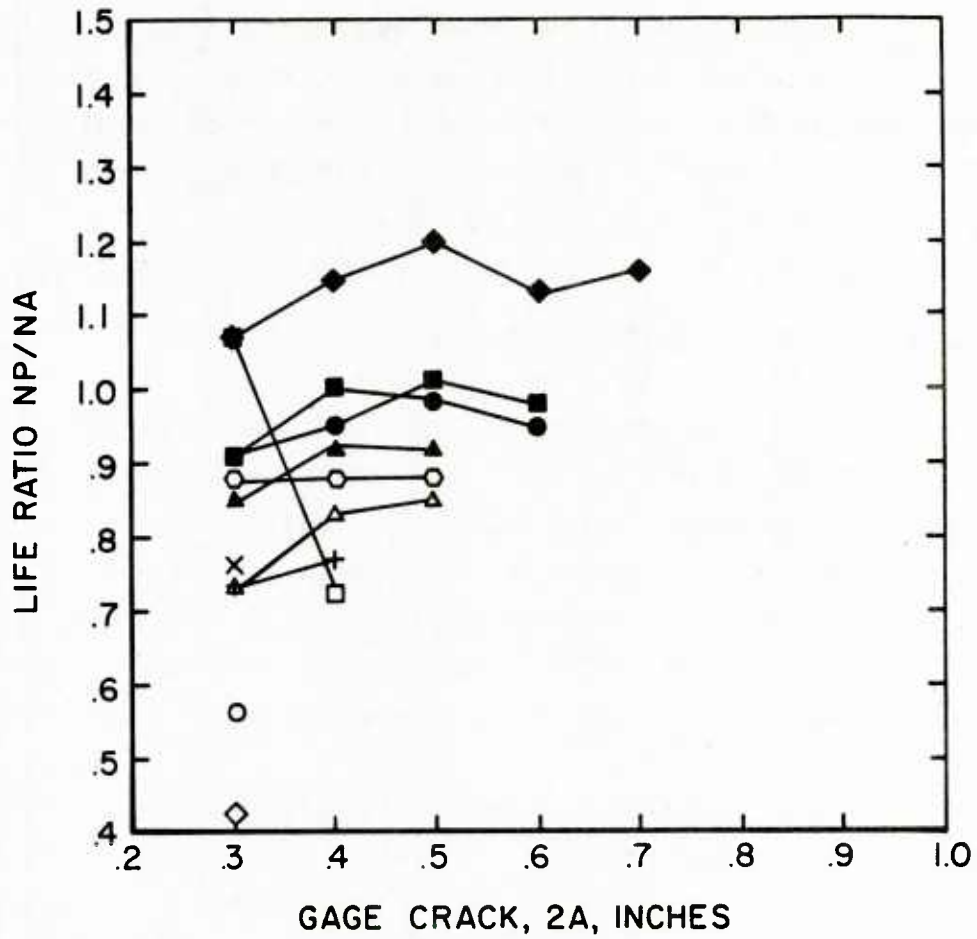
The variation of the modified Type 2 gage, while not within the desired range for unqualified acceptability, shows much more tightly grouped results than the Type 2 gage. However, the modified Type 2 gage shows results almost entirely on the non-conservative side and the Type 2 gage, while showing more spread, is mainly on the conservative side.



Symbol	Test	S_{max} , Ksi	R
□	022	25.0	-0.1
○	023	25.0	+0.1
△	041	16.0	-0.1 (50% overload)
+	042	16.0	+0.1 (50% overload)
x	045	25.0	-0.1 (30% overload)
◇	010	23.4	Var. F-4 Baseline
◆	011	28.7	Var. F-4 High-Baseline
■	012	23.4	Var F-4 Severe
▲	013	23.4	Var F-4 (Baseline (M002))

(Test 020 is Reference)
 $S_{max} = 16.0$ Ksi, R = +0.1

Figure 53. Life Ratio Plots for the Type 2 Crack Growth Gage



Symbol	Test	S_{max} , Ksi	R
□	021	16.0	+0.3
○	024	25.0	+0.3
△	041	16.0	-0.1 (50% overload)
+	043	16.0	+0.3 (50% overload)
X	044	25.0	-0.1 (30% overload)
◇	046	25.0	+0.3 (30% overload)
◆	054	30.0	Var. T-38 Mild
■	057	30.0	Var. T-38 Baseline
●	060	30.0	Var. T-38 Severe
▲	015	28.7	Var. F-4 High-Baseline
○	014	23.4	Var. Baseline

(Test 019 is Reference)
 $S_{max} = 16.0$ Ksi, $R = -0.1$

Figure 54. Life Ratio Plots for the Modified Type 2 Crack Growth Gage

The cause of these observed variations must be determined and corrected, if possible, if the crack growth gage is to be an acceptable IAT device. Analyses were thus performed to determine if the variation was to be expected in the light of acknowledged possible variations in other parameters.

The first consideration is the expected variation in the material properties. The results of a crack growth variability study of 2024-T3 aluminum specimens at constant load amplitude [3] showed that a coefficient of variability between 5 and 10 percent could be expected. Using the results of tests 054, 057, and 060, the T-38 spectrum tests with the modified Type 2 gage, a mean power law curve was fit to each test. As the coefficient of the power law equation is representative of material property variation, a 7 percent coefficient of variation was used to perform analytical transfer function development. A series of 30 random pairs of coefficients were selected for each test. The values at a gage total crack length, $2a$, of 0.7 inches were selected for an analysis of variance. The results shown in the ANOVA table of Table 12 show that the null hypothesis that the means of the distributions are equal is rejected at the .0005 level of significance. Thus, the differences seen in the crack growth rates between the three spectra tests are not due to the material variation. Figure 55 presents a plot of the mean values resulting from this analysis. Also shown is the 95% confidence bound of the mean at the analysis point.

This is a significant observation because it shows that the crack growth gage is quite sensitive to spectrum variations. Without having any other information than the crack growth gage history, it would not be possible to adequately track an aircraft that had been subjected to a changed usage.

For example, consider the case of a T-38 aircraft that moves from the ATC (mild) usage to the LIF (severe) usage. The tracking program had been based on the transfer function derived from the mild usage. If no adjustment is made to the transfer

TABLE 12

ANALYSIS OF VARIANCE TABLE FOR MODIFIED
TYPE 2 GAGE FOR T-38 SPECTRUM TESTS

<u>SOURCE</u>	<u>DEGREES OF FREEDOM</u>	<u>SUM OF SQUARES</u>	<u>MEAN SQUARE</u>	<u>F</u>
Spectra	2	0.3188	0.1594	22.33
Error	87	0.6208	0.0071	
Total	89	0.9396		

$$F_{2, 87, .9995} = 8.31$$

(F statistic at .0005 level of significance)

∴ since 22.33 > 8.31 Null hypothesis is rejected

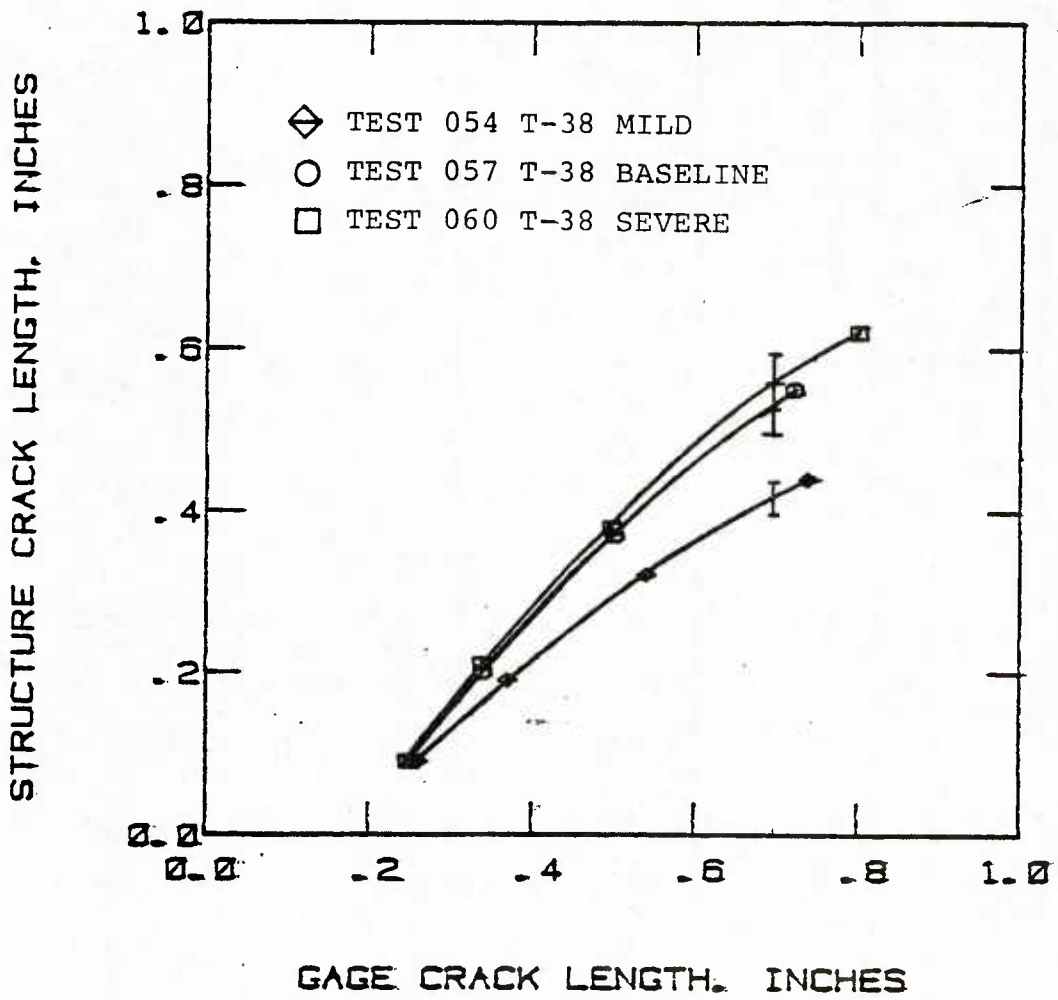
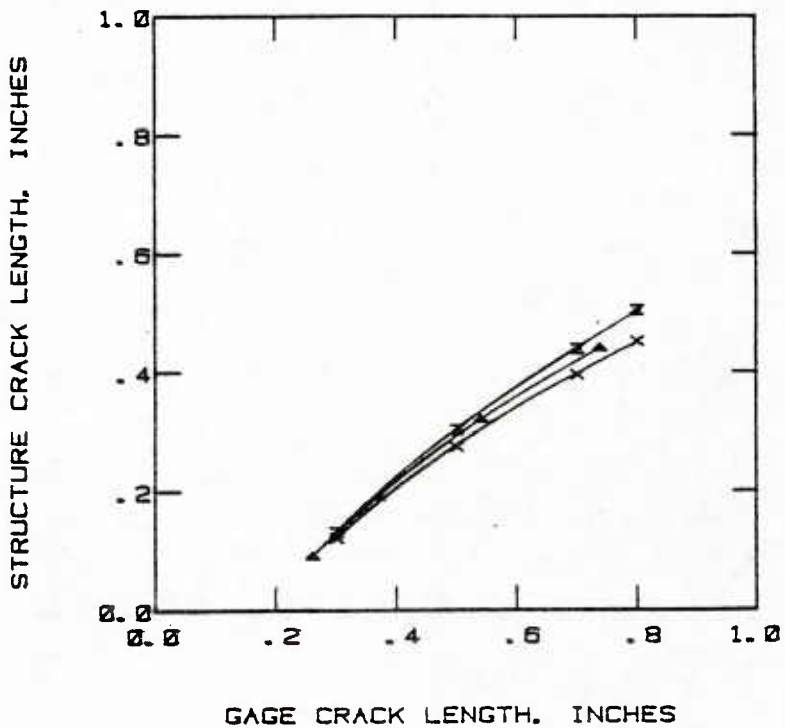


Figure 55. Computed Mean Values for Spectrum Tests Based on a 7 percent Material Property Coefficient of Variance.

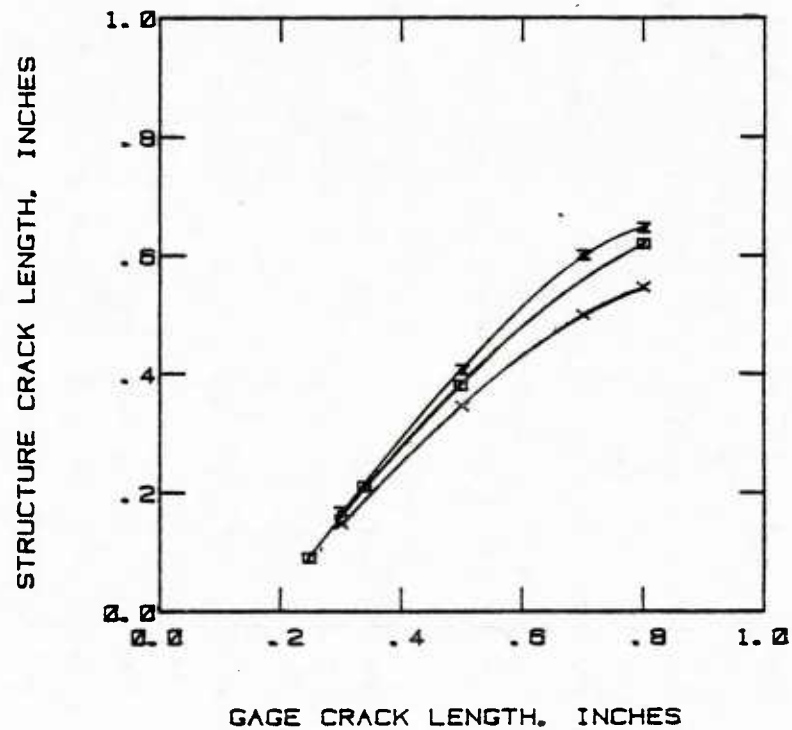
function used in the analysis, the predicted structural crack growth increments for the new usage will be too small. This is true even though the crack growth gage is now experiencing the new usage. To account for the change, the transfer function for the severe usage must be inserted into the analysis. In the case of an obvious change in usage this would probably be done. However, the problem arises when usage has changed slowly but significantly without any change in the analytical transfer function.

An analysis of the effect of dimensional variations, based on measured values is presented in Figures 56 through 61. Each analysis was repeated for the same thirty material variations presented in Figure 55. However, only the mean value data is plotted. It is seen that only the variations of the cracked section thickness, T_1 , and the adhesive thickness, TG , show any appreciable effect on the transfer function. An analysis of variance was performed on these results. The hypothesis that the means are the same was rejected at the .05 level of significance for both sets of data when comparing the closest variations from each spectra. Since this is a very unlikely combination, the .05 level of significance is considered to be sufficient to allow the statement that the variation between the spectra data is not due to the variation in any of the dimensional parameters.

The Type 3 gage data presented in Figure 24 of Volume II was also analyzed using the life ratio method. Test AF30, constant amplitude at 22,000 psi maximum stress and $R=-0.1$ was used as the reference. These results show that the life variation due to load history effects is much greater than the desired limit of $\pm 10\%$ and that the estimates are mostly nonconservative. This gage design is also considered unsatisfactory as a stand-alone IAT device. The range in life ratios for this gage is from 0.22 to 2.16 (a factor of 9.8). This is more than three times the range for the Type 2 gage which was from 0.55 to 1.47 (a factor of 2.7) and for modified Type 2 gage which was from 0.41 to 1.07 (a factor of 2.6). A change in the reference test would not change this range of variation, although, it might make the predictions conservative.

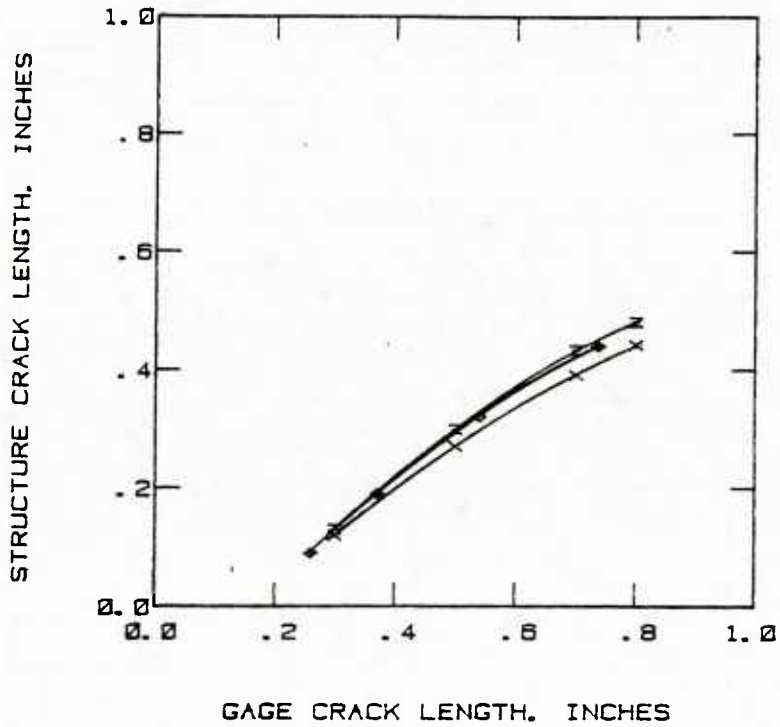


T1, INCHES
 X 0.1449
 Z 0.1541
 Δ 0.1500
 T-38 Mild Spectrum

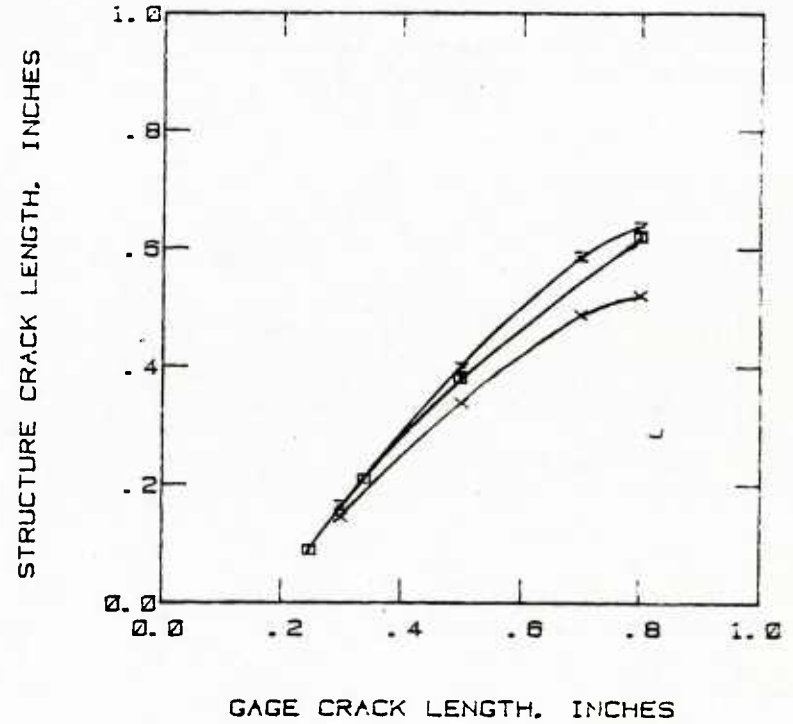


T1, INCHES
 X 0.1449
 Z 0.1541
 □ 0.1500
 T-38 Severe Spectrum

Figure 56. Effect of Variation in Unbonded Thickness, Modified Type 2 Gage

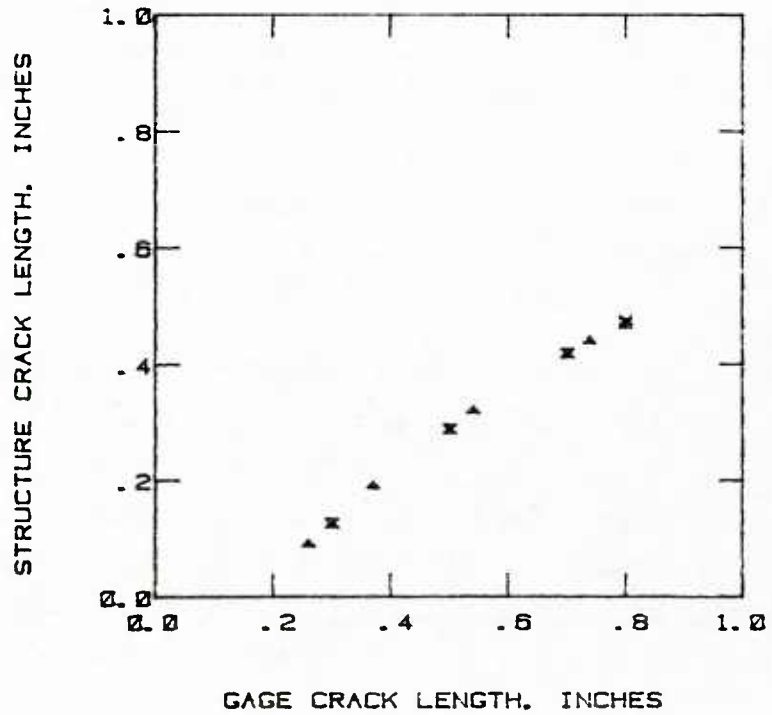


TG, INCHES
 X 0.004
 Z 0.010
 ◊ 0.008
 T-38 Mild Spectrum

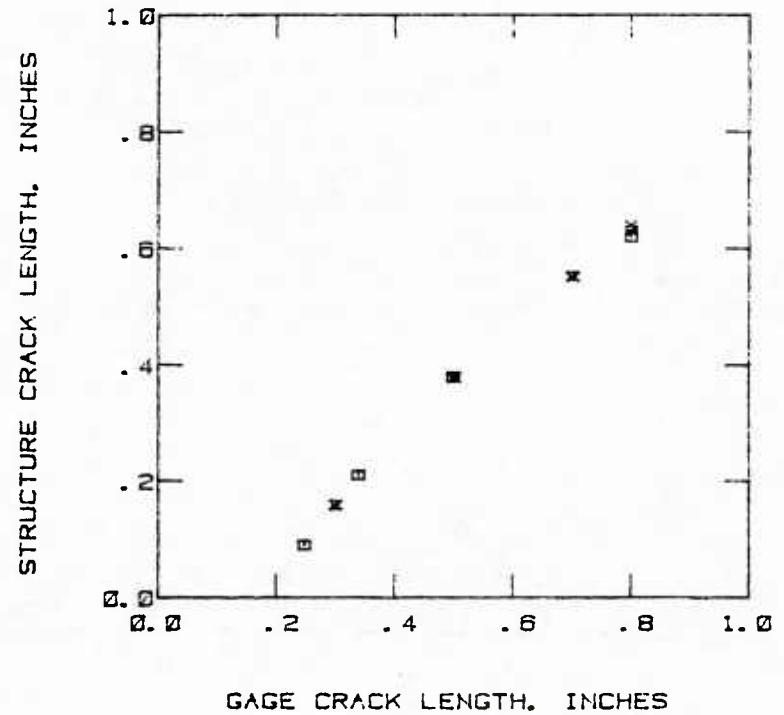


TG, INCHES
 X 0.004
 Z 0.010
 ◻ 0.008
 T-38 Severe Spectrum

Figure 57. Effect of Variation in Adhesive Thickness, Modified Type 2 Gage

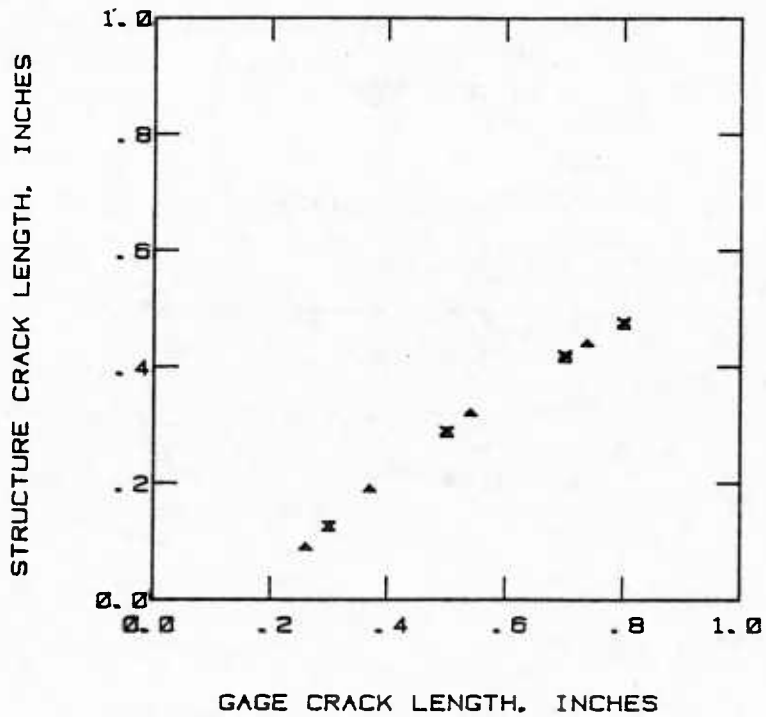


L1, INCHES
 X 0.395
 Z 0.405
 Δ 0.400
 T-38 Mild Spectrum

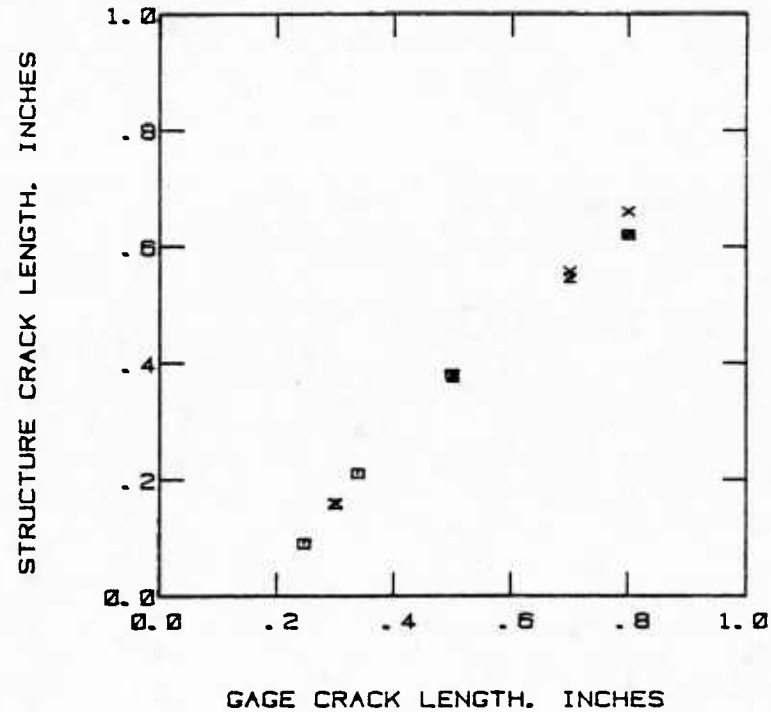


L1, INCHES
 X 0.395
 Z 0.405
 □ 0.400
 T-38 Severe Spectrum

Figure 58. Effect of Variation in Length of Narrow Section, Modified Type 2 Gage

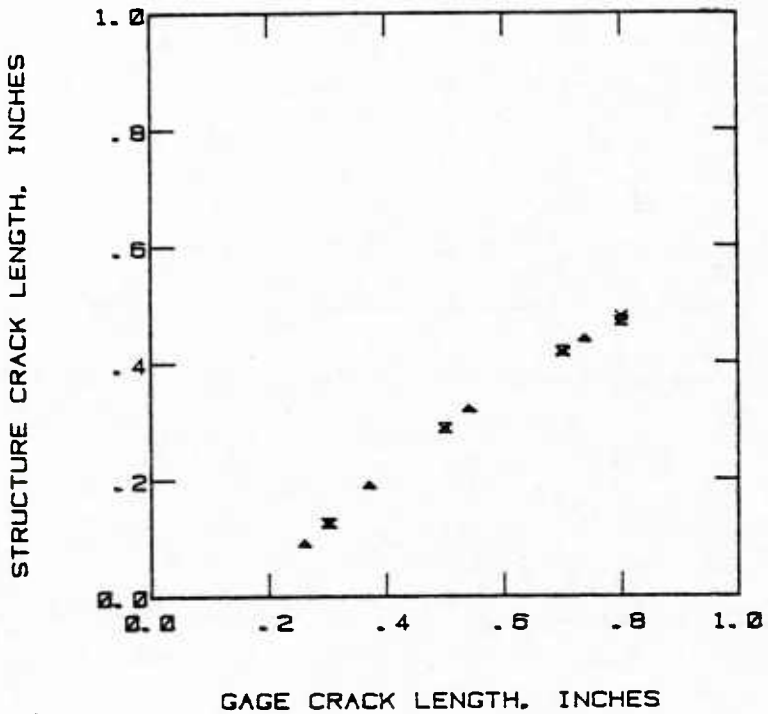


L2, INCHES
 X 0.595
 Z 0.605
 Δ 0.600
 T-38 Mild Spectrum

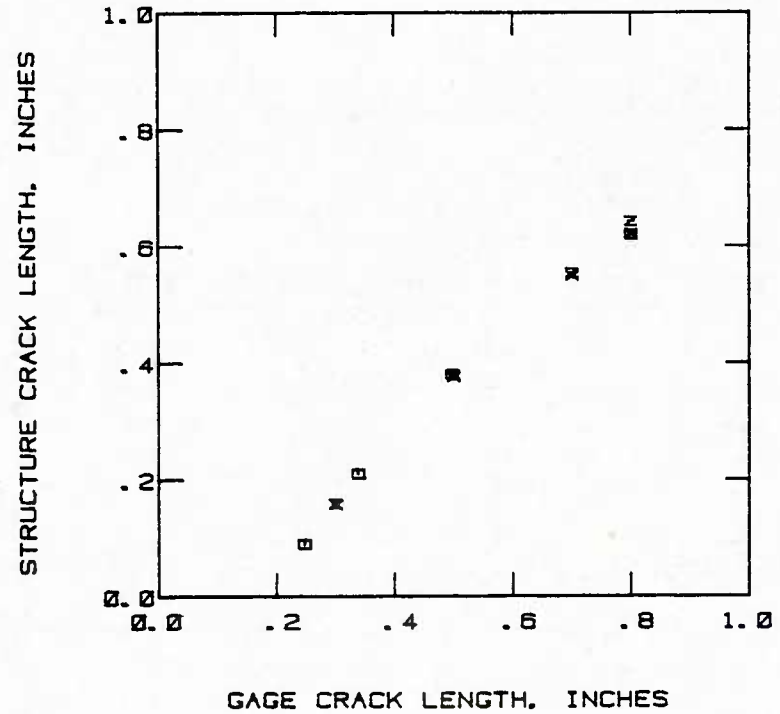


L2, INCHES
 X 0.595
 Z 0.605
 □ 0.600
 T-38 Severe Spectrum

Figure 59. Effect of Variation in Length of Wide Section, Modified Type 2 Gage

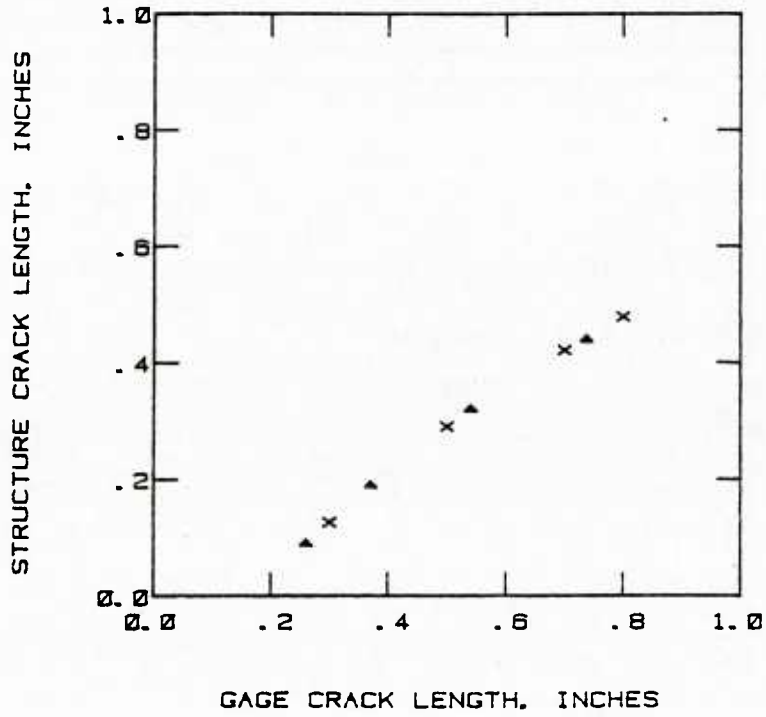


W1, INCHES
 X 0.997
 Z 1.001
 Δ 1.000
 T-38 Mild Spectrum

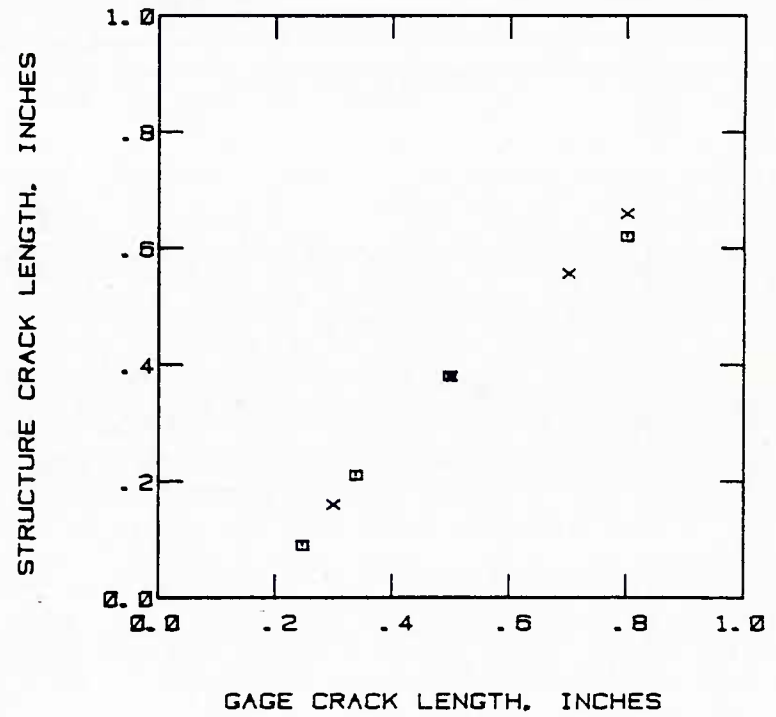


W1, INCHES
 X 0.997
 Z 1.001
 □ 1.000
 T-38 Severe Spectrum

Figure 60. Effect of Variation in Width of Narrow Section, Modified Type 2 Gage

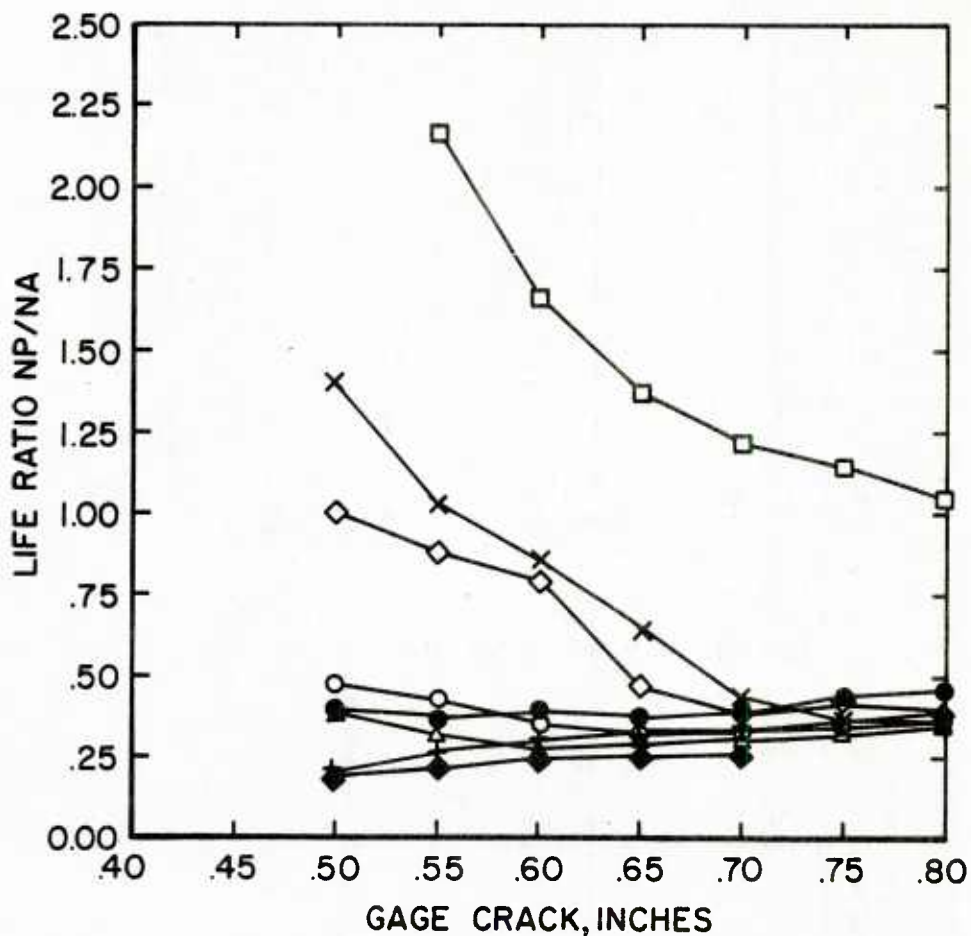


W, INCHES
 X 1.9475
 △ 1.9560
 T-38 Mild Spectrum



W, INCHES
 X 1.9475
 □ 1.9560
 T-38 Severe Spectrum

Figure 61. Effect of Variation in Width of Wide Section, Modified Type 2 Gage



Symbol	Test	Max Stress	R	Symbol	Test	Max Stress	R
□	AF-31	22,000	0.1	X	AF-52	22,000	0.3
○	AF-32	22,000	0.3		(with overolad)		
△	AF-50	22,000	-0.1	◇	AF-55	30,000	T-38 Mild
	(with overload)			◆	AF-58	30,000	T-38 B/L
+	AF-51	22,000	0.1	●	AF-61	30,000	T-38 Severe
	(with overload)						

Figure 62. Life Ratio Plots for the Type 3 Crack Growth Gage

SECTION VII
CONCLUSIONS

Based on the results obtained from the tests and analysis described in this report, the following conclusions are presented.

1. The crack growth gage, when mounted on a structure which is thicker than the gage, responds differently than the structure when subjected to variable amplitude loading histories. This results in a wide variation in the crack length transfer function. Although the designs tested in this program were specifically selected to reduce this effect, they did not eliminate it. Thus, the transfer function that relates the crack growth gage behavior to the structural behavior is not spectrum independent.

2. The crack growth gage does provide a reasonable ranking of relative severity of different applied load spectra. However, the changing of load spectra severity, i.e., increasing the periodic maximum loads, is not adequately reflected by the gage.

3. Because of the spectrum dependence of the crack length transfer function, application of the crack growth gage as a stand-alone IAT device will result in unknown variations in the predicted damage accumulation rates whenever the usage changes.

4. Observed variations in crack growth gage/structural behavior could not be attributed to the effects of variation in material properties and gage dimensions.

5. Because the gage does not provide a history of the cause of any changes in crack growth response in a structure, the crack growth gage is considered to be unacceptable as a stand-alone IAT device. However, it certainly can be used to enhance IAT data interpretation as a supporting device.

SECTION VIII
RECOMMENDATIONS

Based on the results and conclusions of this program, the following recommendations are made.

1. Further investigations of the crack growth gage as an IAT device should only be made on the basis of it being a supporting component of a total tracking system.

2. Additional work needs to be done to continue the development of criteria for the evaluation of tracking systems.

3. Any additional work should concentrate on reducing the variability of device response to spectrum loading. Constant amplitude testing should be minimized since the results are misleading.

4. A program should be developed for the evaluation of other tracking systems in a manner similar to that used in this program. Such evaluations either have not been done or the results are not available in a form to allow direct comparisons among various tracking systems. The evaluation program should utilize statistical methods to account for the uncertainties inherent in many aspects of the tracking problem.

APPENDIX A
DESCRIPTION OF GAGE BONDING PROCEDURE

I. SURFACE PREPARATION

Protect polished and cracked areas of carrier and gages with teflon tape during this procedure.

1. Wipe clean with MEK.
 2. Wipe clean with 1,1,1-Trichloroethan, apply teflon tape to the center area of the gage between the bonding areas.
 3. Abrade with aluminum oxide scotch-brite pads.
 4. Wipe clean with cotton pads to remove dust debris.
 5. Phosphoric Acid Nontank Anodize:
12% Solution: 73 ml of water (D.I. or distilled)
12 ml of 85% phosphoric acid ($P_3P_2O_4$) Fisher A242
20-26 grams of cabosil M-5
- A - Apply uniform coat of gelled solution on aluminum part.
- B - Place two or three layers of gauze over coated part: apply another coat of gelled solution.
- C - Secure a piece of stainless steel screen over coat gauze: apply another coat of gelled solution.

NOTE: Be sure the stainless steel screen does not contact any part of aluminum part.

- D - Connect screen as cathode (-);
Aluminum part as a node (+)
- E - Apply a dc potential of 6 volts for 10 minutes
(4-6 volts for 10-12 minutes are satisfactory).

NOTE: A rectifier may be used to supply to voltage and current during anodizing. Current density should be in the range of 1 to 7 amps/ft².

F - At the end of anodizing time, open the circuit, remove the screen, and gauze.

G - In the laboratory, the parts were rinsed with dioxized water spray until the gelled solution was completely removed.

NOTE: In the field, moisten clean gauze with water. Lightly wipe off the gelled acid with moistened gauze immediately. The rinse delay time is limited to less than five minutes. Do not rub the anodized surface. Immersion or spray should be used if possible.

H - The anodized surface is forced air dried with a hot air gun. (Air dry a minimum of 30 minutes at room temperature is acceptable.)

6. Check quality of prepared surface. A properly anodized surface will show an interference color* when viewed through a polarized filter rotated 90° at a low angle of incidence to fluorescent light or day light.

*Original color changes to complementary color when polarizing filter is rotated 90°.

7. If no color is observed, repeat steps 5 through 7.

II. MOUNTING GAGES

1. Cut adhesive (FM73) to the approximate size of the bonding area of gage and apply to gage. (Do not remove protective film from one side of adhesive and trim to gage.)

2. Remove the protective teflon tape and replace with new tape in the areas between the bonding surface and the polished gage section.

3. Remove protective film from adhesive, trim any excess adhesive from gage.

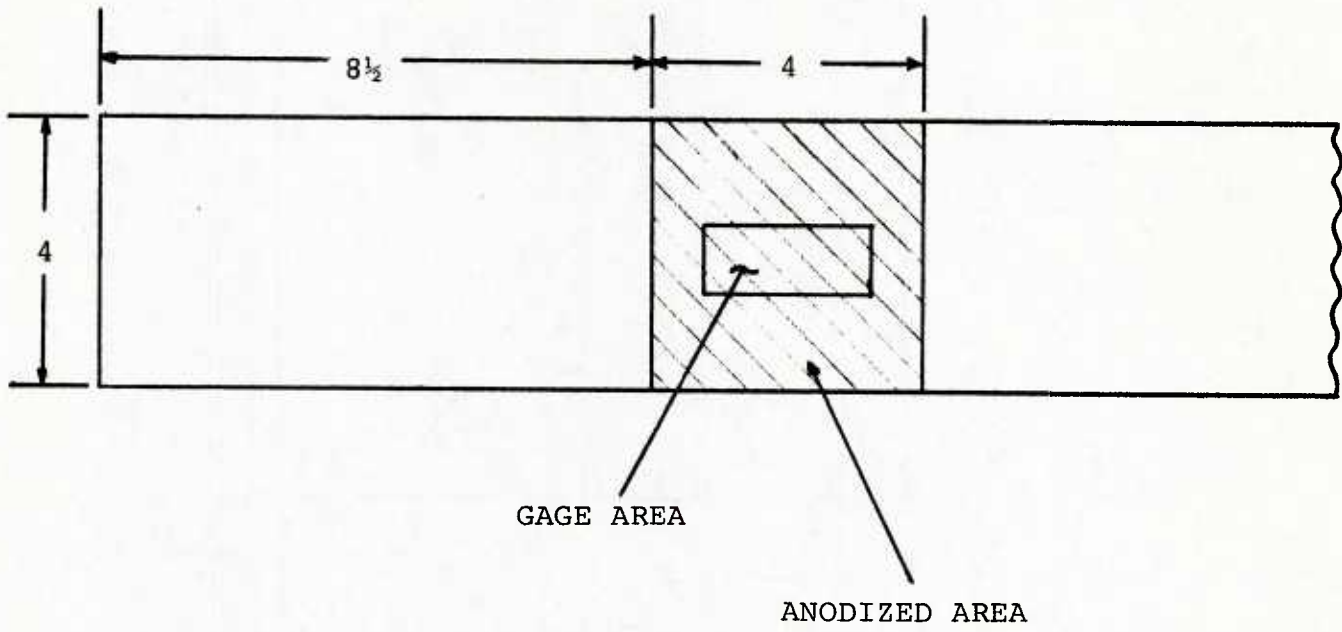
4. Align and place gage on carrier. (In the Lab, a machinist square was used to determine the location from the end of carrier and a parallel bar and special locating fixtures were used to determine the gages side location.)
5. Locate and tape spacer on gage to make a uniform surface over bond area. (Two places on each gage.)
6. Locate and tape 1/8" silicone pads over bond area (to distribute an even load on bond area).
7. Place two carrier and gage assemblies side-by-side in circulating oven, locate thermocouples, one on gage and one on the carrier, both of which are within 1/2 inch of one another.
8. Locate upper cawl plate and dead weight load so that the load is applied evenly to all bonding surfaces. (Alternately, enclose specimens in vacuum bag and connect to vacuum pump).
9. Start cure cycle.

NOTE: Vacuum bag method was used for all tests after 006.

10. Cure Cycle
 - a. Set oven temperature for 205°F.
 - b. Record initial temperatures of specimen assemblies.
 - c. Start strip chart temperature recorders.
 - d. Record time to reach cure temperature (this should be 70 to 120 minutes).
 - e. Maintain cure temperature for 180 minutes.
 - f. Monitor vacuum bag pressure (this should be approximately 29.5 inches Hg).
 - g. Turn off oven and allow to cool down in oven (approximately 50 to 80 minutes to reach 120°F).

- h. Remove from oven and allow to cool at room temperature overnight.
- i. Remove wrappings and visually check bond.

Figure A-1 illustrates the area of the carrier specimen which is anodized. Figure A-2 illustrates the set-up for the curing cycle when using the dead weight pressure application.



NOTE: ALL DIMENSIONS
IN INCHES

Figure A-1. Anodized Area

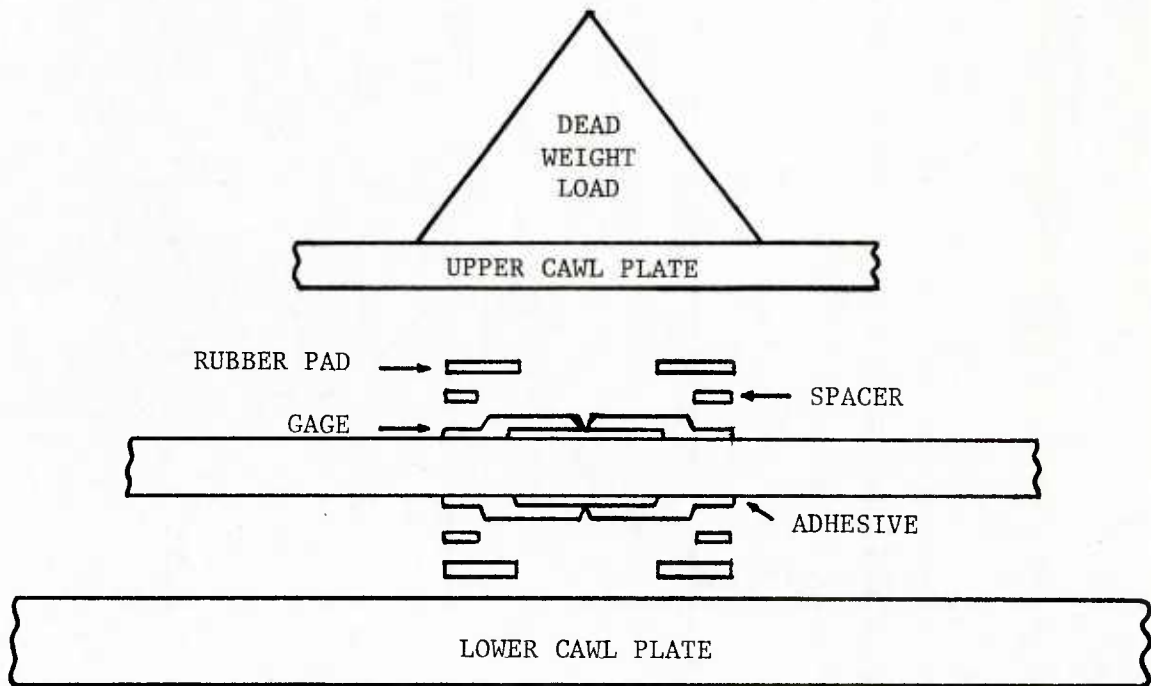


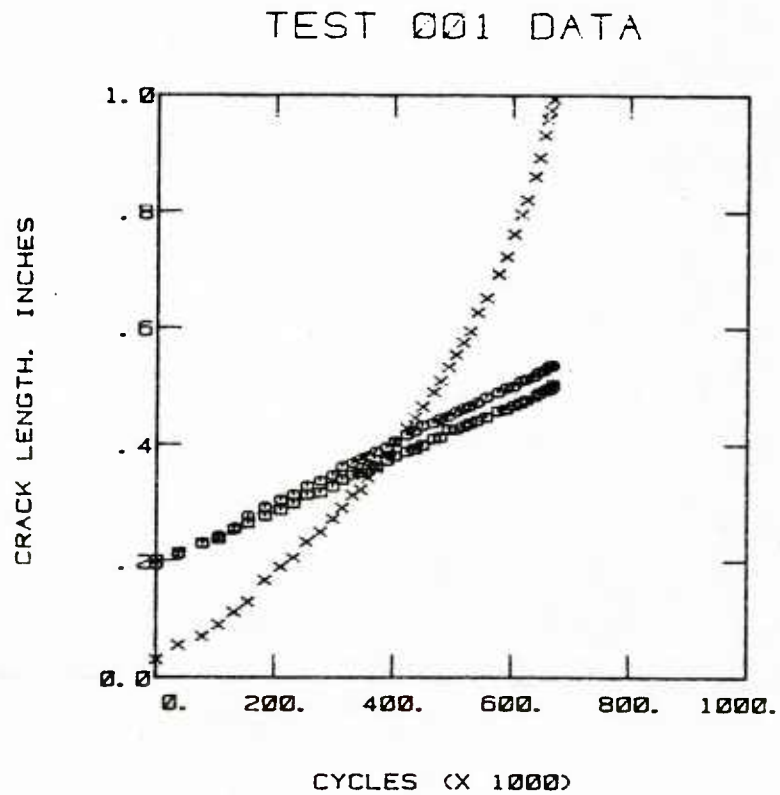
Figure A-2. Bonding Assembly

APPENDIX B
TEST DATA PLOTS

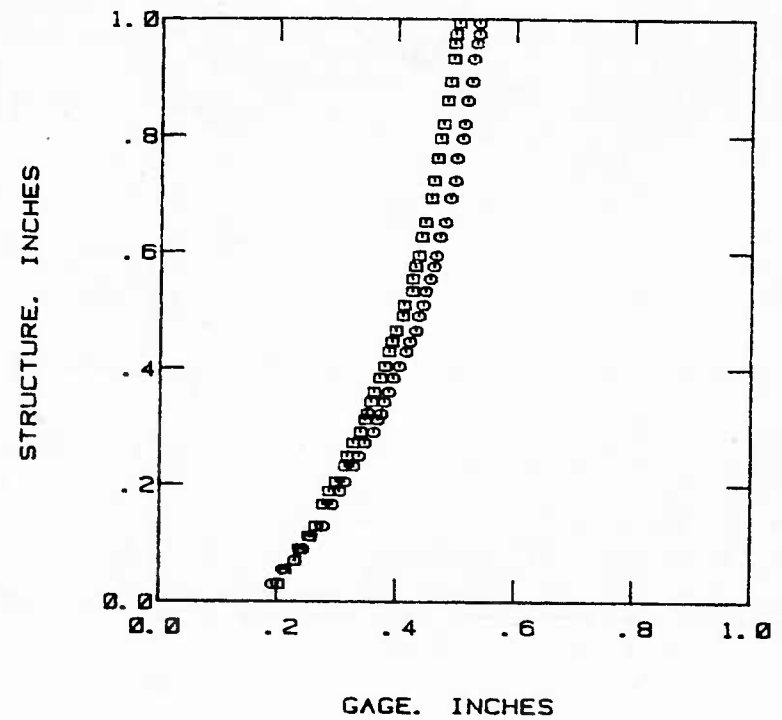
The plots of the crack growth data collected during this program are presented in this Appendix. Two types of plots are shown: the total measured crack length versus the number of cycles and the structural crack length versus the gage crack length. The second plot is commonly called the gage transfer function.

The gage identifications on each structural carrier are: Gage 1, top front; Gage 2, top rear; Gage 3, bottom front; Gage 4, bottom rear.

All structural cracks are single through-the-thickness radial cracks of length "a" out of a three-eighths inch hole. All gage cracks are through-the-thickness center cracks of length 2a.

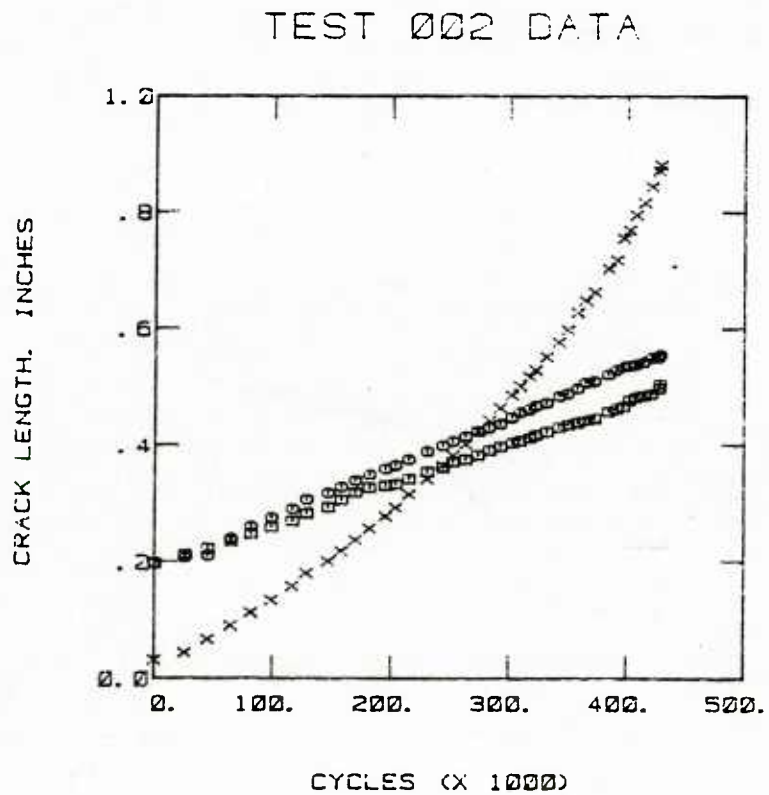


TEST 001 TRANSFER FUNCTION

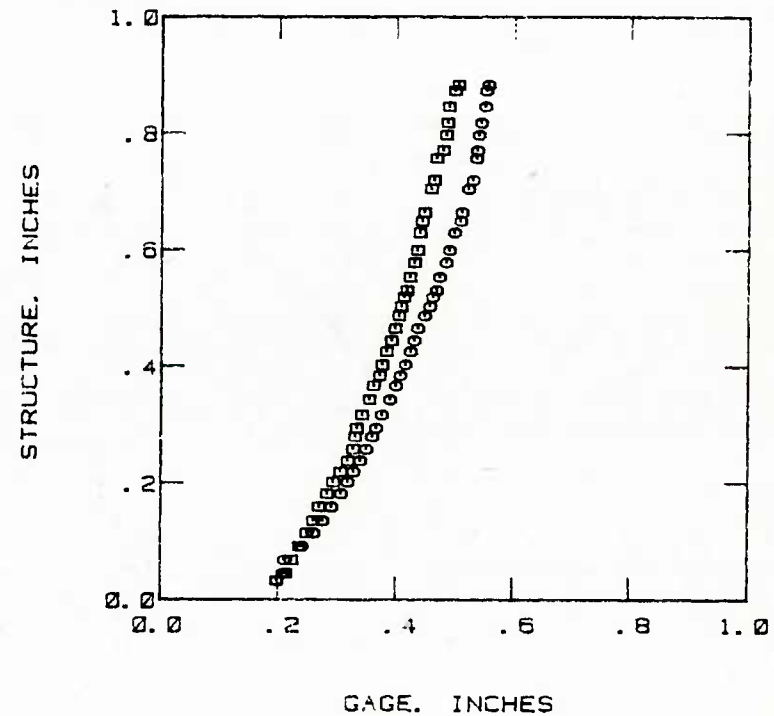


Type 1 Crack Growth Gage
 F-4 Baseline Spectrum
 X Structure
 O Gage No. 1
 □ Gage No. 2

Figure B-1. Crack Growth Data for Test 001

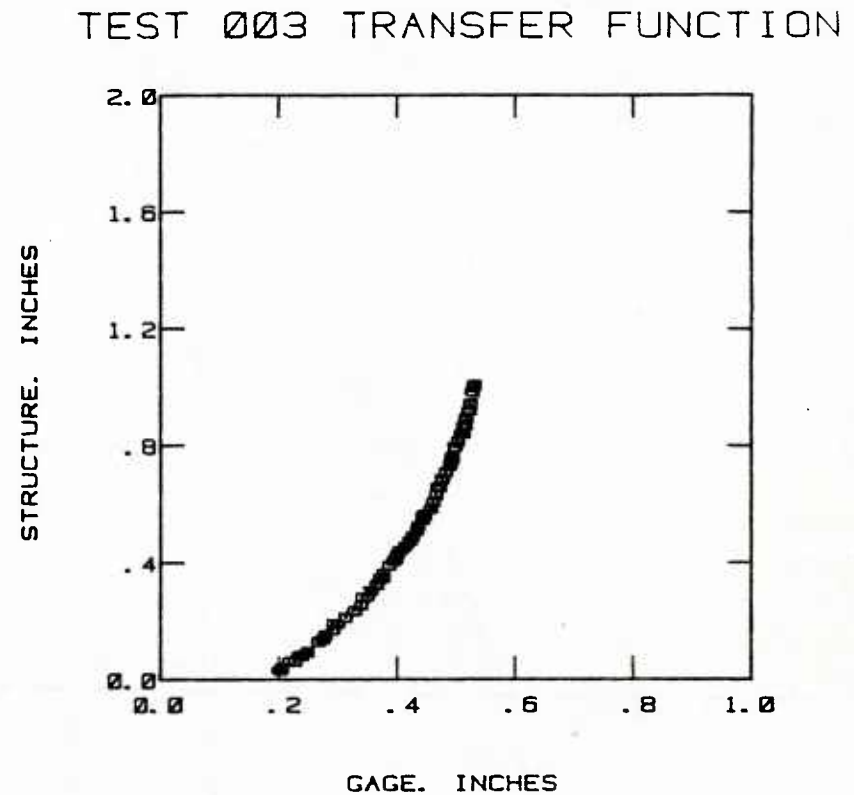
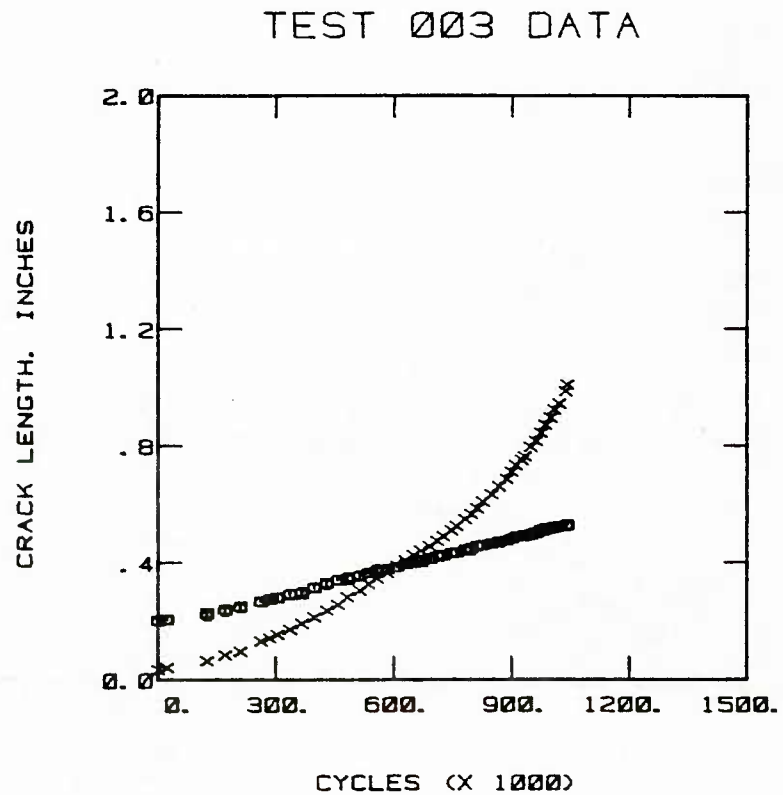


TEST 002 TRANSFER FUNCTION



Type 1 Crack Growth Gage
 F-4 Severe Spectrum
 X Structure
 O Gage No. 1
 □ Gage No. 2

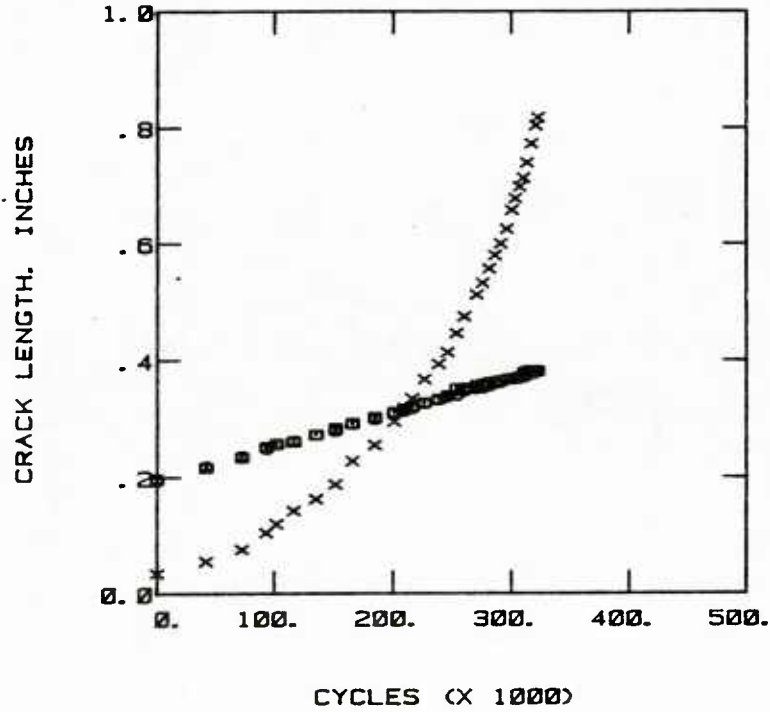
Figure B-2. Crack Growth Data for Test 002



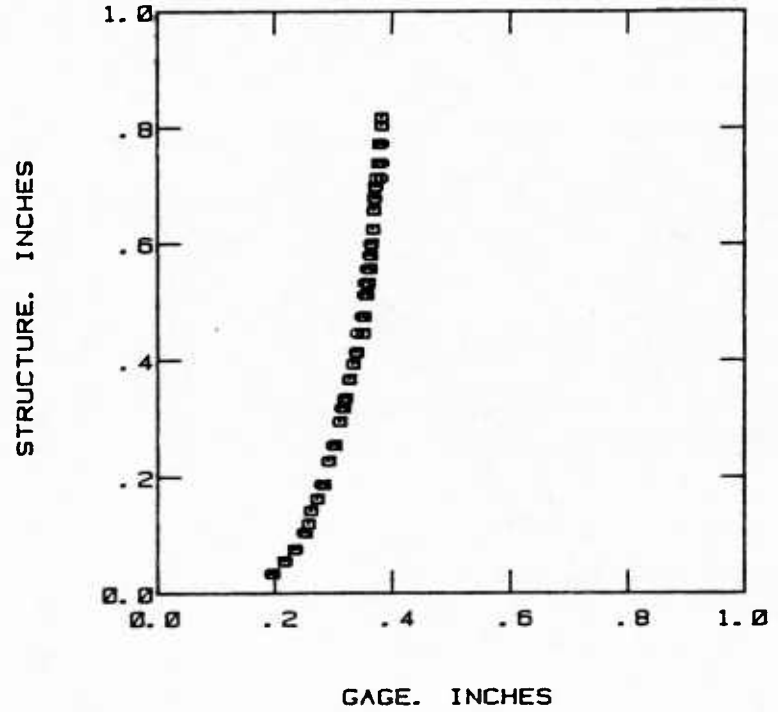
Type 1 Crack Growth Gage
 F-4 Mild Spectrum
 X Structure
 O Gage No. 1
 □ Gage No. 2

Figure B-3. Crack Growth Data for Test 003

TEST 004 DATA

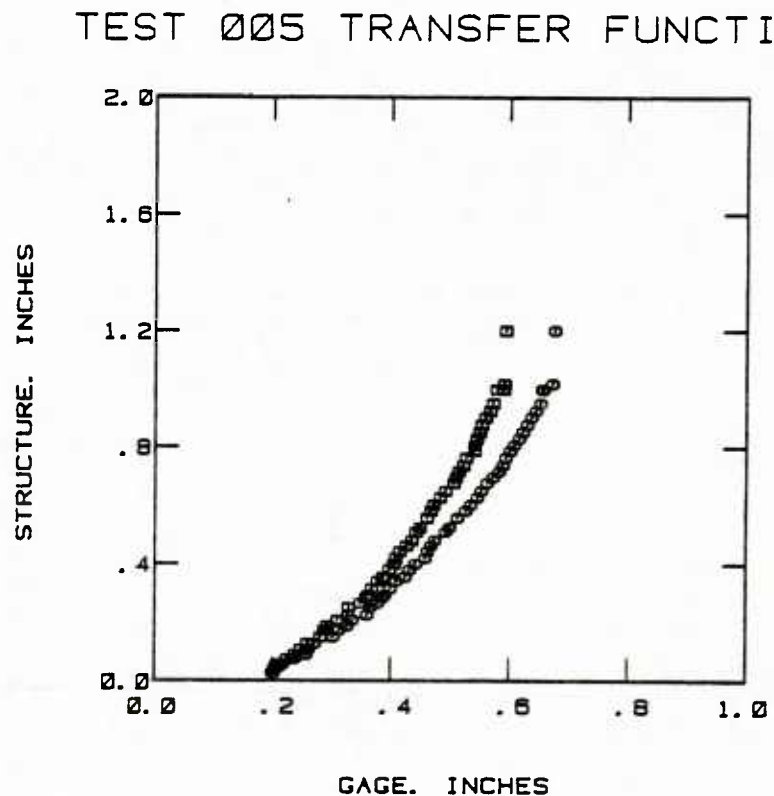
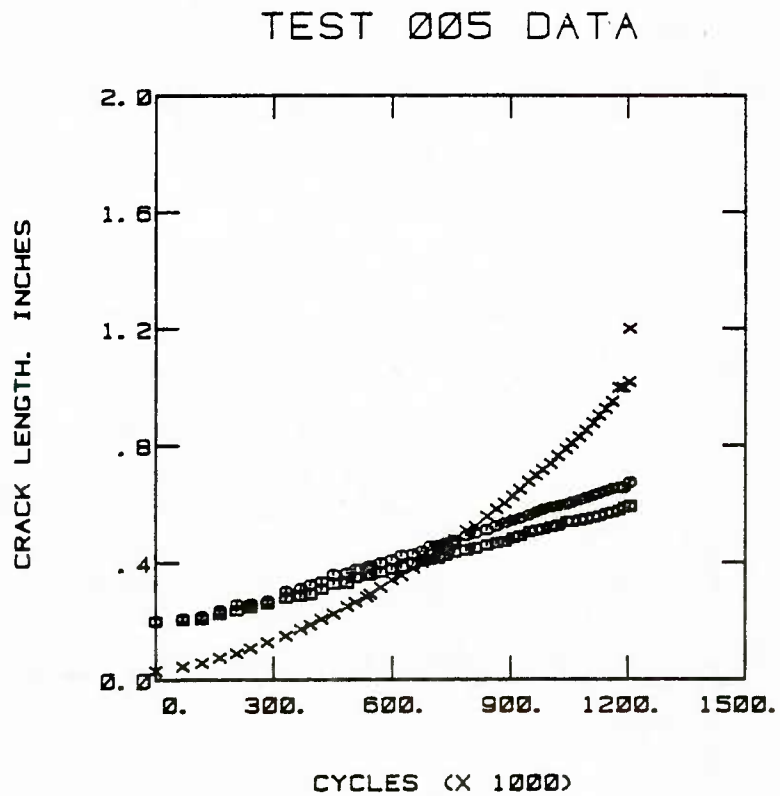


TEST 004 TRANSFER FUNCTION



Type 1 Crack Growth Gage
F-4 High Level Baseline
X Structure
O Gage No. 1
□ Gage No. 2

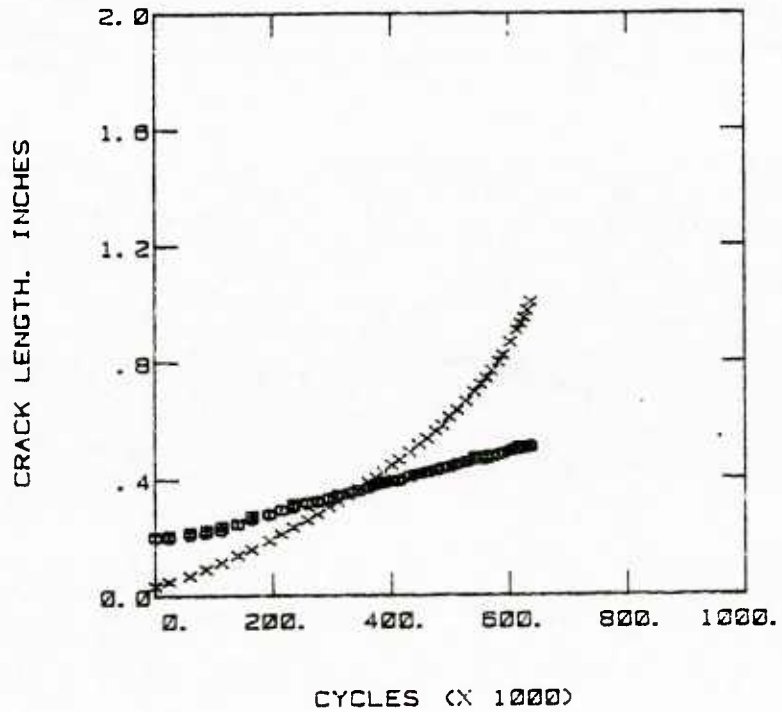
Figure B-4. Crack Growth Data for Test 004



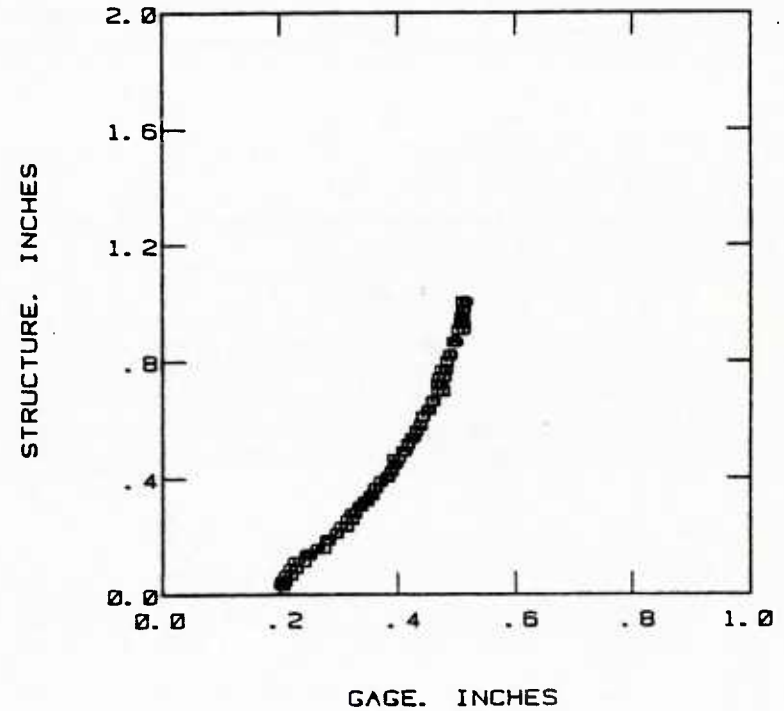
Type 1 Crack Growth Gage
F-4 Low Level Baseline
X Structure
o Gage No. 1
□ Gage No. 2

Figure B-5. Crack Growth Data for Test 005

TEST 006 DATA



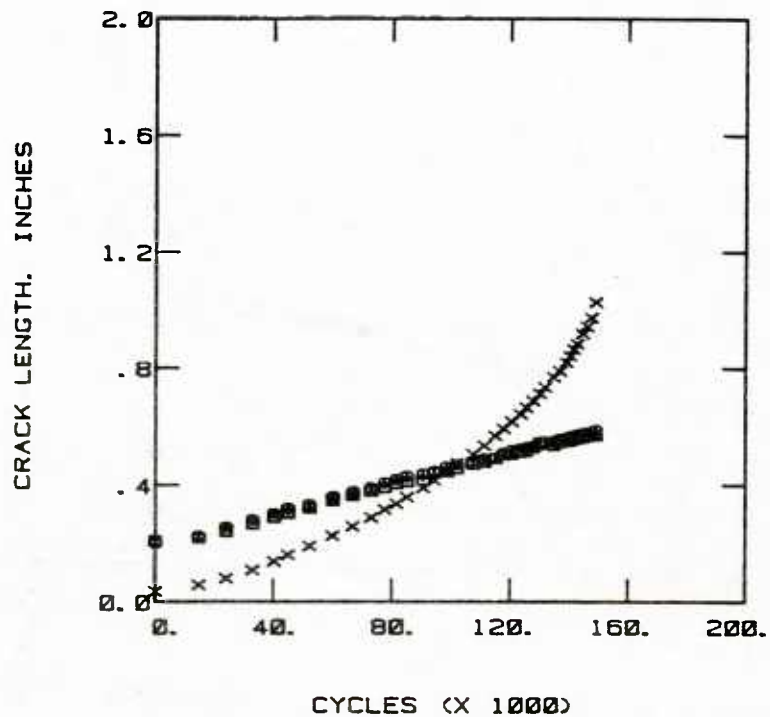
TEST 006 TRANSFER FUNCTION



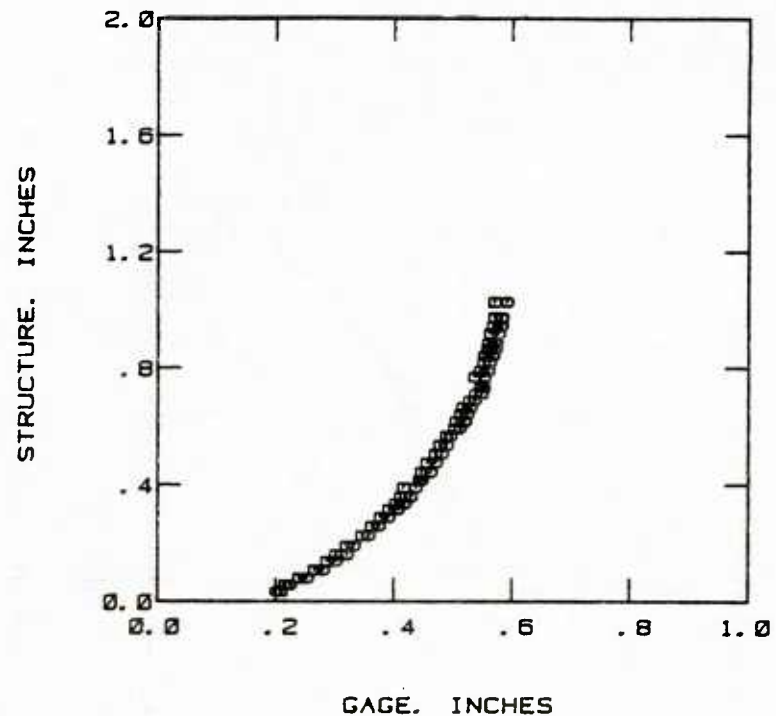
Type 1 Crack Growth Gage
 F-4 Baseline Spectrum (Repeat)
 X Structure
 O Gage No. 1
 □ Gage No. 2

Figure B-6. Crack Growth Data for Test 006

TEST 007 DATA



TEST 007 TRANSFER FUNCTION



Type 1 Crack Growth Gage

F-4 Baseline Spectrum (Deleted Cycles Less Than 50% of Maximum)

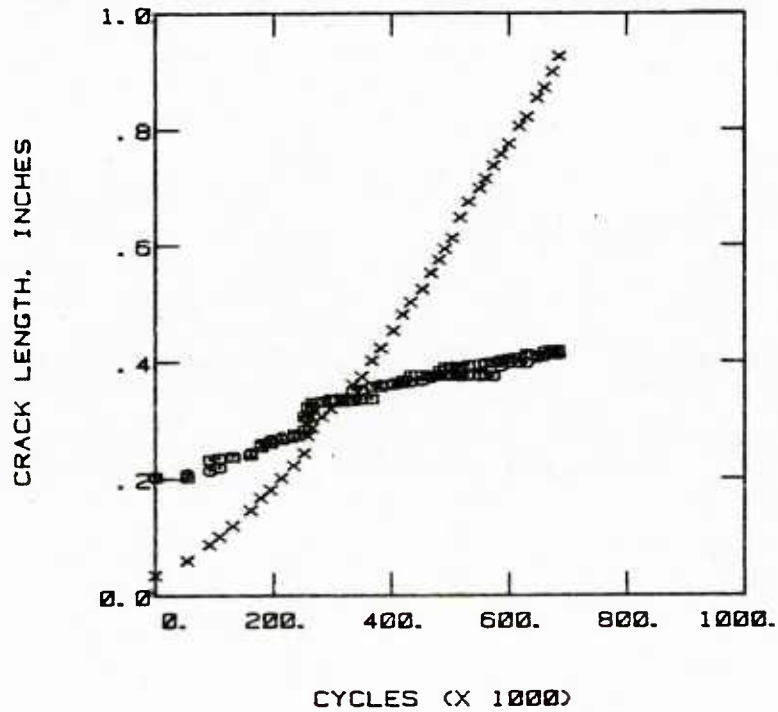
X Structure

○ Gage No. 1

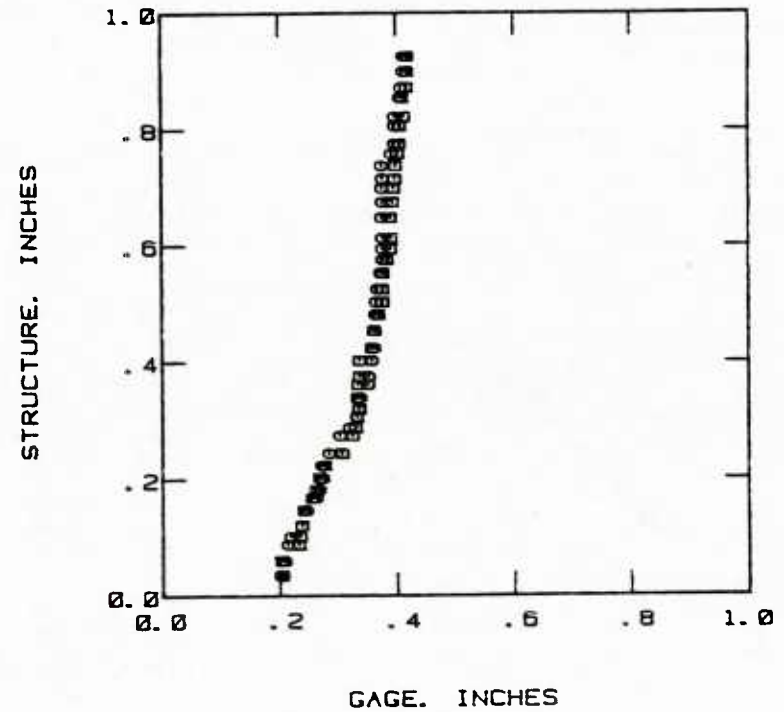
□ Gage No. 2

Figure B-7. Crack Growth Data for Test 007

TEST 008 DATA



TEST 008 TRANSFER FUNCTION

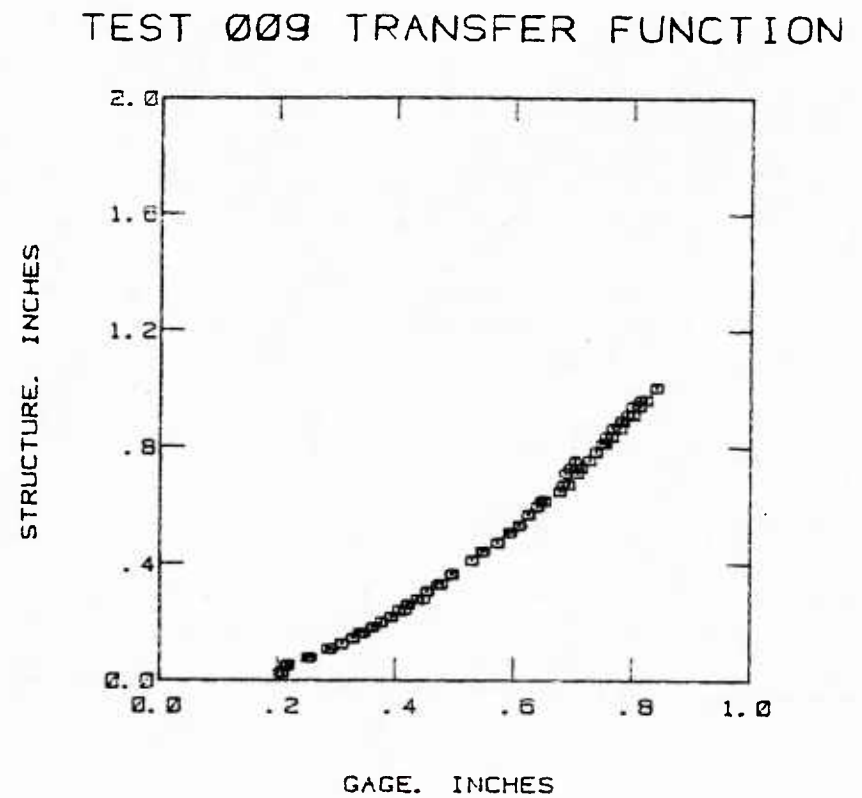
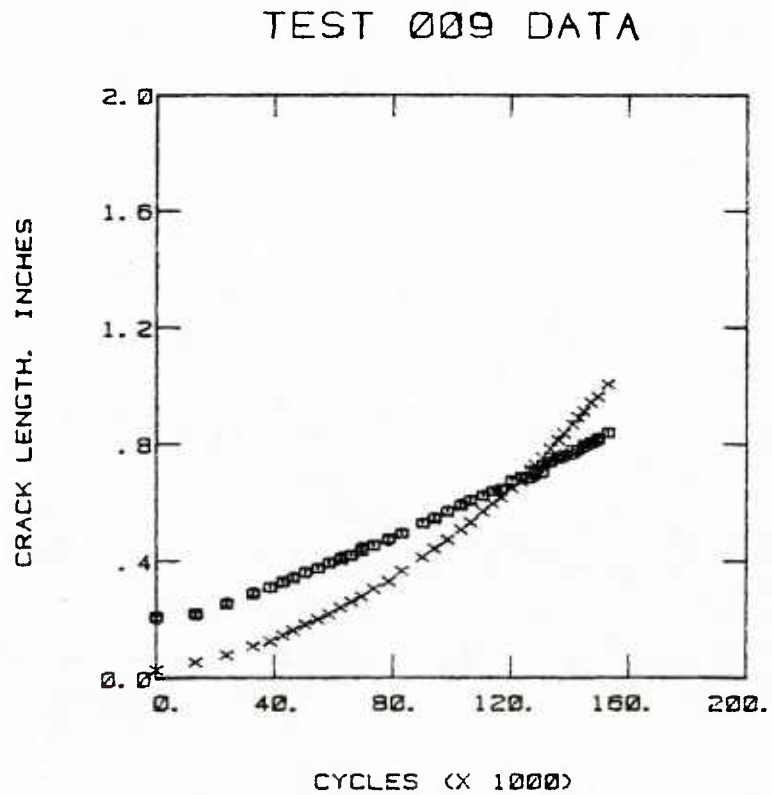


Type 1 Crack Growth Gage

F-4 Baseline (Added 125% Overload Every
2100 Cycles After First 251,000 Cycles)

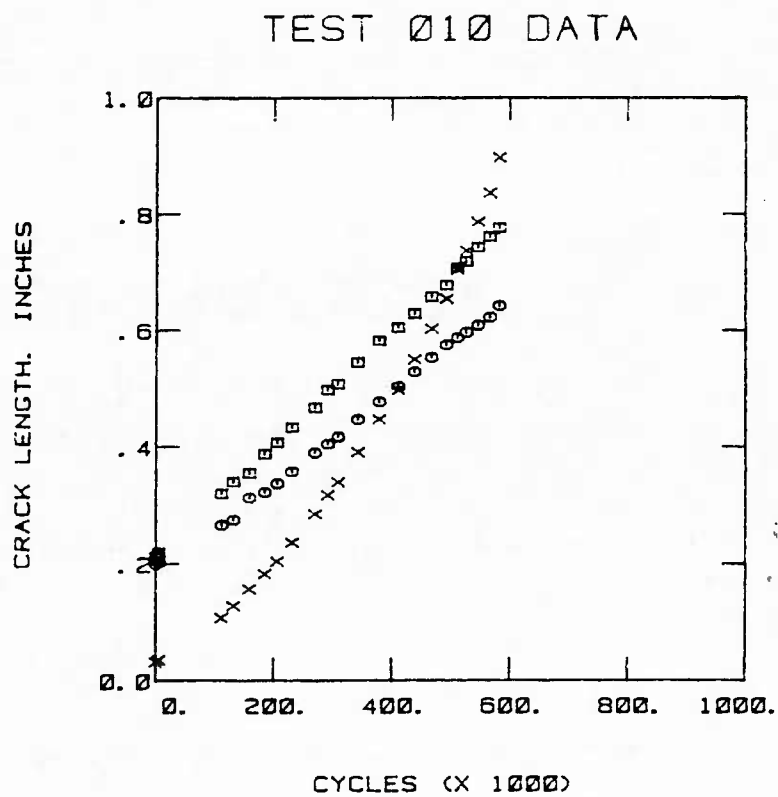
- X Structure
- O Gage No. 1
- Gage No. 2

Figure B-8. Crack Growth Data for Test 008

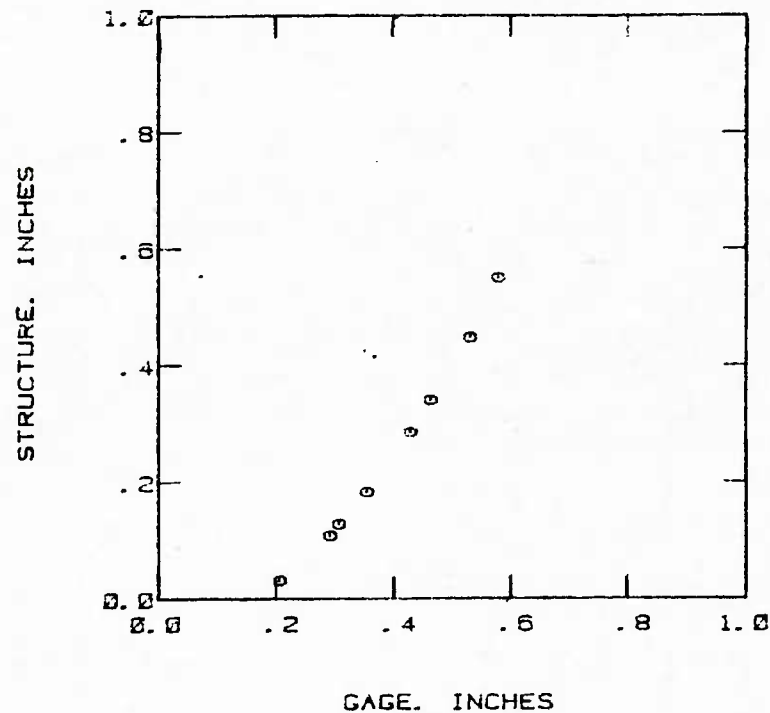


Type 1 Crack Growth Gage
 F-4 Baseline (Deleted Cycles
 Greater Than 70% of Maximum)
 X Structure
 O Gage No. 1
 □ Gage No. 2

Figure B-9. Crack Growth Data for Test 009

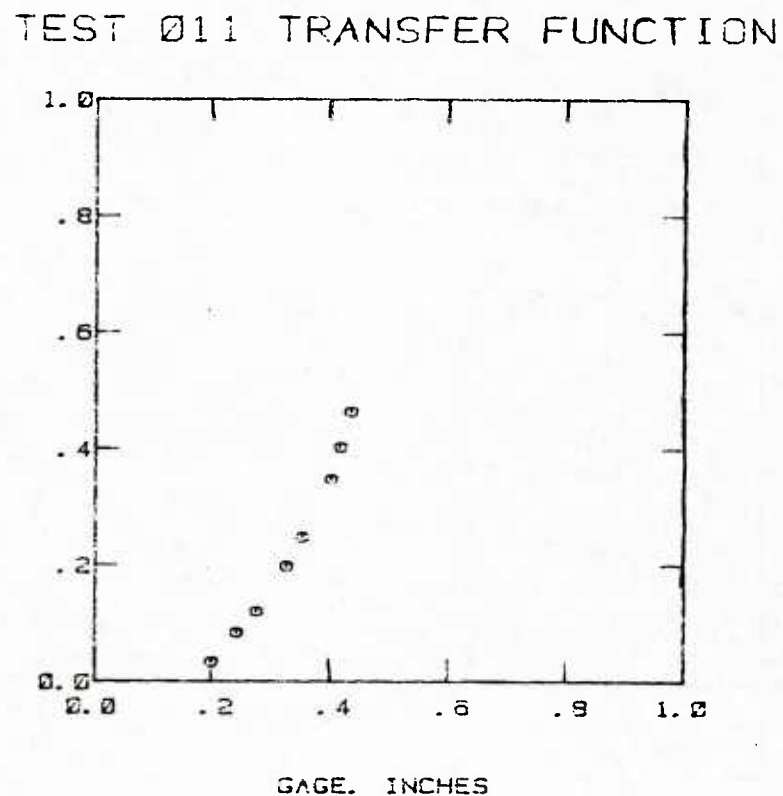
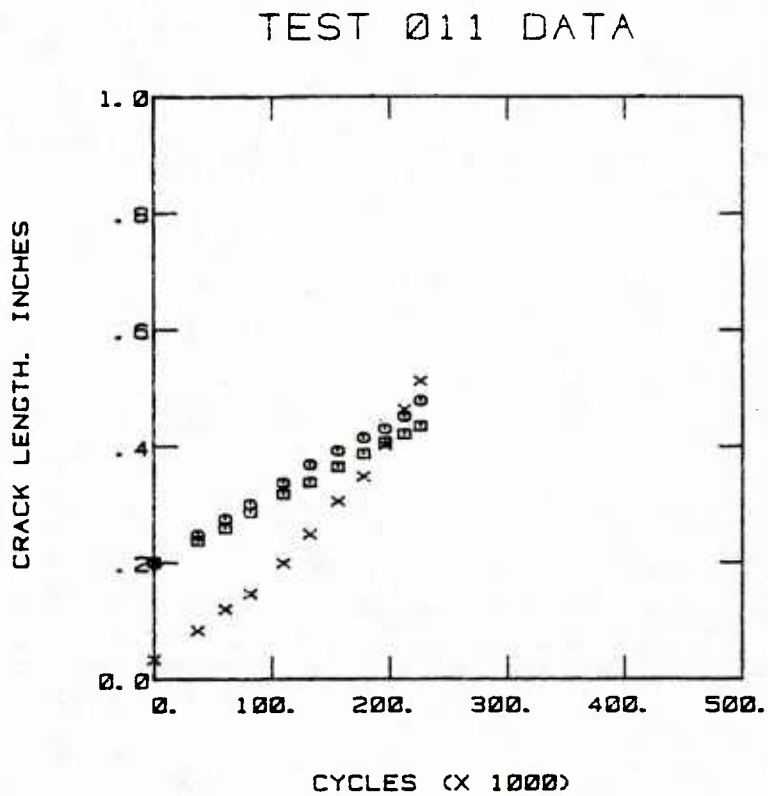


TEST 010 TRANSFER FUNCTION



Type 2 Crack Growth Gage
 F-4 Baseline Spectrum
 X Structure
 O Gage No. 1
 square Gage No. 2

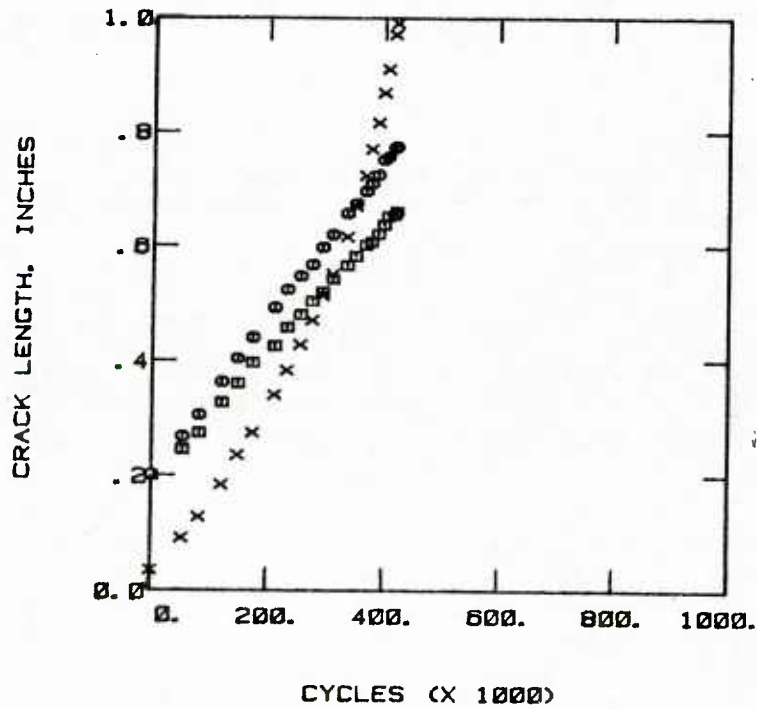
Figure B-10. Crack Growth Data for Test 010



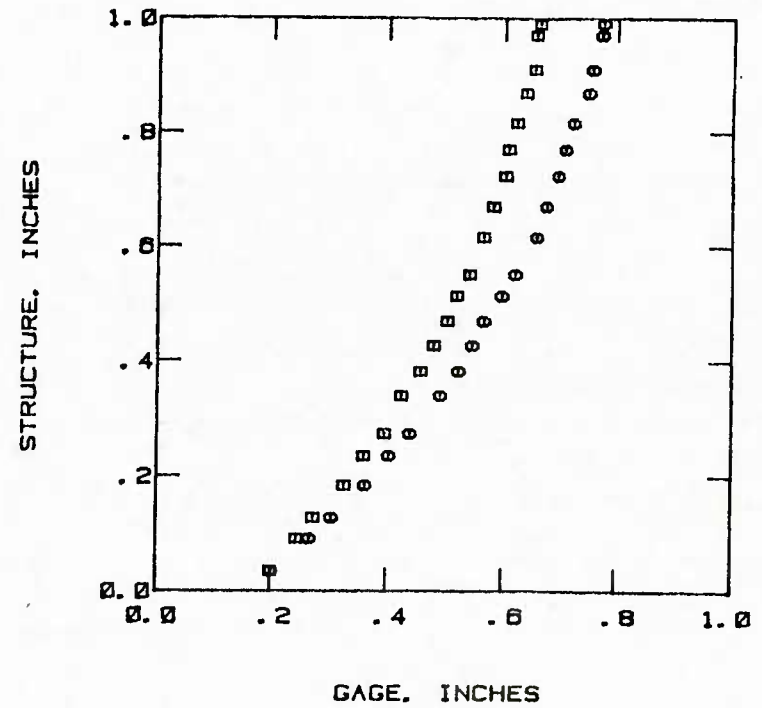
- Type 2 Crack Growth Gage
- F-4 High Level Baseline Spectrum
- X Structure
- O Gage No. 1
- Gage No. 2

Figure B-11. Crack Growth Data for Test 011

TEST 012 DATA



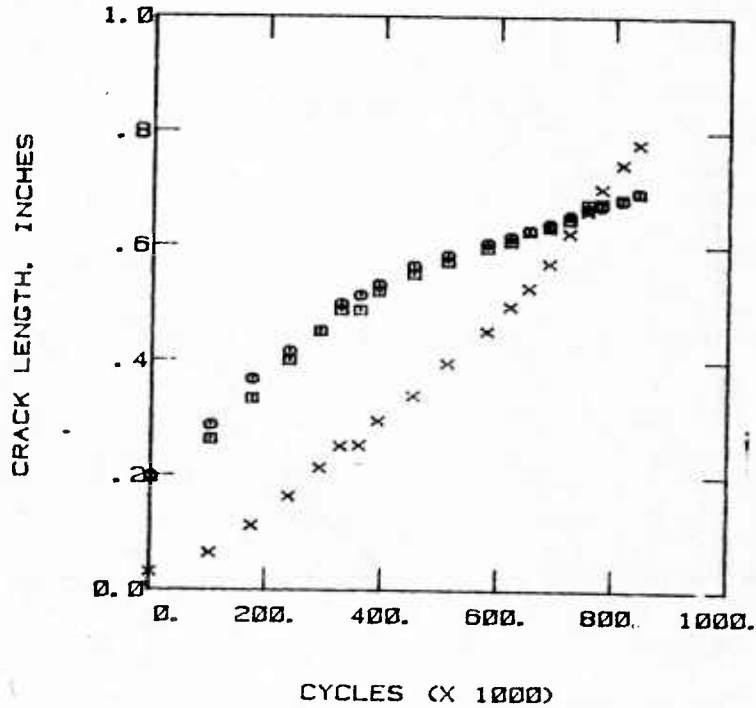
TEST 012 TRANSFER FUNCTION



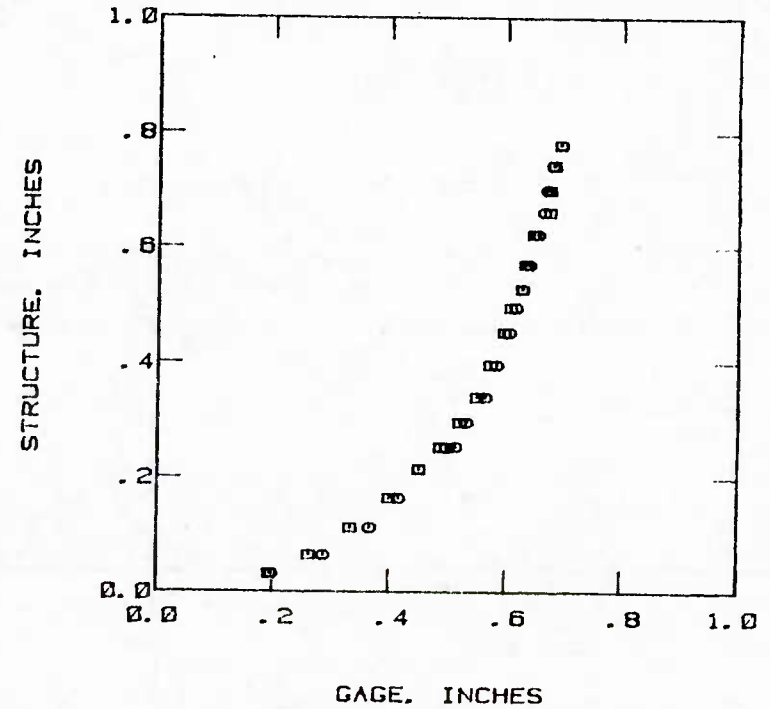
Type 2 Crack Growth Gage
 F-4 Severe Spectrum
 X Structure
 O Gage No. 1
 □ Gage No. 2

Figure B-12. Crack Growth Data for Test 012

TEST 013 DATA



TEST 013 TRANSFER FUNCTION



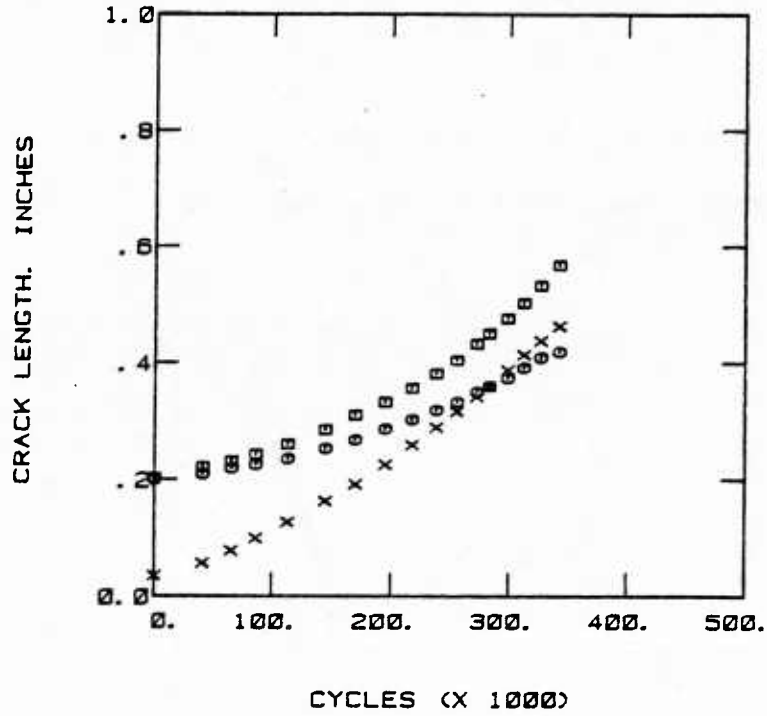
Type 2 Crack Growth Gage

F-4 Baseline (Added 125% Overload Every 2100 Cycles After First 330,000 Cycles)

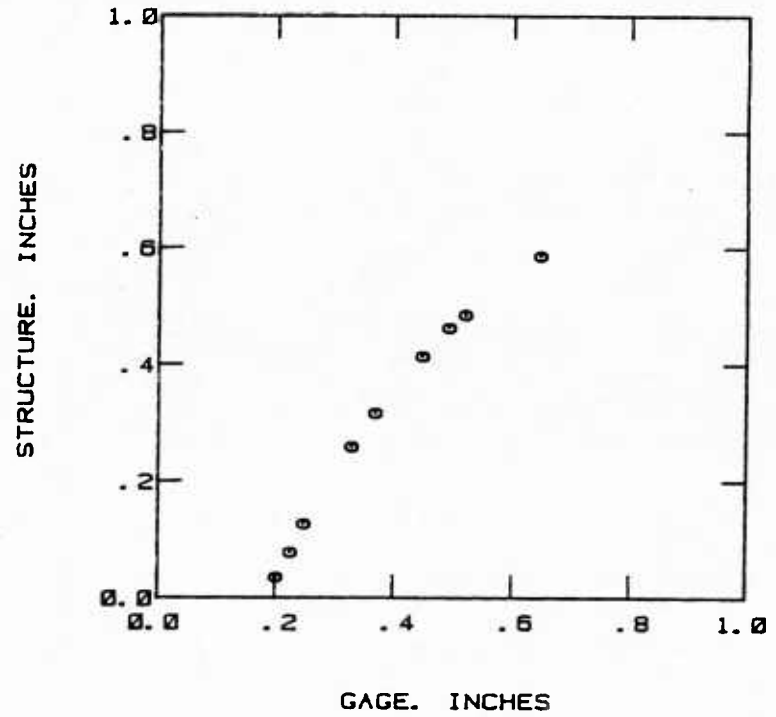
- X Structure
- O Gage No. 1
- Gage No. 2

Figure B-13. Crack Growth Data for Test 013

TEST 014 DATA

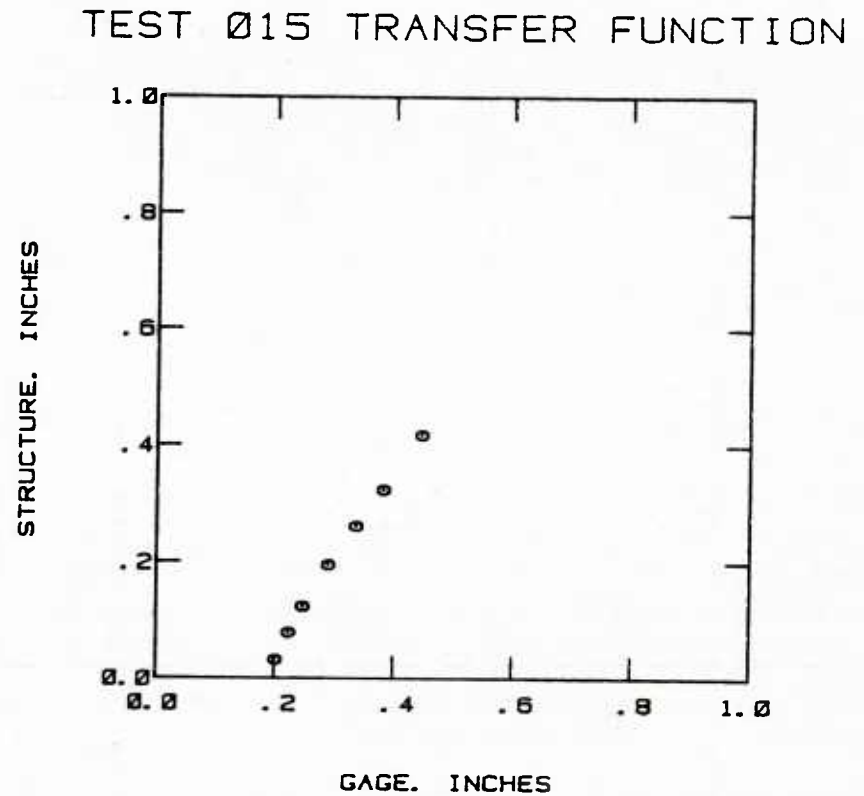
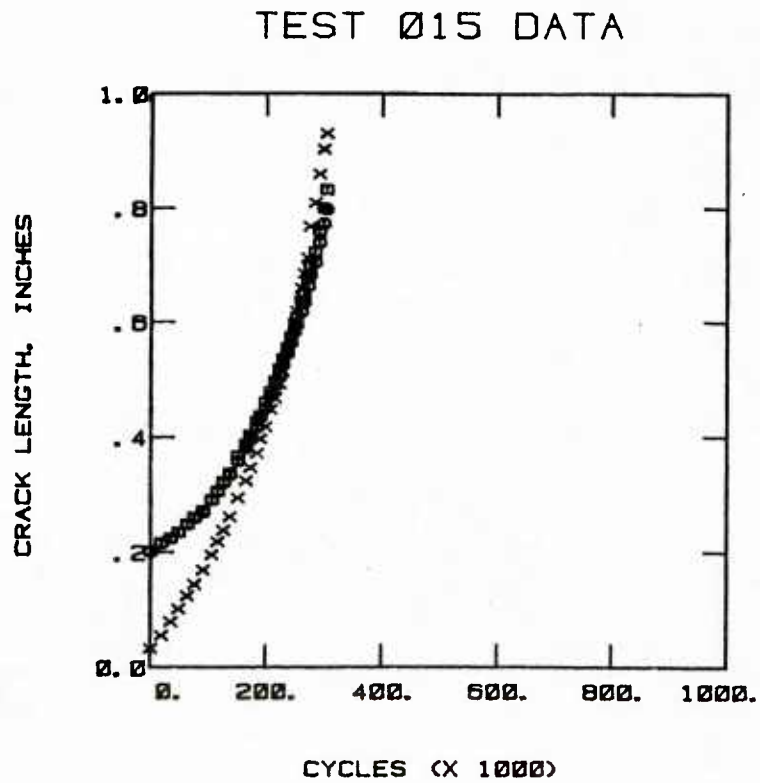


TEST 014 TRANSFER FUNCTION



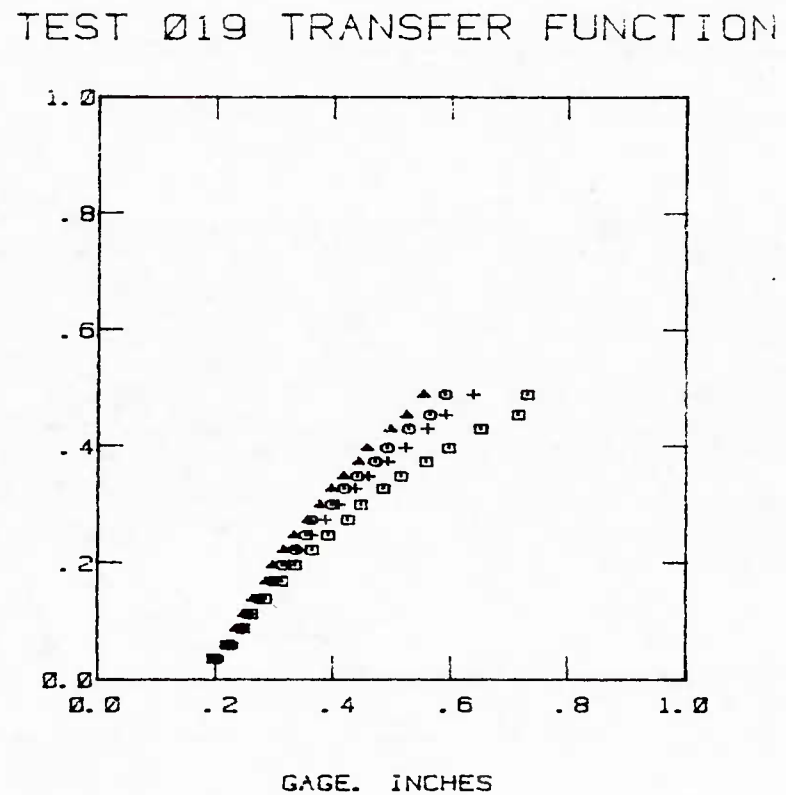
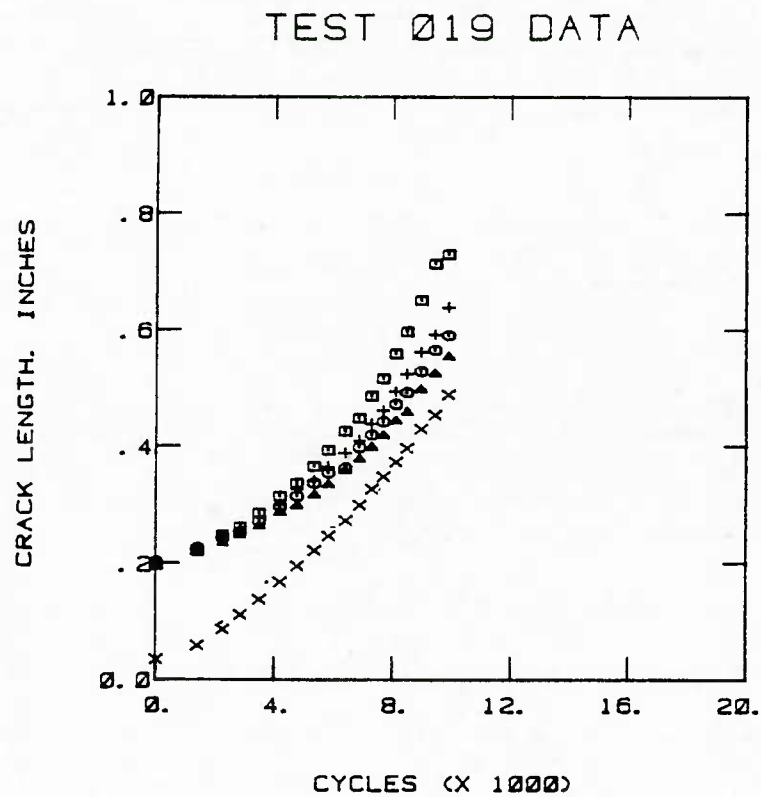
Modified Type 2 Crack Growth Gage
 F-4 Baseline Spectrum
 X Structure
 O Gage No. 1
 □ Gage No. 2

Figure B-14. Crack Growth Data for Test 014



Modified Type 2 Crack Growth Gage
 F-4 High Level Baseline Spectrum
 X Structure
 O Gage No. 1
 □ Gage No. 2

Figure B-15. Crack Growth Data for Test 015



Modified Type 2 Crack Growth Gage

16 KSI Max Stress, $R = -0.1$

X Structure

○ Gage No. 1

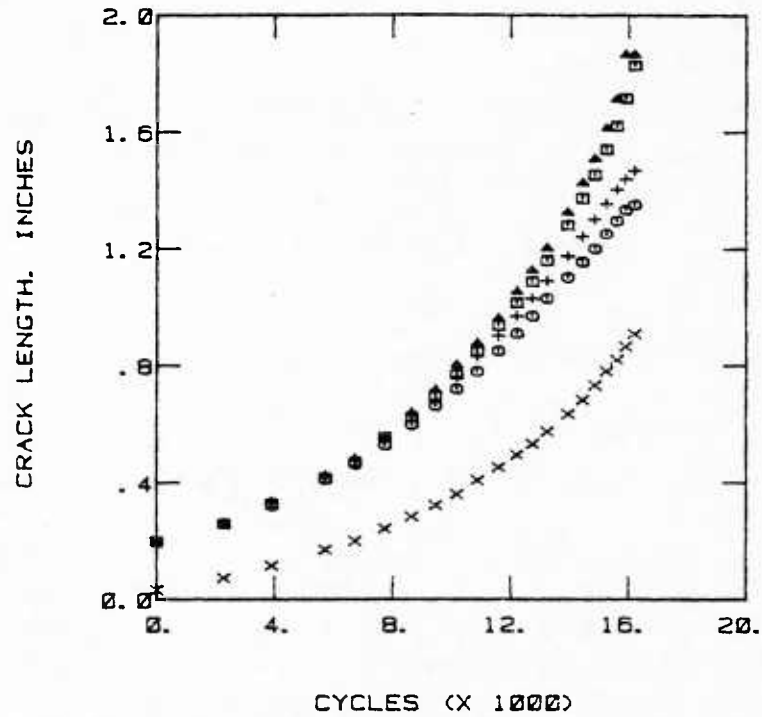
□ Gage No. 2

△ Gage No. 3

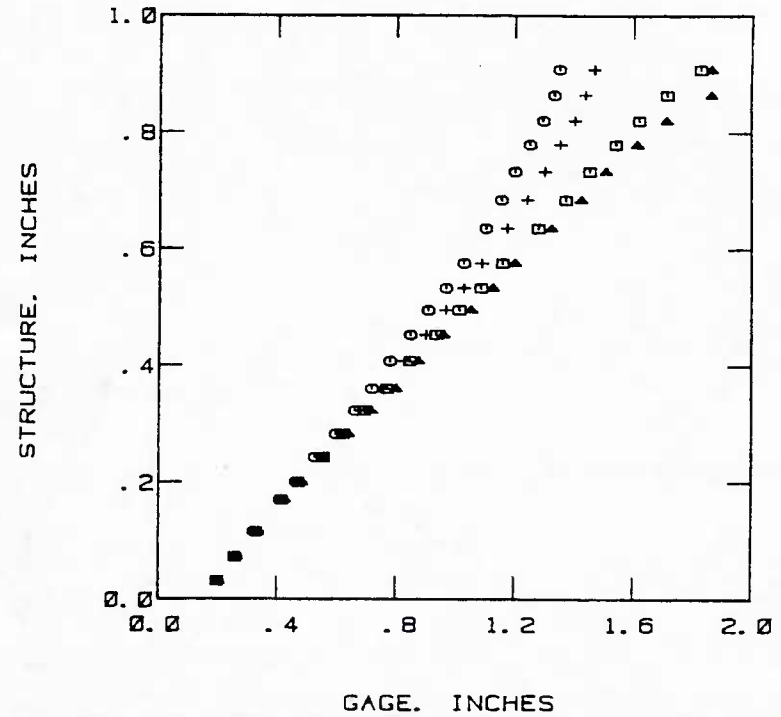
+ Gage No. 4

Figure B-16. Crack Growth Data for Test 019

TEST 020 DATA

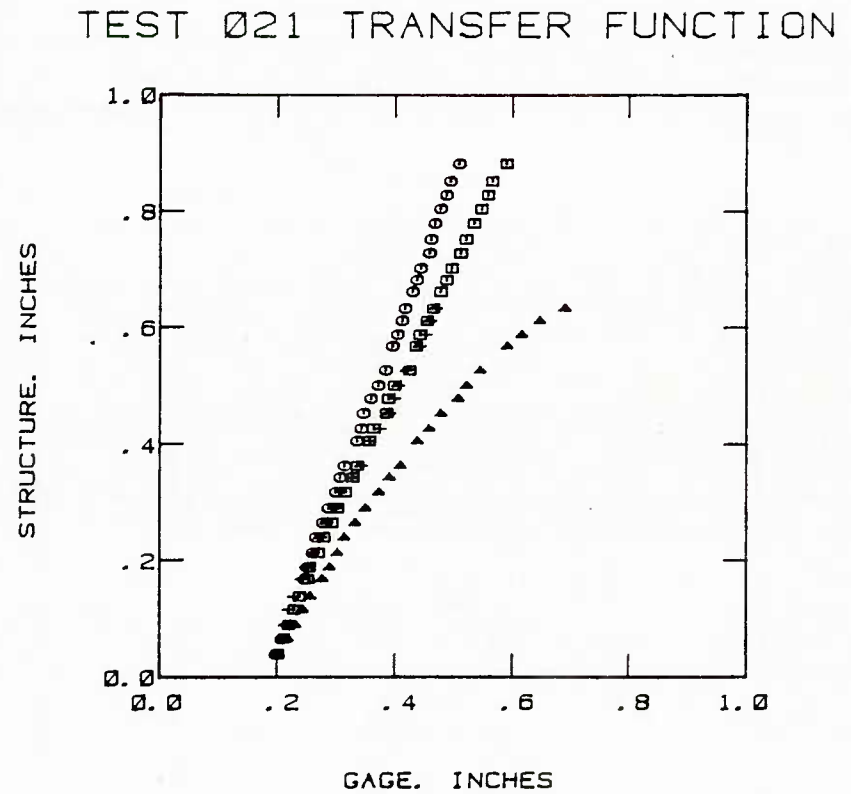
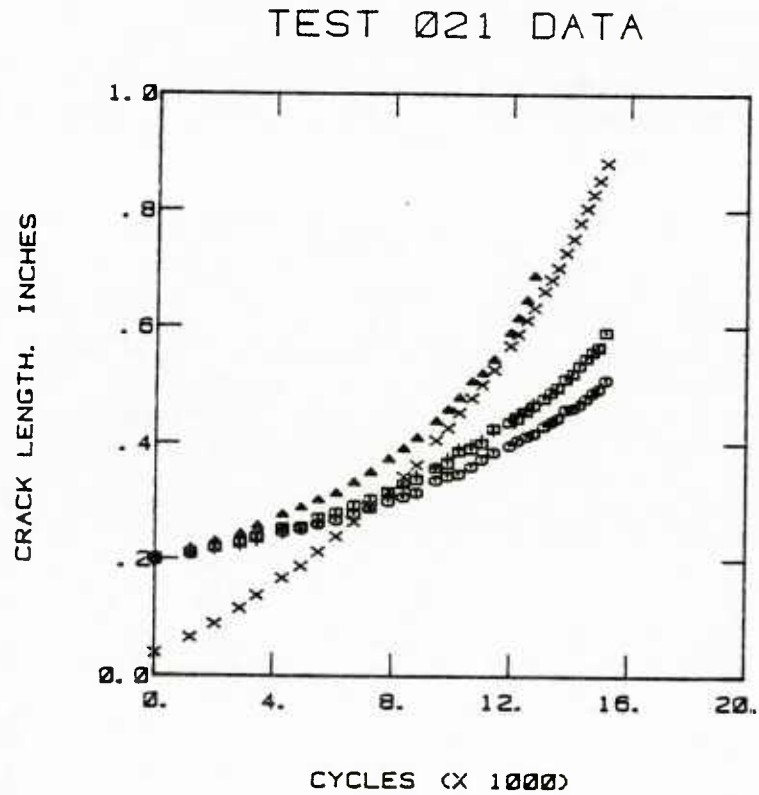


TEST 020 TRANSFER FUNCTION



Type 2 Crack Growth Gage
 16 KSI Max Stress, $R = 0.1$
 X Structure
 O Gage No. 1
 □ Gage No. 2
 △ Gage No. 3
 + Gage No. 4

Figure B-17. Crack Growth Data for Test 020



Modified Type 2 Crack Growth Gage

16 KSI Max Stress, $R = 0.3$

X Structure

○ Gage No. 1

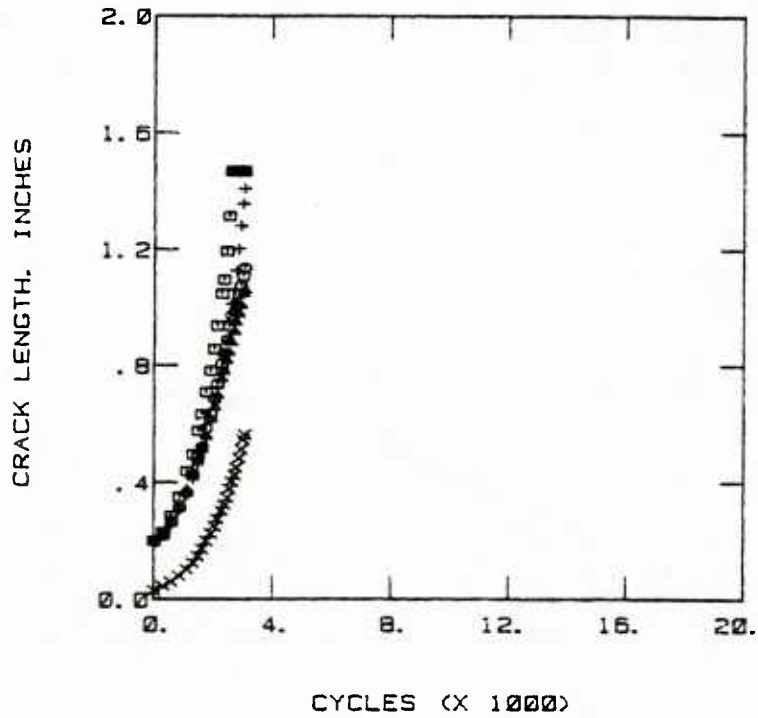
□ Gage No. 2

△ Gage No. 3

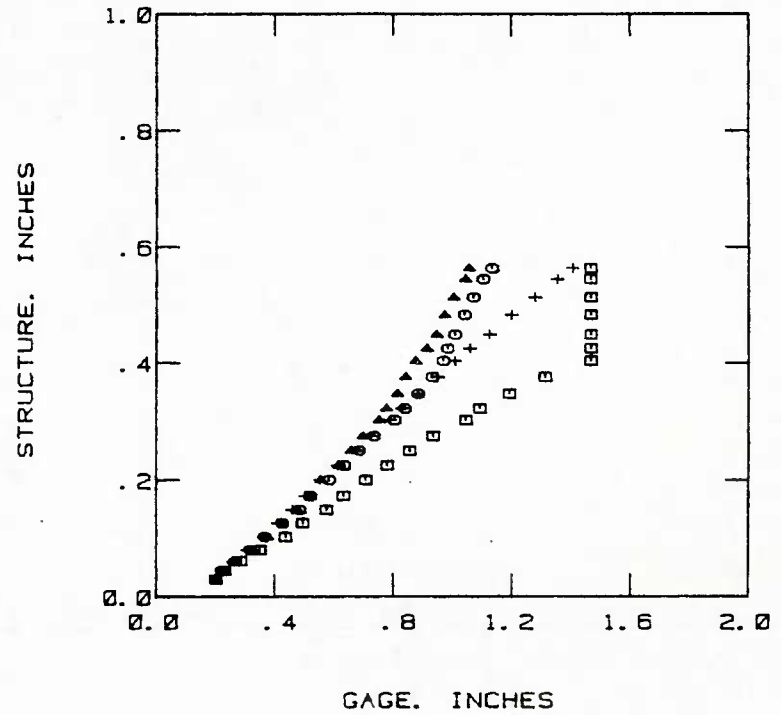
+ Gage No. 4

Figure B-18. Crack Growth Data for Test 021

TEST 022 DATA

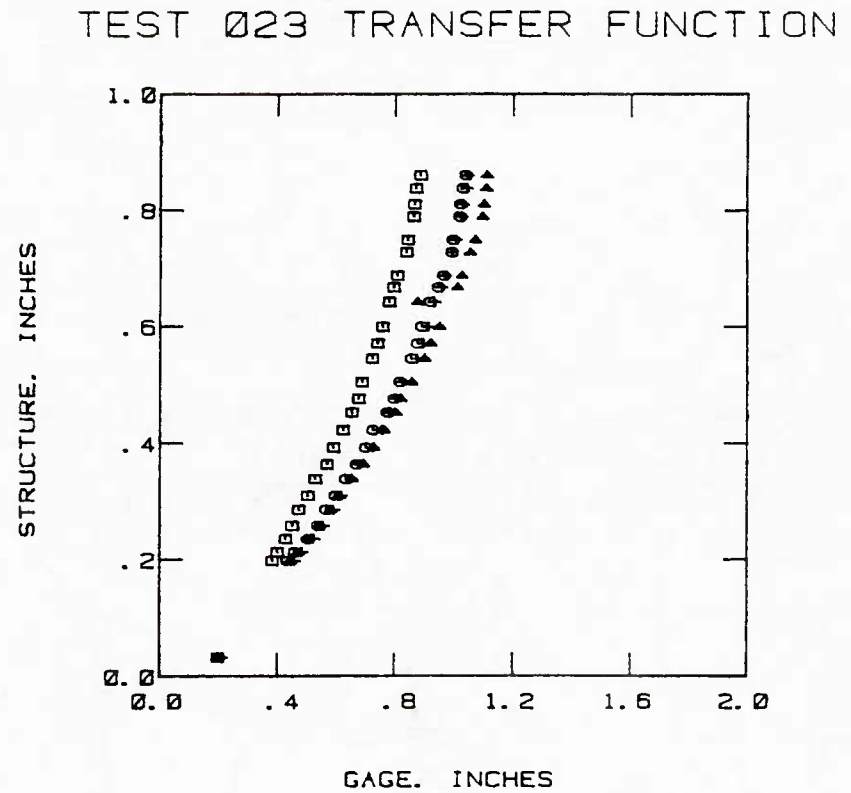
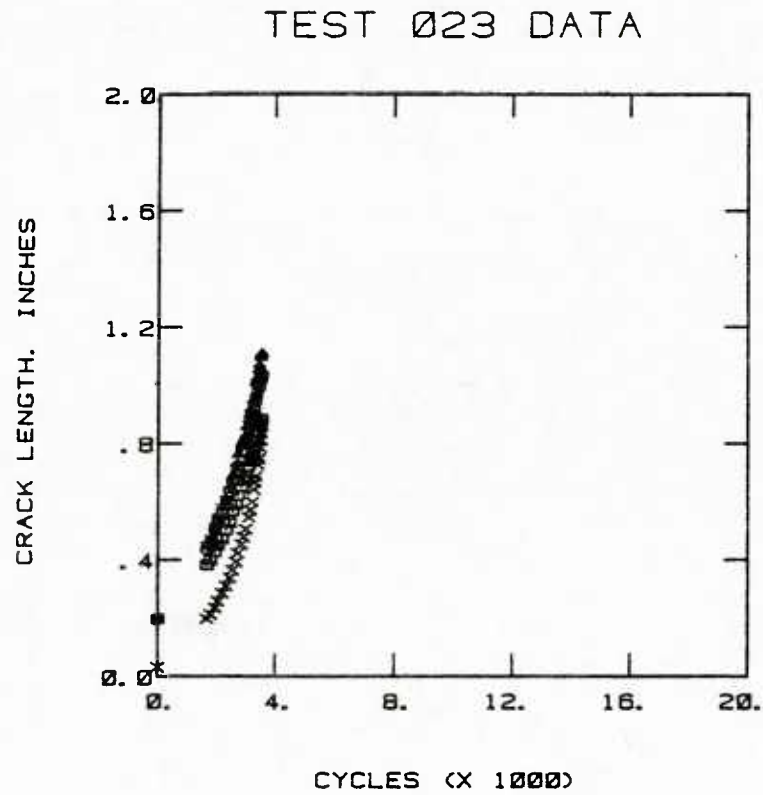


TEST 022 TRANSFER FUNCTION



- Type 2 Crack Growth Gage
- 25 KSI Max Stress, $R = -0.1$
- X Structure
- Gage No. 1
- Gage No. 2
- △ Gage No. 3
- + Gage No. 4

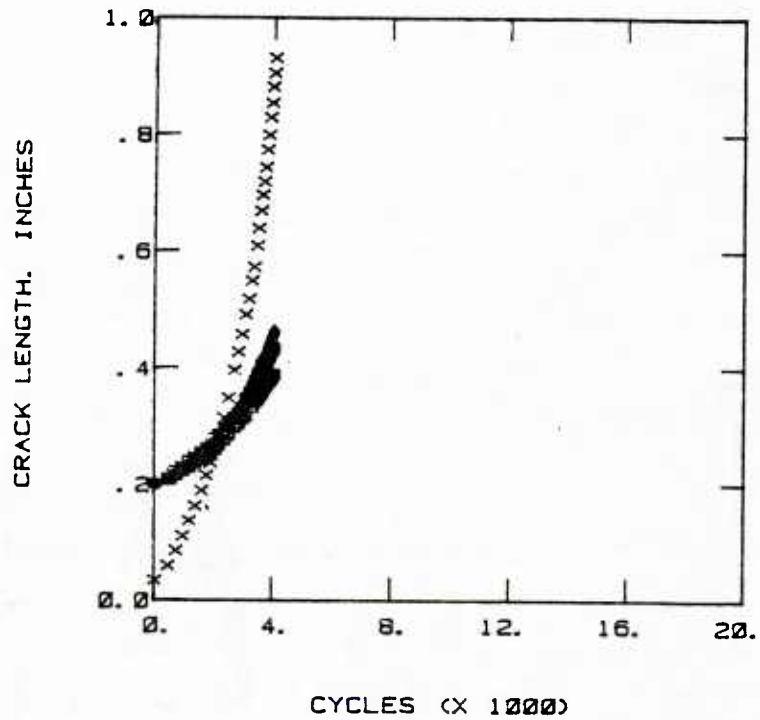
Figure B-19. Crack Growth Data for Test 022



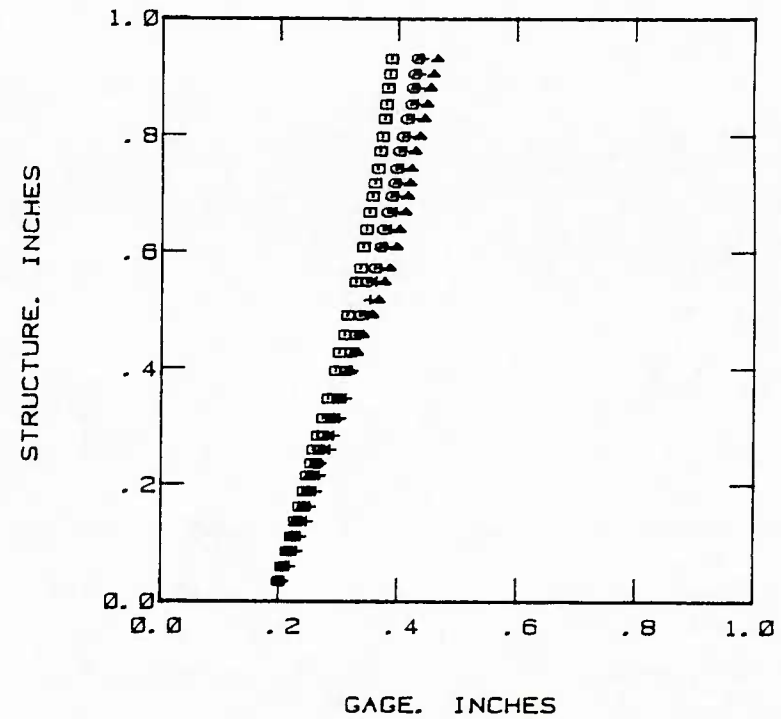
Type 2 Crack Growth Gage
 25 KSI Max Stress, $R = 0.1$
 X Structure
 O Gage No. 1
 □ Gage No. 2
 △ Gage No. 3
 + Gage No. 4

Figure B-20. Crack Growth Data for Test 023

TEST 024 DATA



TEST 024 TRANSFER FUNCTION



Modified Type 2 Crack Growth Gage

25 KSI Max Stress, $R = 0.3$

X Structure

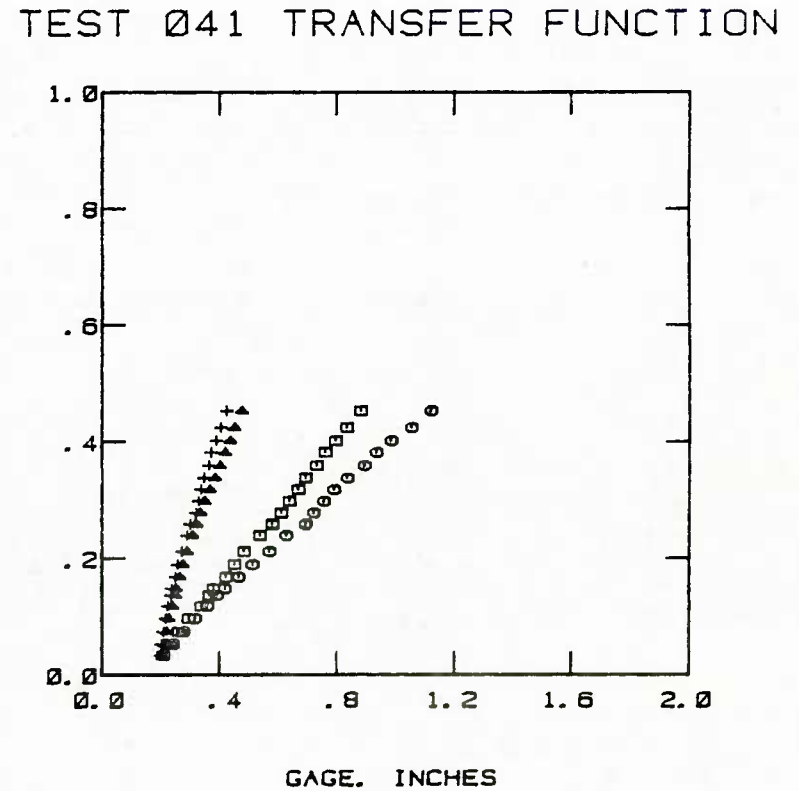
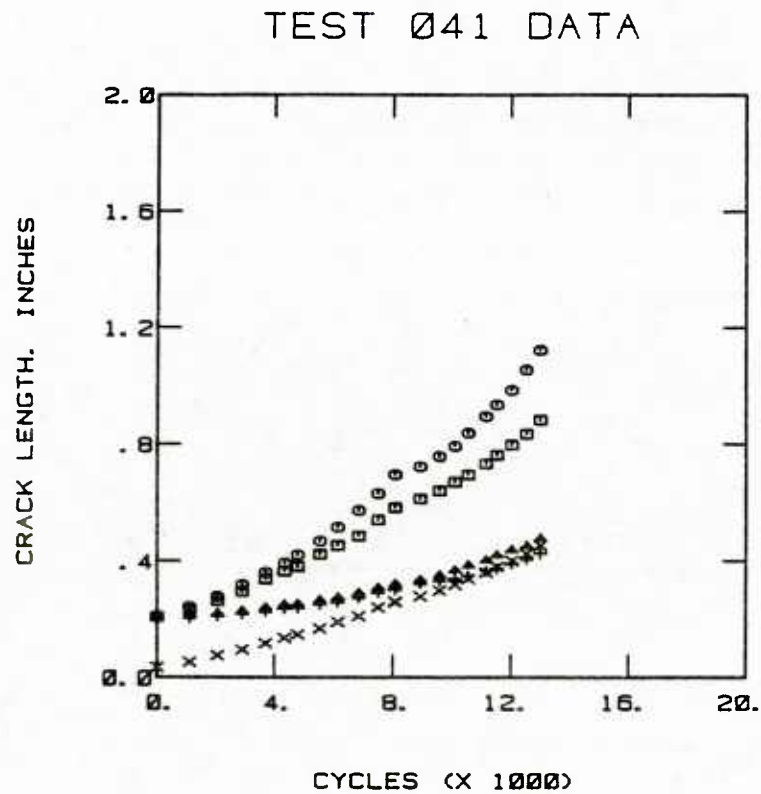
○ Gage No. 1

□ Gage No. 2

△ Gage No. 3

+ Gage No. 4

Figure B-21. Crack Growth Data for Test 024



Modified Type 2 Crack Growth Gage (Nos 1, 2)

Type 2 Crack Growth Gage (Nos 3, 4)

16 KSI Max Stress, $R = -0.1$, (150% Overload
Cycle After 8080 Cycles)

X Structure

O Gage No. 1

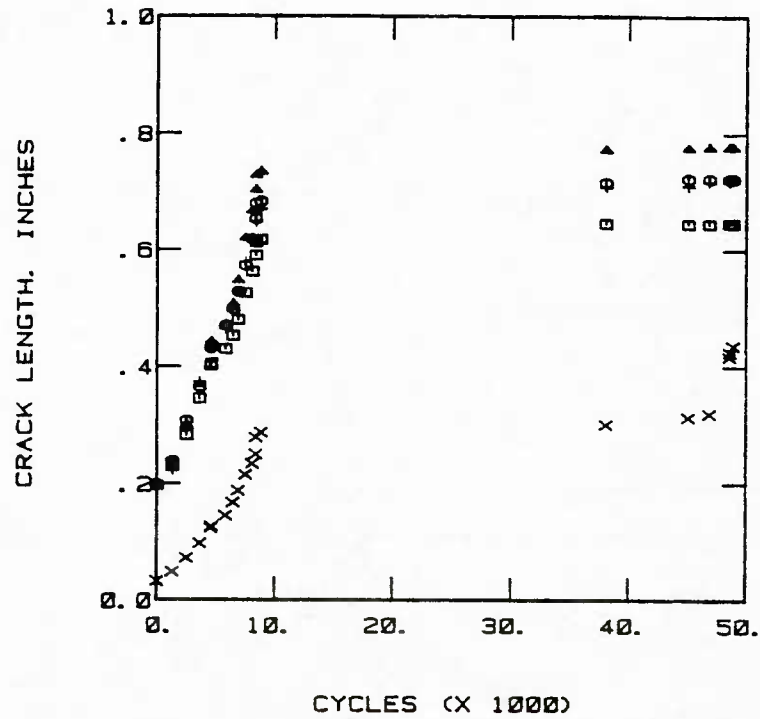
□ Gage No. 2

△ Gage No. 3

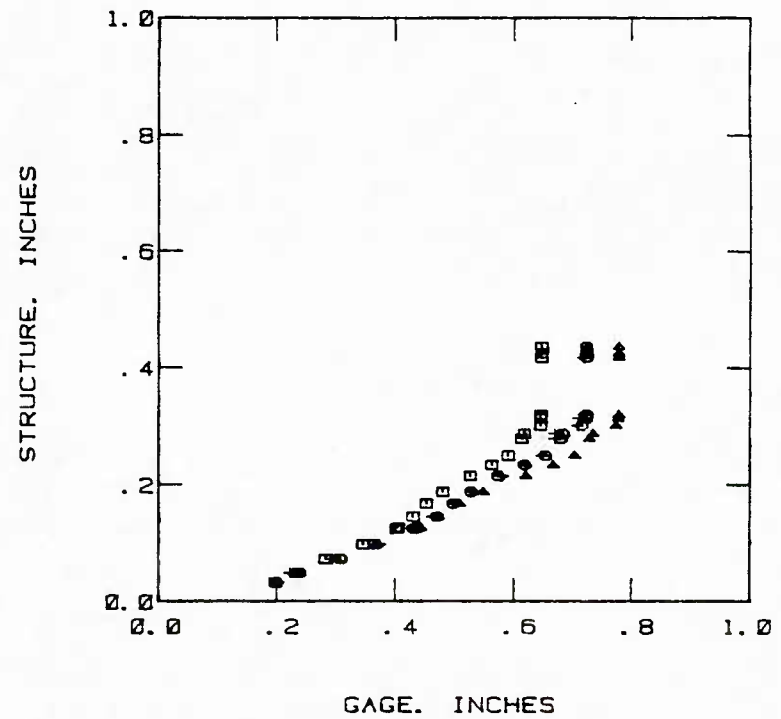
+ Gage No. 4

Figure B-22. Crack Growth Data for Test 041

TEST 042 DATA



TEST 042 TRANSFER FUNCTION



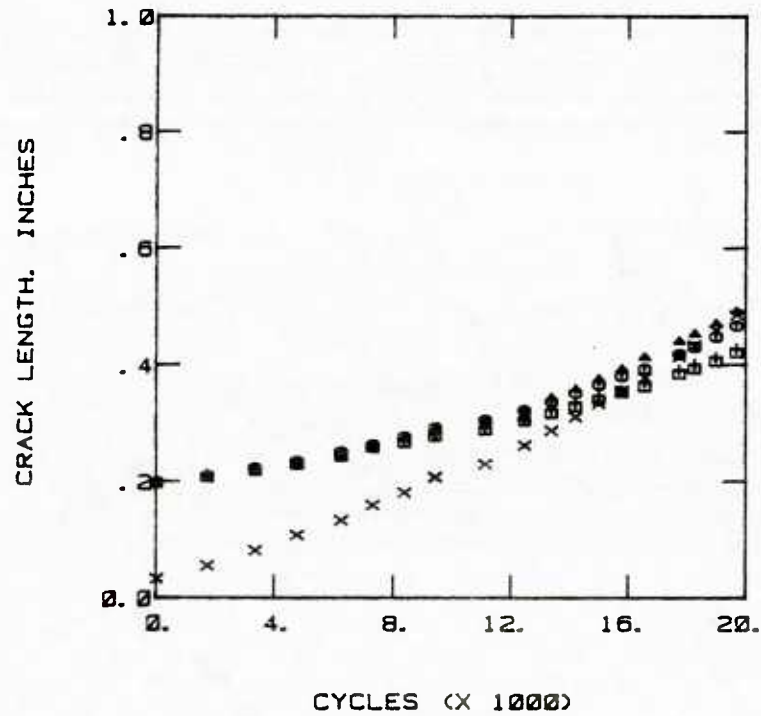
Type 2 Crack Growth Gage

16 KSI Max Stress, $R = 0.1$ (150%
Overload Cycle After 4500 Cycles)

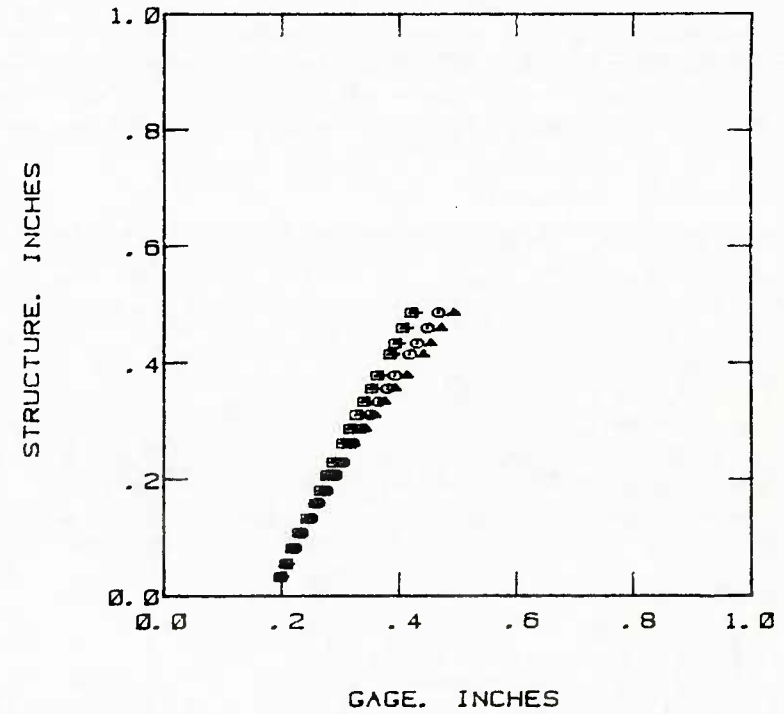
- X Structure
- O Gage No. 1
- Gage No. 2
- △ Gage No. 3
- + Gage No. 4

Figure B-23. Crack Growth Data for Test 042

TEST 043 DATA



TEST 043 TRANSFER FUNCTION



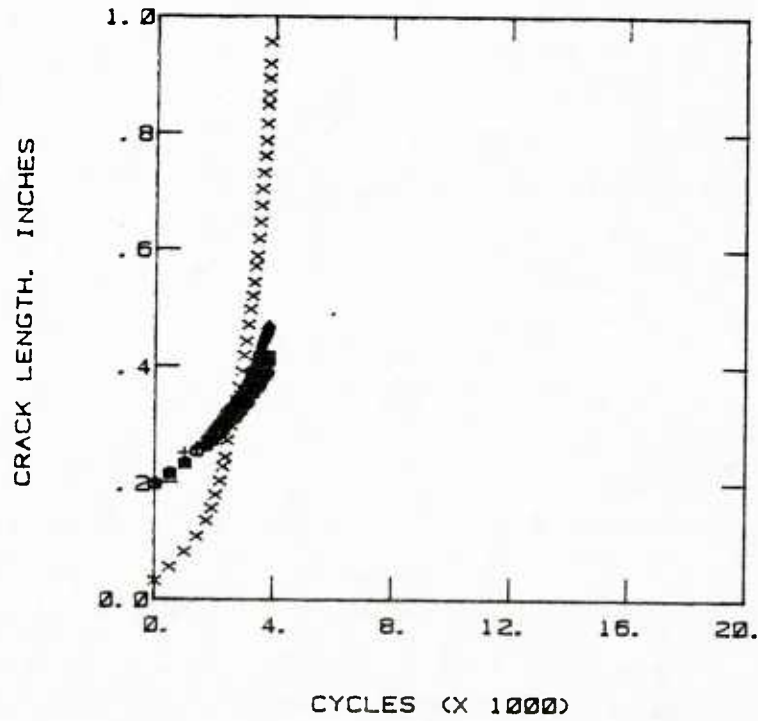
Modified Type 2 Crack Growth Gage

16 KSI Max Stress, $R = 0.3$ (150%
Overload Cycle After 9435 Cycles)

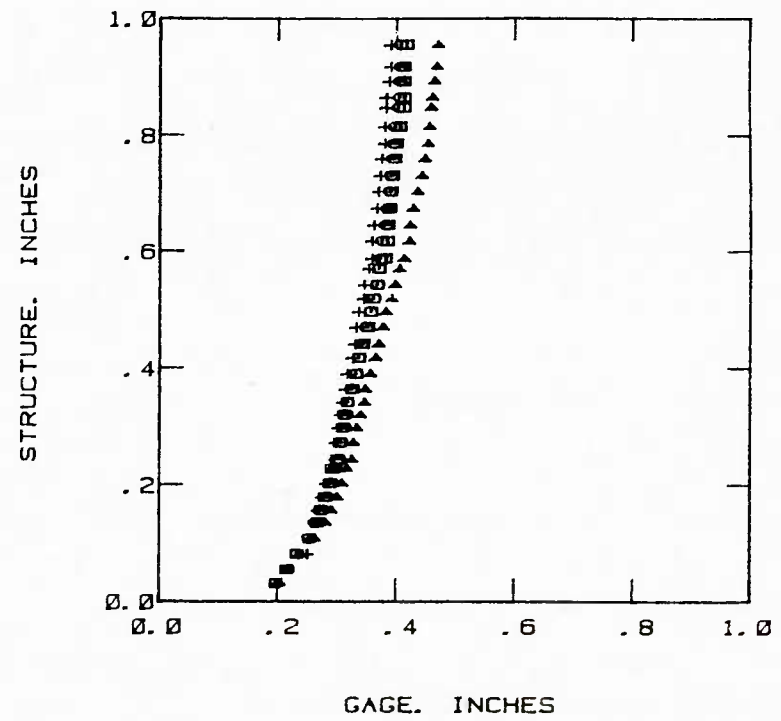
- X Structure
- O Gage No. 1
- Gage No. 2
- △ Gage No. 3
- + Gage No. 4

Figure B-24. Crack Growth Data for Test 043

TEST 044 DATA



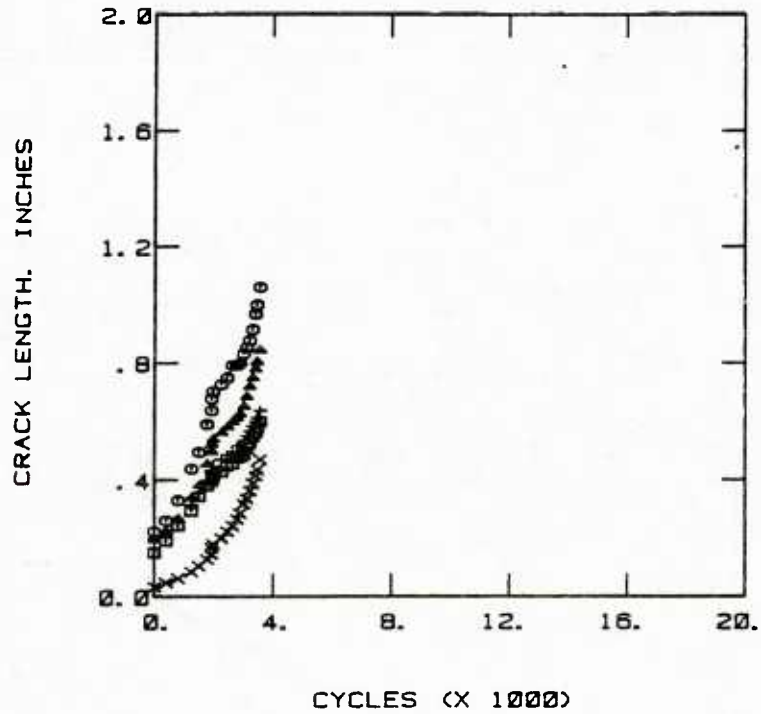
TEST 044 TRANSFER FUNCTION



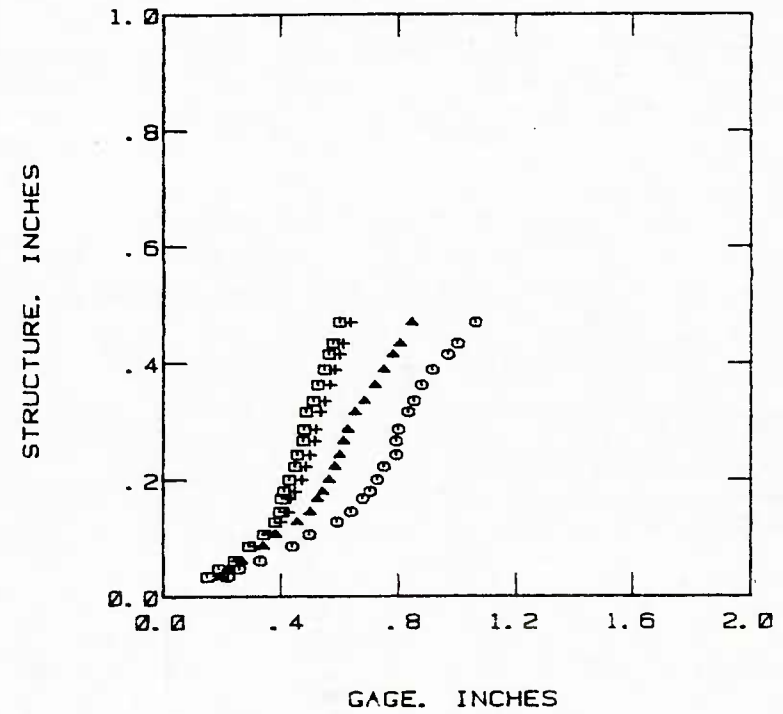
Modified Type 2 Crack Growth Gage
 25 KSI Max Stress, R = -0.1 (130%
 Overload Cycle After 2383 Cycles)
 X Structure
 O Gage No. 1
 □ Gage No. 2
 △ Gage No. 3
 + Gage No. 4

Figure B-25. Crack Growth Data for Test 044

TEST 045 DATA



TEST 045 TRANSFER FUNCTION



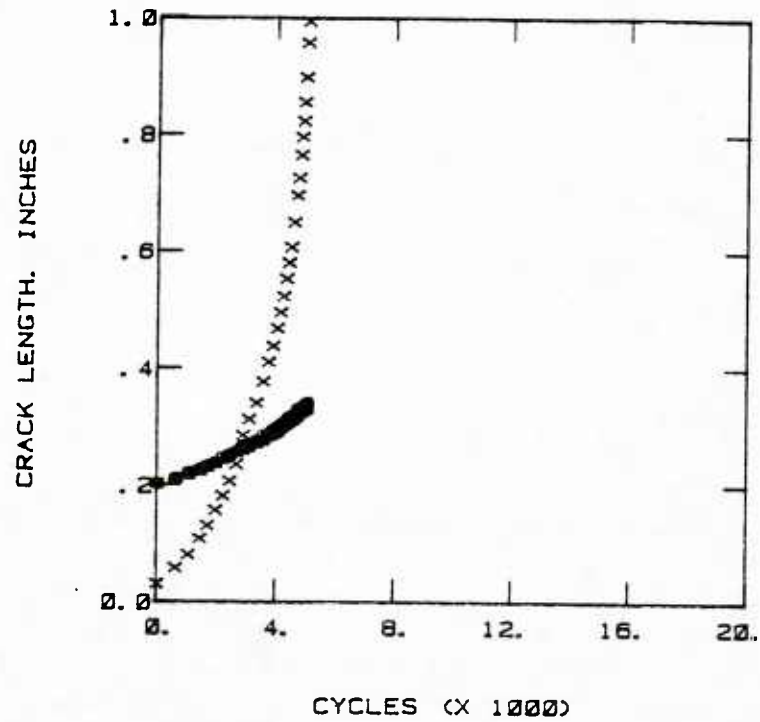
Type 2 Crack Growth Gage

25 KSI Max Stress, $R = 0.1$ (130%
Overload Cycle After 1920 Cycles)

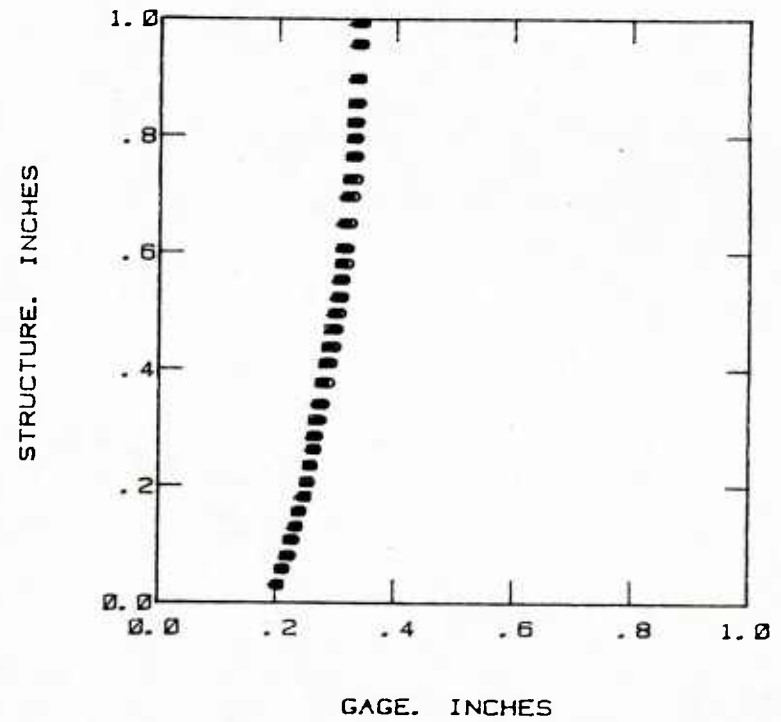
- X Structure
- Gage No. 1
- Gage No. 2
- △ Gage No. 3
- + Gage No. 4

Figure B-26. Crack Growth Data for Test 045

TEST 046 DATA



TEST 046 TRANSFER FUNCTION



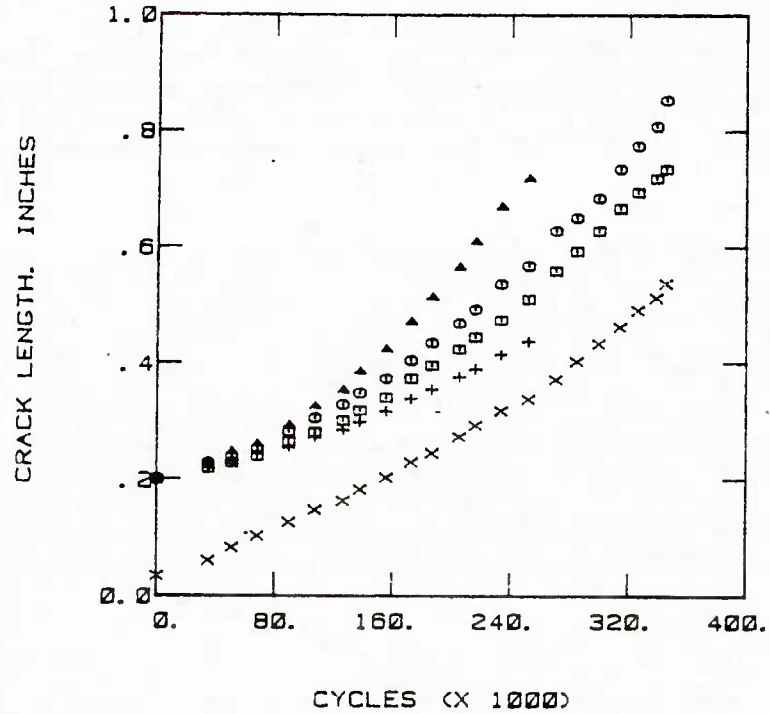
Modified Type 2 Crack Growth Gage

25 KSI Max Stress, $R = 0.3$, (130%
Overload Cycle After 2883 Cycles)

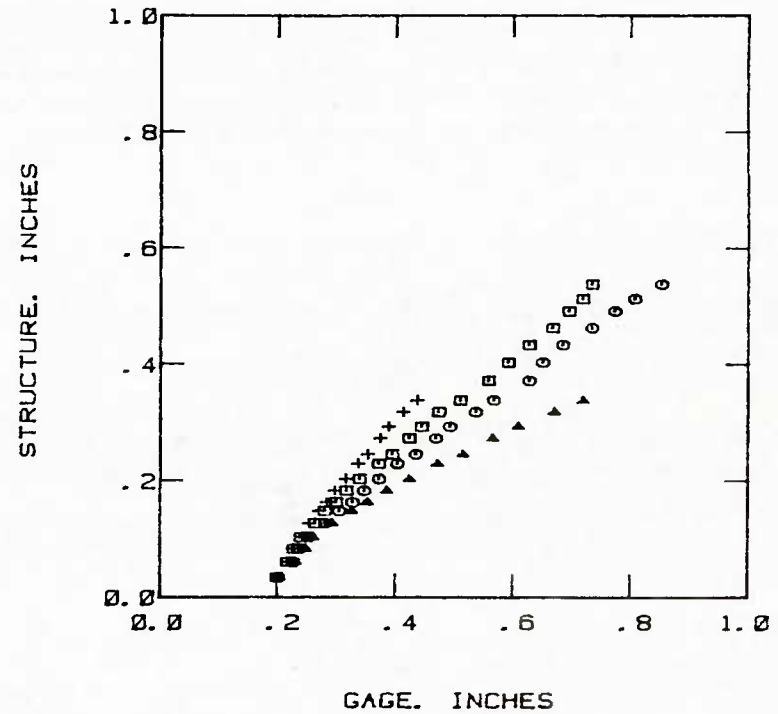
- X Structure
- Gage No. 1
- Gage No. 2
- △ Gage No. 3
- + Gage No. 4

Figure B-27. Crack Growth Data for Test 046

TEST 054 DATA

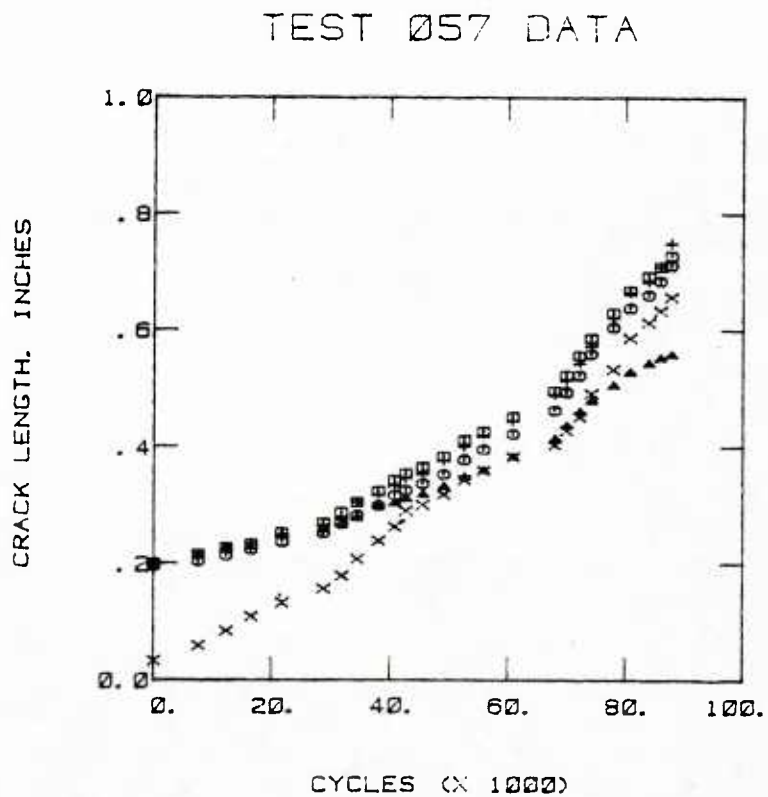


TEST 054 TRANSFER FUNCTION

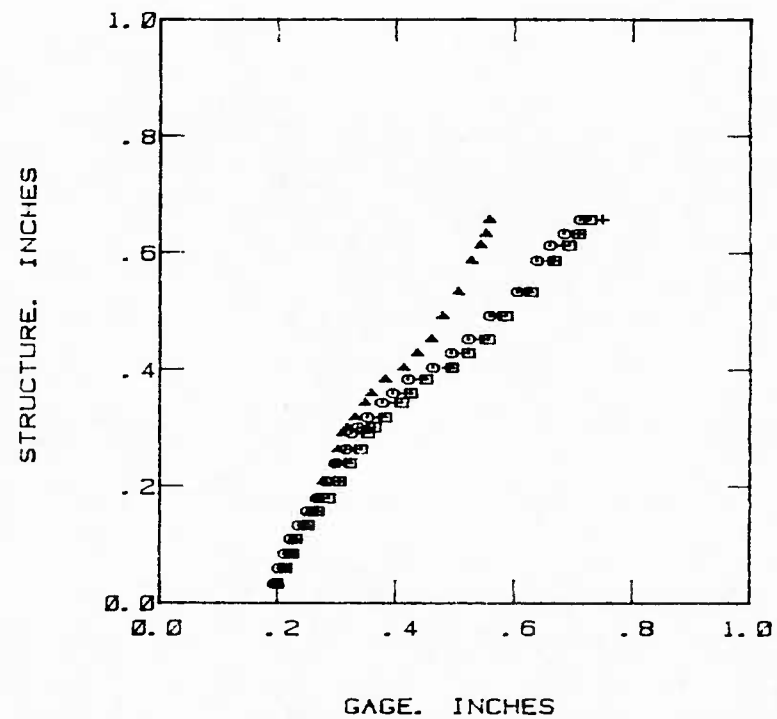


- Modified Type 2 Crack Growth Gage
- T-38 Mild Spectrum
- X Structure
- Gage No. 1
- Gage No. 2
- △ Gage No. 3
- + Gage No. 4

Figure B-28. Crack Growth Data for Test 054



TEST 057 TRANSFER FUNCTION



Modified Type 2 Crack Growth Gage

T-38 Baseline Spectrum

X Structure

O Gage No. 1

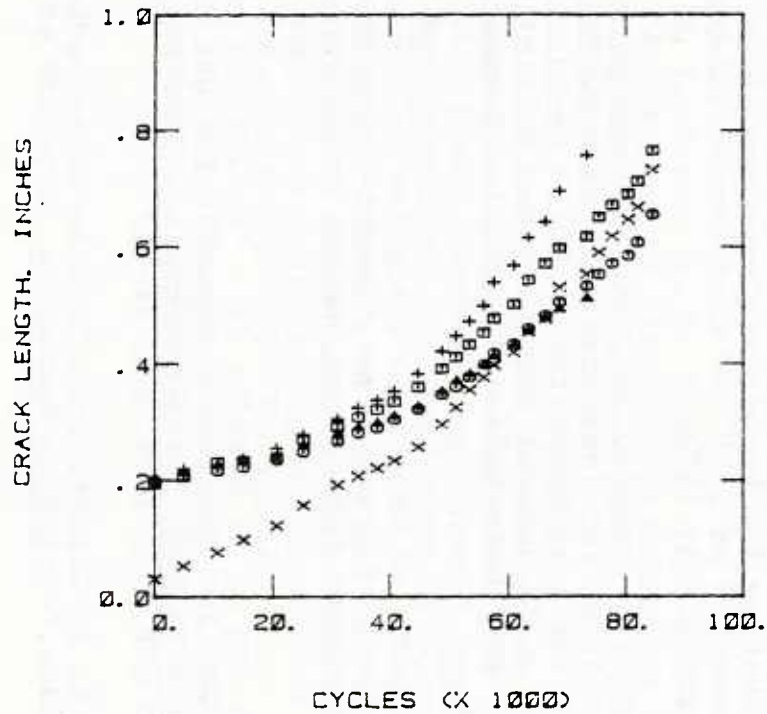
□ Gage No. 2

△ Gage No. 3

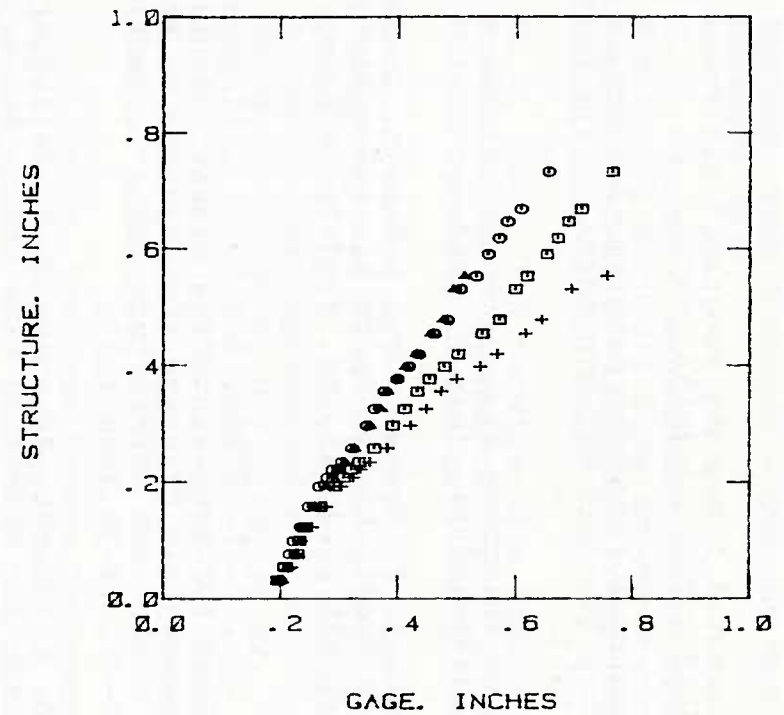
+ Gage No. 4

Figure B-29. Crack Growth Data for Test 057

TEST 060 DATA



TEST 060 TRANSFER FUNCTION



Modified Type 2 Crack Growth Gage

T-38 Severe Spectrum

X Structure

O Gage No. 1

□ Gage No. 2

△ Gage No. 3

+ Gage No. 4

Figure B-30. Crack Growth Data for Test 060

U210202